MECHANISTIC INVESTIGATION OF INACTIVATING BACTERIAL FOOD PATHOGENS WITH NANOPARTICLES

A Dissertation

by

YAGMUR YEGIN

Submitted to the Office of Graduate and Professional Studies of
Texas A&M University
in partial fulfillment of the requirements for the degree of

DOCTOR OF PHILOSOPHY

Chair of Committee,	Alejandro Castillo
Co-Chair of Committee,	Mustafa Akbulut
Committee Members,	T. Matthew Taylor
	Luis Cisneros-Zevallos
Head of Department,	Bhimu Patil

December 2020

Major Subject: Food Science and Technology

ABSTRACT

This research aimed to investigate the inactivation of foodborne pathogens with essential oil containing nanoparticles. Foodborne microbial pathogens continue to impose significant public health and financial burden in the U.S. despite the advent of numerous food processing technologies and food safety oversight systems designed to prevent pathogen transmission to consumers.

Antimicrobial nanoparticles (NPs) were synthesized with geraniol essential oil component using the triblock copolymer Pluronic® F-127. Physico-chemical properties and antimicrobial effects were tested. Different sizes of NPs from 26 to 412 nm were obtained by adjusting concentrations of Pluronic® F-127 and geraniol. NPs displayed sustained release with a time constant of 24 hr. NPs showed better stability at neutral pH and room temperature compared to their stability at acidic and alkaline pH conditions (pH 4.0, 10.0) and decreased and elevated temperatures (4, 37, 50 °C). Antimicrobial NPs inhibited *S.* Typhimurium and *E. coli* O157:H7 growth at 0.4 and 0.2 wt.%, respectively. Nanoencapsulation of geraniol enhanced antimicrobial activity of geraniol by lowering the required amount of essential oil component (EOC) for inhibition through improved transport of EOC to pathogen membranes.

The interactions between *Salmonella* Typhimurium, *Escherichia coli* O157:H7, *Listeria innocua*, and *Staphylococcus aureus* and geraniol-loaded polymeric nanoparticles/non-encapsulated geraniol were investigated to gain new insight into their mechanisms of action against bacteria cells. Bacteria cells were treated with different concentrations of geraniol-loaded polymeric nanoparticles and non-encapsulated geraniol. Zeta (ζ) potential of bacteria cells increased from negative towards less negative in an antimicrobial concentration-dependent

increase due to adsorption of cationic amine groups onto the negatively charged surface lipids. After the bacteria cells were treated with antimicrobial, cell membrane was disrupted and caused the death of the cells. Non-encapsulated geraniol also caused the aggregation of the cells and increased mean size value. Nanoencapsulation of geraniol enhanced its interaction with bacteria cells and increased its adsorption into internal compartments of the cells resulting breaking of the cells. Size measurements for NP-treated cells also showed that the size of the cells was smaller than untreated cells.

Based on the present work it has been reported that 1) the use of antimicrobial nanoparticles can significantly increase the efficiency of encapsulated essential oil components by penetrating cell membrane, 2) encapsulated geraniol shows significantly better efficacy against pathogenic bacteria than non-encapsulated geraniol, 3) greater alteration on the surface charges of the cells were measured for the NP-treatment having stronger antimicrobial properties than free geraniol-treatment, 4) mean size value decreased for NP-treated bacteria cells due to break down of the cells while mean size value increased for non-encapsulated geraniol-treated cells due to aggregation of the cells.

Overall, results of this research will be utilized to provide helpful information to the food industry for a better understanding of inactivating bacterial food pathogens with nanoparticles.

DEDICATION

To my husband, Cengiz.

To my parents, Mujgan & Ismail Hakki, and my sister Irmak.

ACKNOWLEDGEMENTS

I would like to express my sincerest and deepest gratitude to my PhD advisors, Dr. Alejandro Castillo and Dr. Mustafa Akbulut for their support, encouragement, advises, and guidance throughout my research at Texas A&M University. I would like to thank to my committee members, Dr. Taylor and Dr. Cisneros for their invaluable guidance, publication preparations, and time throughout my study. I would like to thank current and previous my lab-mates Dr. Jun Oh, Dr. Ming Zhang, Dr. I-Cheng Chen, Shuhao Liu, Michael Bae, and my other group members for their support, technical discussions, collaboration, friendship, laughs, and making my PhD a great experience for the rest of my life.

Finally, very special thanks to my parents Müjgan and Ismail Hakkı, and my sister Irmak for their unconditional love, support, and help during my all education life. To my husband, Cengiz Yegin, thank you for your full support, care, love, and courage throughout my research and internships. I could not wish a better husband. Thank you for your unconditional love.

My sincere thanks all people supported me with their prayers.

CONTRIBUTORS AND FUNDING SOURCES

Contributors

This work was supervised by a dissertation committee consisting of Professor Alejandro Castillo (advisor), Professor Mustafa Akbulut (co-advisor), Professor Matthew Taylor of the Department of Animal Science, and Professor Luis Cisneros-Zevallos of the Department of Horticultural Sciences

All other work conducted for this dissertation was completed by the student independently. Some parts of the work were completed in collaboration with my former and current group members at Texas A&M University: Dr. Jun-Kyun Oh, Dr. Ming Zhang, Dr. I-Cheng Chen, Dr. Cengiz Yegin, Dr. Nirup Nagabandi Shuhao Liu and Michael Bae.

Funding Sources

This work was made possible by Agriculture and Food Research Initiative Competitive Grant No. 2011-67017-30028 from the USDA National Institute of Food and Agriculture. Its contents are solely the responsibility of the authors and do not necessarily represent the official views of the awarding office.

TABLE OF CONTENTS

Page

LIST OF FIGURES

Page

LIST OF TABLES

Page

1. ESSENTIAL OILS AS ANTIMICROBIALS

1.1. Introduction

Foodborne microbial pathogens continue to impose significant public health and financial burden in the U.S. despite the advent of numerous food processing technologies and food safety oversight systems designed to prevent pathogen transmission to consumers. According to the U.S. Centers for Disease Control and Prevention (CDC; Atlanta, GA), approximately 48 million incident cases of human foodborne disease occur annually, resulting in an estimated cost to the U.S. economy of 77.7 billion USD.[1–3] Bacterial pathogens such as *Salmonella enterica* and the Shiga toxin-producing *Escherichia coli* (STEC), including *E. coli* O157:H7, have been transmitted to consumers by a variety of food vehicles, including fresh and minimally processed produce, dairy products, meat and poultry.[4]

1.2. Essential Oils

Demand for healthy foods by consumers has been an increasing trend and influenced food ingredients. Therefore, there has been a huge search for alternative food preservation methods. Natural antimicrobials can be obtained from many different natural sources such as microorganism, animals, and plants.[5] These antimicrobial compounds can extend the shelf life of food products by killing or inhibiting microorganisms. Essential oils and herbs are also known as natural antimicrobials and show wide range of antimicrobial properties. Herbs and spices have been used in food product to add flavor and their antimicrobial effect is well known.[6] Essential oils can be derived from different parts of plants. Most of the antimicrobial active components of essential oils are produced by plants as a result of defense mechanism.[7] Their active compounds may show antimicrobial effect against different microorganisms such as molds, yeast, and bacteria. Essential oils can be obtained different parts of the plants, for ex: fruits, seeds, bulbs, and leaves.[6]

Parts containing higher concentration of essential oils can show more antimicrobial effect. There are many different types of phytophenols in plants, for example, sesamol in sesame oil, eugenol in cloves, vanillin in vanilla, thymol in thyme, and cinnamic acid and eugenol cinnamon.[8] Essential oils obtained from basil and marjoram can show antimicrobial activity against *Salmonella, E. coli, and Bacillus cereus*.[9] Cinnamon essential oil can show antimicrobial activity against *L. monocytogenes*, *S.* Enteritidis, and *Campylobacter jejuni*.[10] Flavonoids show antimicrobial activity by penetrating on membranes.[8] Flavonoids are antimicrobial to some of bacteria such as *Staphylococcus aureus* and *Pseudomonas* spp.[11] They are show antimicrobial activity against fungi such as *Penicillium* spp. and *Aspergillus* spp.[12] Saponins show an antimicrobial effect by interacting with fatty acids and sterols on membranes of microorganisms.[8] They also show antibacterial activity against *S. aureus*[13] and antifungal activity against *Aspergillus* spp.[14]

1.3. Geraniol

Geraniol (3,7-Dimethyl-2,6-octadien-1-ol) is one of the aromatic constituents of essential oils. Since it is natural compound it can be a desirable alternative of synthetic antimicrobial materials in food industry. Compounds obtained from *Rosa damascene* such as citronellol, geraniol, and nerol show better antimicrobial effect individually than in a combination of all these compounds.[15] Some of the studies have shown antimicrobial and antifungal activity of geraniol (Figure 1).[16] However, its low solubility in water and high volatility are limiting factors for its formulation and use in food products. Antimicrobial effectiveness of sixty-six types of essential oils were evaluated by Si et al.[17] Their research showed that geraniol exhibited ≥80% inhibition towards *S.* Typhimurium and *Escherichia coli* O157:H7 with 500 μg/ml concentration. Geraniol in gas displayed antimicrobial activity against bacterial pathogens, including, *Streptococcus pneumoniae*, *S. aureus*, *Streptococcus pyogenes*, and *Haemophilus influenzae*.[18] The rose oil

component geraniol (*trans*-3,7-Dimethyl-2,6-octadien-1-ol) has been previously reported to exert growth-inhibiting activity against various foodborne bacterial and fungal microbes.[16,19] Kim et al.[20] reported minimum inhibitory concentrations (MICs) and minimum bactericidal concentrations (MBCs) of the compound in 1% Tween 20 against *E. coli* O157:H7, *L. monocytogenes*, *S.* Typhimurium, and *Vibrio vulnificus* ranged between 500 and 1,000 μg/ml. Friedman et al.[21] reported bactericidal activity of geraniol against *Salmonella* and *E. coli* O157:H7 was observed rapidly at 21°C, achieving 50% lethality of inoculated *E. coli* O157:H7 and *Salmonella* cells at levels of 0.089 and 0.031%, respectively, in clarified apple juice. An MIC for geraniol of 0.05% against *E. coli* O157:H7 grown in medium adjusted to pH 4.5 was reported, though researchers observed that at pH 7.2 the MIC of geraniol against the pathogen was >0.1%.[22]

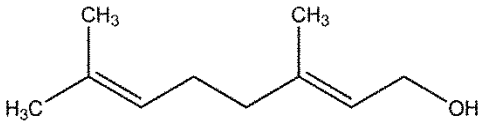

Figure 1: Chemical structure of geraniol.[16]

1.4. The Mechanism of Essential Oils as Natural Antimicrobials

Various mechanisms of bacterial inhibition have been proposed for the antimicrobial activities of essential oils and essential oil components. At first, the destruction of the bacterial cytoplasmic membrane was accepted as a mechanism of inactivation. However, different mechanisms of inhibition of bacterial cells have been proposed. Possible mechanisms of action of essential oil compounds include disruption of cytoplasmic membrane, leakage of cell contents, cell wall degradation, pH disturbance, destabilization of proton motive force, coagulation of cell

contents, damage to membrane proteins.[23–25] The mechanisms of action of essential oils and their components are not very well understood. However, cytoplasmic membrane disruption is a commonly accepted mechanism.[26] Hydrophobic properties of essential oils enable interactions of essential oils to the lipid bilayer of cell membranes and increase their antimicrobial efficiency.[27] Figure 2 shows the site of action in the bacterial cell.[23] Cytoplasmic membrane has an important role at the in and out of the substances and maintaining well-being of cells.[28] Damage on the lipid bilayer of cytoplasmic membrane causes increased permeability to the surrounding environment and leakage of cell inside materials.[29] Leakage of intracellular content would consume proton motive force and decreases in ATP synthesis.

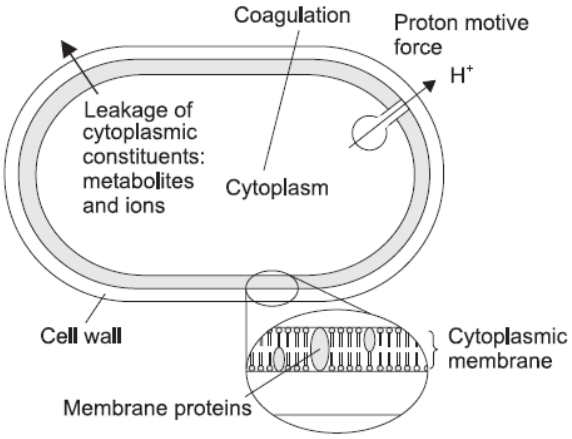

Figure 2: Site of action for essential oils in the bacterial cell.[23] (Reproduced with permission from Burt, S. Essential oils: their antibacterial properties and potential applications in foods-a review. *Int. J. Food Microbiol* 94, 223–253 (2004)).

1.5. Benefits of Nanoscale Drug Delivery

Drug delivery is method of releasing bioactive agents at a target site at a desired rate. There are various advantages of nanoparticles[30] such as protecting the bioactive compounds from degradation[31], increasing the solubility of the drug in aqueous environment[32], improving the bioavailability of the drug[33], making drugs easier to penetrate cells.[34]

1.6. Nanoencapsulation for Controlled Release Applications

Antimicrobial preservatives are used for the microbial growth inhibition. Natural antimicrobials have received a significant attention of consumers due to their increasing food safety awareness.[35] Biological activity of active compounds may decrease when added into a food system.[36] Therefore, it is essential to use the antimicrobial compounds at the concentrations which are enough to inhibit bacterial growth without altering the quality attributes of the food products.[35]

The application of essential oils as antimicrobials in foods can be challenging task due to different reasons. Bacteria are generally suspended in aqueous portions of food matrices. Essential oils are hydrophobic. Therefore, their hydrophobicity requires the higher concentrations of essential oils to inhibit foodborne pathogens since their low water solubility significantly limits their effectively contact with bacterial pathogen cells.[37] When bacterial cells and hydrophobic antimicrobials contact, antimicrobial compounds inhibits bacteria cells by partition into the bacterial cell membrane.[23,38] Besides low solubility of essential oils, their low flavor threshold also limits their use since their effective antimicrobial concentrations negatively affects sensory attributes.[39] Encapsulation of essential oils can increase their solubility in aqueous environment and decrease negative sensory impacts. A wide range of materials such as lipids, proteins, polysaccharides, and synthetic polymers can be used for encapsulation.[40] Nanoencapsulation of compounds can be an efficient way to improve the stability of active compounds and decrease

their interactions with other food additives. Encapsulation of antimicrobial compounds can help the distribution of these compounds in food matrices where bacteria locate.[35] Nanoencapsulation of essential oils can be a solution for improving their dispersion in water and increasing their stability by protecting them from degradation.[41] Application of nanotechnology has brought solutions in food industry such as stability, solubility, and improved bioavailability.[42]

Nanoencapsulation can bring solutions to many problems in food processing. Nanoencapsulation involves wall material to encapsulate substances. Wall material serves as a barrier between encapsulated substances and environment factors. It protects inside material from negative environmental factorssuch as light, pH and oxygen. Nanoencapsulation also protects againstoxidative degradation and photo degradation.[43] In addition, it can increase antimicrobial effectiveness of essential oils by increasing the interaction between essential oils and target microorganisms.

In recent years a great deal of research has been completed detailing the efficacy of plant-derived essential oil components (EOC) (e.g., thymol, carvacrol, allicin, geraniol, limonene, etc.) to inhibit the growth of foodborne bacterial pathogens.[44] Nevertheless, their utility in foods may be limited by their impact on organoleptic properties of the food at levels sufficient to inhibit microbial growth or by low solubility in the aqueous phase of various foods.[23,35] One functional solution to these limitations is that of encapsulation within food-grade encapsulating materials (e.g., lipid, polymers).[45,46] Gaysinsky et al.[47,48] reported entrapment of eugenol and carvacrol within surfactant micelles resulted in decreased growth in a liquid medium over 24 hr at pH 7.0 of *E. coli* O157:H7 and *Listeria monocytogenes* when compared to non-encapsulated EOCs. Gomes et al.[49,50], likewise, reported inhibition of bacterial pathogens on spinach surfaces treated with β-

cyclodextrin-entrapped cinnamon and clove oils, reporting reduced minimum inhibitory concentrations (MIC) of encapsulated antimicrobial oils versus non-encapsulated EOC.

1.7. Pluronic® F-127

Poloxamers are also known with their trademark Pluronics® (BASF). They show amphiphilic properties due to their hydrophilic poly (ethylene oxide) (PEO) blocks and hydrophobic poly (propylene oxide) (PPO) block. Traditional surfactants are low molecular weight while block copolymers are long chain monomers. Chemically dissimilar properties (non-polar and polar) of monomers makes block copolymers amphiphilic. Poloxamers displays an amphiphilic property in aqueous environment due the solubility of PEO and insolubility of PPO in water. Polymeric nanoparticles can enhance solubility and bioavailability of hydrophobic compounds.[51]Pluronics are amphiphilic triblock copolymers. They can form micelles by self-assembly in an oil-in-water emulsion and the use of Pluronic® F-127 as a pharmaceutical additive has been approved by Food and Drug Administration.[52] Pluronic® F-127 was selected because it is inexpensive, non-toxic, bears high biocompatibility, and has been repeatedly utilized in drug delivery systems.[53–56]

Dorn et. al. proposed the formation of micellar block copolymer drug complexes first time.[57] Hydrophobic drugs accumulate inside of the PPO core when hydrophobic drugs are mixed with Pluronic. In addition, hydrated PEO coronas can prevent the removal of hydrophobic drug from the cores. Therefore, Pluronic can increase solubility of hydrophobic drugs and enhance their bioavailability.[58]

2. SURFACE CHARGE INTERACTIONS

2.1. Definition

Zeta potential is defined as a physical measurement of electric potential of particles' shear plane.[59] It can also be defined as the potential difference phase boundaries between liquids and solids. Electrical charge of the particles can be measured after they are suspended in a liquid medium. Unit for zeta potential measurement is in millivolts (mV). Schematic representation of zeta potential is shown in Figure 3.

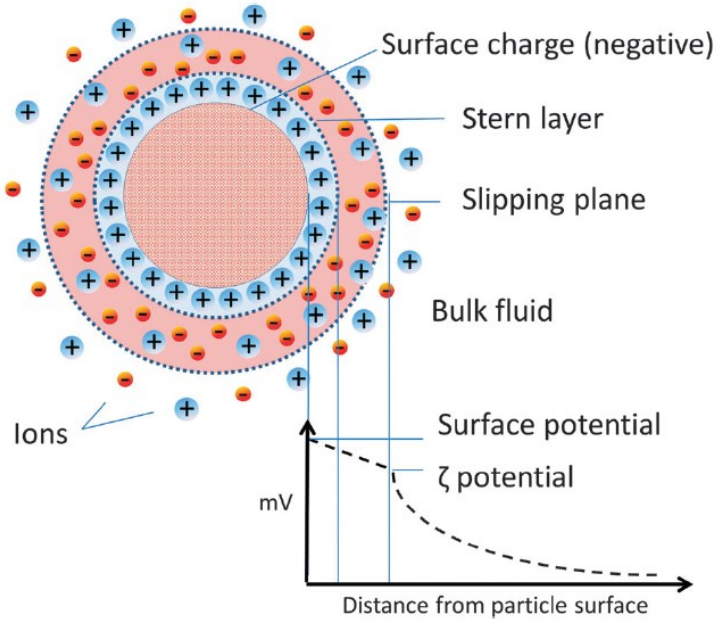

Figure 3: Schematic representation of zeta potential: ionic concentration and potential differences as a function of distance from the charged surface of a particle suspended in a medium.[60] (Reproduced with permission from Liese, A. & Hilterhaus, L. Evaluation of immobilized enzymes for industrial applications. Chem. Soc. Rev. 42, 6236–6249 (2013))

Zeta potential plays a significant role in suspension stability. If particles in a suspension repel each other with their high enough (+) or (-) zeta potentials, particles will not precipitate. However, if the particles do not repel each other in other words if the repulsion forces are not more than van der Waals forces, particles will precipitate (Figure 4).

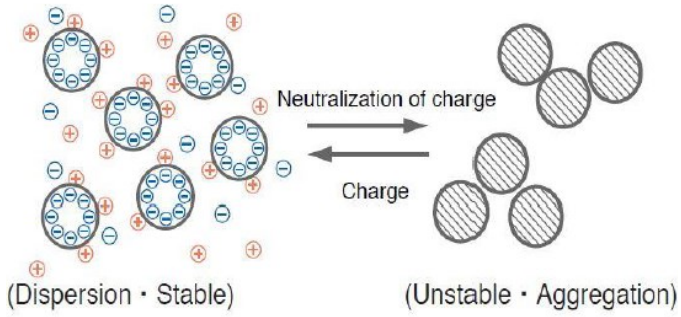

Figure 4: Evaluation of dispersion stability by zeta potential/particle size.[60]

The measurement of zeta potential can provide information about the degree of interactions between particles in a colloid system and the stability of a system. Zero zeta potential value and near neutral zeta potential values show an unstable system. Particles will not be stable and will aggregate. However, zeta potential values less than -30mV and more than +30mV (strongly negative or positive zeta potentials) indicate a stable system since particles will be stable and will repel each other.[61] Zeta potential values can also be used to determine the zeta potential values because zeta potential of a particle strongly depends on its surface charge. Zeta potential values will be less than surface charge values due to the ions in the double electrical layers.[61]

Electrophoretic mobility of a particle is measured to determine zeta potential values. The data can be correlated to zeta potential values. Henry equation can be used:[62]

$$U(E) = \frac{2\ x\ \varepsilon\ x\ Z\ x\ f(\kappa a)}{3\eta}$$ Equation 1

Electrophoretic mobility (U(E)) can be affected by various factors such as zeta potential (Z) of a particle, viscosity (ŋ) of the medium, and dielectric constant (ε) of the medium.[61] The Henry function f (κa) in the equation can be defined as a ratio between thickness of electrical double layer and particle radius.

Zeta potential values may be affected by pH of a solution. For example, zeta potential value of a particle in an acid medium has a more positive zeta potential while zeta potential value of a particle in an alkaline medium has a more negative zeta potential.[61]

2.2. Bacterial surface charge (zeta potential)

Cell surface charge has been described by the zeta potential. Zeta potential is defined as the electrical potential of the region in between surface of the cell and aqueous region. The bilayer supports the membrane structure.[63] Hydrophilic headgroups of membrane modified lipds are located toward aqueous environment while hydrophobic tails are located on the inside of the membrane. Bilayer has a significant role in the bacteria cell surface charge. Outer membranes of all bacterial cells consist of amino, carboxyl, and phosphoric groups. Those groups can be ionized and join the cell surface net charge. Polysaccharides on the cell wall and cell membrane components (exp: phospholipids, peptidoglycans) makes microorganisms negative charged. In addition, degree of the surface charge can be obtained depending on electrostatic mobility of cell.

Surface charge of most of the bacteria is negative and their negative surface charges are balanced by opposite charged ions present in the surrounding environment.[64] Bacteria cell membranes are negatively charged or have negative zeta potential due to their cell wall components for exp: carboxylate groups, phosphates, and proteins.[65] Zeta potential plays an important role in the maintenance of the cellular functions and gives a crucial information related

to cell surface.[66,67] Electrostatic interactions can affect the interactions between bacterial cell surface and agents. Those interactions may cause changes on zeta potential. As a result of the interactions, cell surface permeability may be changed and result to death of bacteria cell.

Measurement of zeta potential is beneficial since it can indicate the changes on the components of bacteria cell wall. It can be estimated by measuring velocity of bacteria cells in an electric field. The velocity of the bacteria cells can be measured by determining the frequency of laser light scattering. Velocity depends on different factors such as pH of the medium, temperature, ionic strength, and surface charge.[68] Movement direction depends on the charge of bacteria cells or particles. While negative charged particles move towards positive electrode, positive charged particles move towards negative electrode.

Zeta potential can be affected by environmental factors such as heavy metals, temperature, pH, ionic strength, and age of culture. Cell wall composition can be altered by environmental pH.[69] Heavy metals at high pH can alter surface charge of some bacteria cells. Bacteria cells have acidic and basic functional groups on their surfaces. Functional groups are related to lipopolysaccharides, peptidoglycan or phospholipids (exist in Gram (-) bacteria), and teichoic acids (exist in Gram (+) bacteria).[70] Those functional groups plays a crucial role at the electrostatic behavior of bacteria cells[71] and therefore, contributing bacterial adhesion.[72–75] In addition, electrostatic behaviors can also affect their interactions with agents.[76,77]

Surface charge determination of bacterial cells are important for better understanding their behaviors at different environmental conditions. Surface charge measurement of bacterial cells is important to investigate mechanisms of action of sanitizer CPC.

2.3. Cell Surface Charge Measurement

Bacterial cell surface has a significant importance in terms of its physiological functions including turgor support, maintaining shape, cell growth and division, and diffusion.[78] Overall, bacteria spend biggest position of their metabolic energy on cell surface by maintaining and synthesizing its macromolecular components. Therefore, it is important to understand the physiochemical properties of the outer membrane of the bacteria cells. It is not easy to directly determine electrostatic charges of bacteria cell surfaces.[79] Therefore, indirect surface charge measurements are used for the measurement.

2.4. Surface Charge Measurement Methods

2.4.1 Microelectrophoresis Method

Different methods have been employed for the bacteria cell surface charge measurements. Microelectrophoresis method is one of the methods used for charge measurement. In this method, bacteria cell suspension is placed in an electrophoresis cell, then voltage across the cell, movement of a single bacterium over a given distance is observed and electrophoretic mobility of the cell is calculated by using the velocity.[80] After that, surface charge of the bacteria cells can be estimated by using electrophoretic mobility. Mobility rate and direction is affected by pH, temperature, ionic strength, bacteria net surface charge, and electric field strength.

Different types of microelectrophoresis have been used. Abramson microelectrophoresis was an early type used for cell surface measurements. More sophisticated types of the microelectrophoresis has been developed for example: FACE Zeta Potential Meter ZPOM (Kyowa Interface Science, Tokyo, JAPAN), Zeta Meter (Zeta Meter, NY, USA), and Lazer Zee Meter 501 (Pen Kem, Bedford Hills, NY, USA). All these types of microelectrophoresis contain observation chamber placed between electrodes and a microscope for observing cell movement.[80]

Microelectrophoresis method has been employed for surface charge measurements in many studies such as Dyar and Ordal[81], Reynolds and Wong,[82] Gilbert et al.[83], Van deer Mei et al.[84], Mangia et al.[85]. Microelectrophoresis is a quite time-consuming techniques for zeta potential measurements since it requires following individual bacterial cells over time.[86] Therefore, some other methods have been developed for zeta potential measurements.

2.4.2 Aqueous Two-Phase Partitioning Method

Aqueous two-phase partitioning method has been used for characterization of bacterial cell surface charge properties.[87,88] Polyethylene glycol -dextran (PEG-dextran) two-phase system established. PEG is a more hydrophobic phase while dextran is less hydrophobic phase. After that, bacteria cells distributed between two phases. Bacterial cells depending on their polarity influenced by surface charge moved toward more hydrophobic or less hydrophobic phase. It is less laborious compared to microphoresis method. However, this method does not give a data to be used for zeta potential calculations.

2.4.3 Electrostatic Interaction Chromatography (ESIC) Method

ESIC method was developed as an alternative to laborious methods for surface charge measurements. It was mainly used as a method for microorganism isolation,[89] however, it has been employed as a method for microbial physiology.[86,90,91] Pedersen[86] used ESIC method first time for bacterial surface charge measurement. It is also time-consuming method for surface charge measurements.

2.4.4 Isoelectric Equilibrium Analysis Method

Isoelectric focusing method was modified by Sherbet et al.[92] to be used as an isoelectric equilibrium analysis method for surface charge measurements. This method involves the generation of a pH gradient which is stabilized by linear gradients. Then, bacterial cells are loaded

onto the column after the generation of a pH gradient and ampholines addition. Voltage is applied to the cells to maintain the desired flow. After that, around 24h given to the cells to move towards their isoelectric positions. Isoelectric equilibrium analysis method is not commonly used method for bacterial cell surface charge measurements. It takes long time to obtain results.

2.4.5 Electrophoretic Light Scattering (ELS) Method

ELS method has been used for bacteria cell surface charge measurements.[93–96] ELS surface charge measurement method involves the measurement of particle velocity moving in an electric field by the determination of the frequency of change of the laser light scattered, yielding their electrophoretic mobility.[94] Zeta potential estimations are very rapid and easy by ELS method.

2.5. Bacteria cell wall

Bacteria cells can be in various sizes and shapes.[97] Cell wall of bacteria has a significant role in the maintenance of the shape and stress bearing.[98,99] Bacteria are divided into two groups called as Gram-positive and Gram-negative bacteria based on Gram-staining technique. Gram-staining technique distinguishes bacteria depending on their cell wall. The cell wall in Gram-negative bacteria contains inner membrane and outer membrane and these membranes are separated by periplasm. Peptidoglycan layer is the main structural periplasm component. Periplasm of Gram-negative bacteria may have free oligosaccharides protecting bacteria cell against osmotic stress. Periplasm may also contain proteins having role at cell surface assembly and nutrient uptake. In general, Gram-negative bacteria show higher resistance to essential oils than Gram-positive bacteria.[100] There are differences between Gram-negative and Gram-positive bacteria cell wall components (Figure 5).

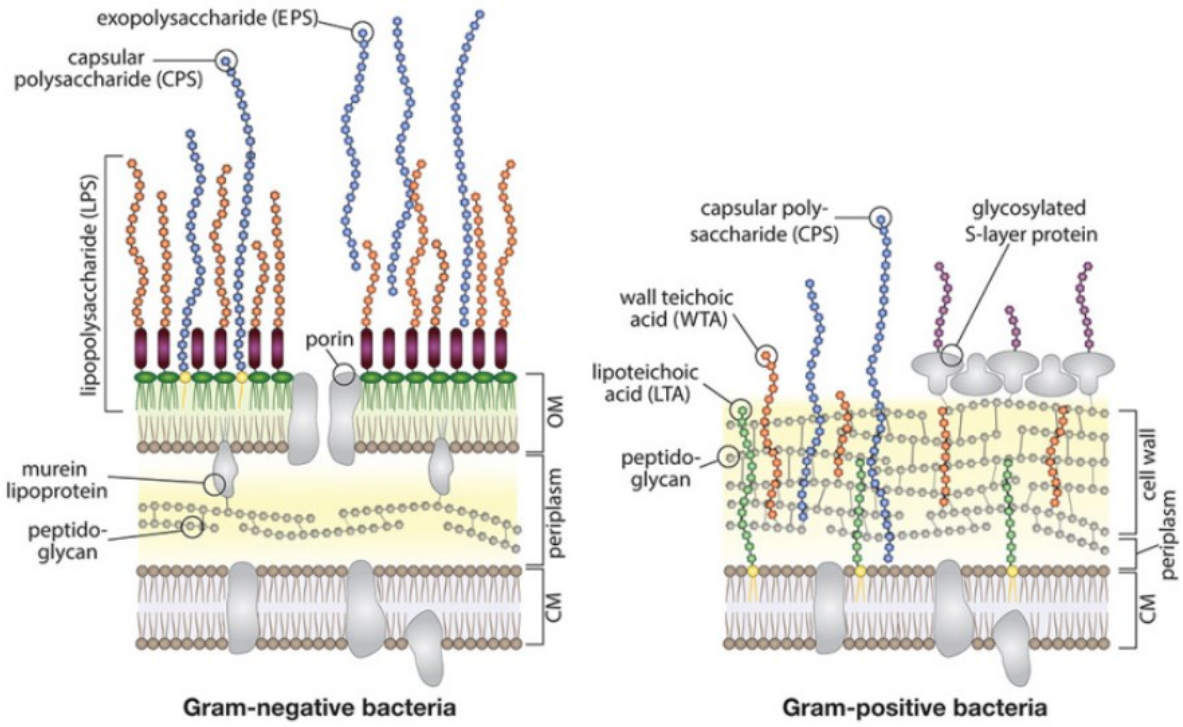

Figure 5: The schematic comparison of the cell walls of Gram-negative bacteria and Gram-positive bacteria.[101]

Gram-positive bacteria do not have outer membrane like Gram-negative bacteria. Outer membrane protects Gram-negative bacteria from the environment. Teichoic acids are also present in Gram-positive bacteria and there two types teichoic acids: lipoteichoic acids and wall teichoic acids. Teichoic acids in Gram-positive bacteria bound to peptidoglycan. They are polyolphosphate polymers. These polymers are strongly negatively charged and can act as a cation-sequestering. The cell wall structure of Gram-positive bacteria allows hydrophobic compounds to pass through the cells and cytoplasm. Essential oils contain phenolic compounds, and they show antibacterial activity against Gram-positive bacteria. Phenolic compounds show different effect depending on their amounts. Phenolic compounds found in essential oils effect enzymes involved in energy production at low concentrations while they cause protein denaturation at high concentrations.[102]

Gram-negative bacteria have much more complex cell wall than Gram-positive bacteria. Peptidoglycan chemical structures of Gram-positive bacteria are very similar to Gram-negative bacteria. The thickness of the layers around plasma membrane is different for Gram-positive and Gram-negative bacteria. Gram-negative bacteria have a lot thinner peptidoglycan layer than Gram-positive bacteria. They have an outer membrane outside of their thin peptidoglycan layer. Braun's lipoprotein links outer membrane and peptidoglycan each other. Braun's lipoprotein embedded in outer membrane and bound to peptidoglycan. The existence of outer membrane in Gram-negative bacteria is one of the differences between Gram-negative and Gram-positive bacteria. Outer membrane consists of a double layer phospholipid. Phospholipids binds to inner membrane by lipopolysaccharides. Outer membrane contains lipopolysaccharides and proteins. Lipopolysaccharides consist of O-side chain, core polysaccharide, and lipid A. One of the reasons that Gram-negative bacteria show resistance to hydrophobic drugs is hydrophilic compounds can pass through outer membrane via protein proteins which serving as hydrophilic transmembrane channels.[103,104] Outer membrane of Gram-negative bacteria quite impermeable to hydrophobic drugs and some of the drug can pass through porins slowly.[105]

Surface charge of bacteria has often called as zeta potential, cell surface electrochemical property.[67,106] Majority of bacteria has negative surface charge and their charges are balanced with oppositely charged ions in their surrounding medium.[64] The electrostatic cell surface charge can be defined as a net charge coming from the cell surface molecules and counter-ions. Antibacterial drug uptake rate and their adsorption are affected by bacterial surface charge. Electrostatic interactions may play a significant role at the interactions between bacterial cell surface and agents. These electrostatic interactions may change zeta potential and cause cell death by altering cell permeability.

2.6. *Salmonella* Typhimurium

Salmonella is a non-spore forming, facultatively anaerobic, Gram-negative bacterium. It is one of the most common food poisonings. Intestinal tract of animals is a reservoir of *Salmonella*. *Salmonella enterica* is the leading cause of foodborne illness.[107] *S. enterica* can cause salmonellosis; and a human got salmonellosis may show enteric fever, septicemia, and gastroenteritis.[108] The infectious dose may range between 10 to 100,000 bacteria cells.[109] It can grow and multiply in the small intestine of their host by colonizing and invading their intestinal tissues and producing enterotoxin.[110]

A foodborne illness outbreak occurred due to the consumption of *S.* Typhimurium contaminated tomatoes in 21 states in the U.S. in 2006 and 183 people were infected.[111] *S.* enteritidis is also linked to the consumption of raw or improperly cooked eggs. Raw eggs should not be eaten and should be stored at refrigerator to minimize the risk of *S.* Enteritidis. *Salmonella* spp. are the most common pathogenic bacteria linked to foodborne outbreaks due to contamination of fresh produce.[112]

Optimum growth pH for *Salmonella* is between pH 6.6 and pH 8.2, and pH 4.05 is the minimum pH.[110] Best growth temperature is between 35 and 37 °C.[113] The minimum water activity for *Salmonella* growth is 0.94, and it can survive in food products having low water activity.[114] Salmonellosis has been also linked to foods with low water activity such as peanut butter, cereal products, fermented meat products, dried milk, hard cheese, and chocolate.[114] *Salmonella* can survive for very long time in chocolate. Low moisture hinders heat transfer and decreases all metabolic activities. Thus, lower the moisture of food higher the D value for *Salmonella*.[115] The other reason is the high fat content of chocolates. Fat protects *Salmonella* and it goes through intestine. Even though *Salmonella* cells are not heat resistant, their toxins are highly heat resistant.

Therefore, storage conditions are highly critical to prevent *Salmonella* food poisoning. Proper handling of foods, controlling irrigation water, proper application of GAP and GMP can help the producers to lower the risk of *Salmonella* food poisoning.

2.7. *Listeria innocua*

Research studies have studied the benefit of using *L. innocua* as an indicator of the presence of *L. monocytogenes*.[116] *L. innocua* can be used as surrogate bacteria for the study of *L. monocytogenes* to eliminate, reduce, and control of this pathogenic bacteria.

Listeria is a Gram-positive , non-spore forming, and rod-shaped bacteria.[117,118] L. monocytogenes can be found at numerous sources such as soil, water, animals, and humans.[119]

L. monocytogenes cause a disease as called as listeriosis, which is caused by the consumption of food contaminated with these bacteria.[120] Hospitalization and mortality rate are quite high for listeriosis. The death rate of listeriosis (34 %) is a lot higher than the death rate of salmonellosis (4.1 %) even though *L. monocytogenes* outbreaks are less prevalent than those related to *Salmonella* spp.[110]

It is very widely occurred in the environment. It usually occur at the environments where lactic acid bacteria (LAB) present.[110] *L. monocytogenes* is commonly associated with soft cheese, pasteurized milk, frankfurters, and vegetables. It can be a problem with the consumption of Mexican-style cheese. Not only pasteurization issues but also hygiene issues are responsible from listeriosis. Post-processing contamination should be prevented since *Listeria monocytogenes* is widely distributed in nature. Raw food products may harbor *Listeria* in low numbers. Meat and poultry carcasses may be contaminated with faces during slaughter, milk during milking, vegetables by water and soil, and fish by contaminated water.

Listeria is generally linked to ready-to-eat foods due to the contamination at the production environment.[121] Prevalence of *Listeria* has been associated with various food products such as ready-to-eat foods[122], fish[123], meat products[124], and dairy products[125]. *L. monocytogenes* has also been linked to the consumption of contaminated fresh produce since there is no killing treatment for these types of foods.

2.8. *Escherichia coli* O157:H7

E. coli O157:H7 is a shiga toxin producing bacteria. *E. coli* is major foodborne illness causing bacteria. First time it was associated human illness at an hemorrhagic colitis outbreak in 1982 and listed as a notifiable disease since 1994 by Center for Disease Control and Prevention (CDC).[126] E. coli can harm by causing disease in immunocompromised people.[110] It is particularly a big health concern in children and seniors due to its relation to hemolytic uremic syndrome which can cause kidney failures.[127,128]

E. coli is rod shaped, facultatively anaerobe, oxidase negative Gram-negative bacteria. E. coli lives in intestinal tracts of warm blooded animals and humans.[110] E. coli O157:H7 is commonly related with meat and meat products; however, it is also a common transmission vehicle for produce contamination.[129] Many outbreaks are associated with *Escherichia coli* 0157: H7 such as lettuce, tomato, meat and meat products. This pathogenic microorganim is highly associated with fecal contamination from soil, dust, packaging materials, washing water, and irrigation water. E. coli can be serologically grouped based on their surface antigens: O (somatic), K (capsule), H (flagellar).[130] There are some virulence groups for E. coli such as enterohemorrhagic E. coli (EHEC), enteropathogenic E. coli (EPEC), enteroaggregative E. coli (EAEC), diffuse-adhering E. coli (DAEC), enterotoxigenic E. coli (ETEC), and enteroinvasive E. coli (EIEC).[110,131] E. coli O157:H7 belongs to EHEC group.[110] Serotype 0157: H7 is the most common in the US.

Escherichia coli 0157:H7 was fist time isolated from the feces of swine.[132] There are two syndromes from EHEC: Hemolytic Uremic Syndrome (HUS) and Thrombotic Thromboctopenic Purpura (TTP).

EHEC group can cause abdominal pain, bloody diarrhea, hemolytic uremic syndrome in which kidney fails.[110] Incubation period for E. coli O157:H7 is between 2 to 5 days.[133] Infectious dose of E. coli O157:H7 is quite small, less than 50 cells can cause illness.[134]

Enterohemorrhagic *E. coli* has greatest impact on the food companies worldwide. The contamination of E. coli O157:H7 does not cause of product loss related to recall of the contaminated food products but also the contamination damages to the brands of the companies. Financial loss to the associated companies could be very high and may also result for going out of business.[135]

2.9. *Staphylococcus aureus*

Staphylococcus aureus food poisoning is one of the most common foodborne illnesses. *S. aureus* is a toxin-producing bacterium. This bacterium may exist in many places such as water, food preparation surfaces, dust, hands of many people, animals, equipment, and utensils. Main sources of *Staphylococcus aureus* are humans and animals. *S. aureus* food poisoning is mainly associated with food commodities which require handling such as salads and sandwiches. Therefore, it is necessary to apply hygiene practices. The other important reason for *S. aureus* poisoning is temperature abuse for the growth of microorganisms. Food commodities should be stored inside of refrigerators. Microorganism needs to grow and produce enough toxin to cause food poisoning. When heat treatment is applied to food product, *Staphylococcus aureus* can be killed but not the toxin. Thus, toxins will stay in the food product and cause intoxication. Foods

having risk of *Staphylococcus aureus* should not be kept at the growth temperature of *Staphylococcus*.[110]

Staphylococcus aureus can be carried in the skin, infected cuts, nasal cavities, and throat. Almost 40% of people are carrier of this pathogen. Thus, all employees should be trained about food safety and hygiene practices. They should wash their hands and nails with soap and water. Gloves should be used during food handling and changed frequently to prevent cross-contamination. Sick person should not work in food handling. Equipment and food preparation areas should be cleaned and sanitized.

Enterotoxins of *Staphylococcus aureus* keep their biological activities during thermal processing since they toxins have high resistance to heat treatments. Therefore, toxins are very likely to cause food poisoning. After the consumption of food commodities, toxins cause diarrhea, cramps, vomiting, and nausea. Patients should take fluids to prevent dehydration.

Few numbers of enterotoxins (20-100 ng) may cause food poisoning (Asao et al., 2003). There are many factors have a role on the production of toxins such as temperature, pH, water activity (a_w), and type of food commodities.[136] *S. aureus* is a problem for food industry since it can grow at big range of pH values.[137] Additionally, it can grow at lower water conditions than many other bacteria can grow.[138] However, the formation of enterotoxin requires higher moisture conditions than the growth of *S. aureus*.[139]

S. aureus may cause food poisoning in milk products since it can occur in raw milk. This pathogenic microorganism is the main reason of mastitis. Hygiene practices, pasteurization, and sufficient cooling should be applied to decrease the risk of staphylococcal food poisoning.

Food companies should prevent the growth of *Staphylococcus aureus* and toxin production in meat products to prevent *S. aureus* food poisoning. A study of Rodriguez-Caturla et al.[140] showed that

biofilm formation can protect *Staphylococcus aureus* and cells can survive on dry surfaces of equipment. Therefore, this pathogenic microorganism can cause cross-contamination of cooked meats.

3. DEVELOPMENT AND CHARACTERIZATION OF GERANIOL-LOADED POLYMERIC NANOPARTICLES WITH ANTIMICROBIAL ACTIVITY AGAINST FOODBORNE BACTERIAL PATHOGENS*

3.1. Overview

This study demonstrates the rose essential oil component (EOC) geraniol can be loaded into polymeric nanoparticles (NPs) with sustainable release profile. Geraniol-loaded NPs were prepared by flash nanoprecipitation and characterized for size, encapsulation efficiency, payload release during storage, inhibition of *Escherichia coli* O157:H7 and *Salmonella enterica* Typhimurium *in vitro* and on spinach surfaces, and NP-assisted transport of EOC into cellular membranes. Adjusting concentrations of stabilizing polymer, Pluronic® F-127, and geraniol produced NPs ranging in size from 26 to 412 nm. Antimicrobial NPs inhibited *S.* Typhimurium and *E. coli* O157:H7 growth at 0.4 and 0.2 wt.%, respectively. Geraniol-loaded NPs displayed sustained release with a time constant of 24 hr, maintaining their anti-pathogenic properties over a prolonged time period. Antimicrobial NPs may be useful for decontamination of various foods and food surfaces from cross-contaminating microbial pathogens.

3.2 Materials and Methods

3.2.1 Materials

Geraniol (>96.0 %; CAS# 106-24-1) (TCI America, Portland, OR), Pluronic® F-127 (PF127; CAS# 9003-11-6) (Sigma-Aldrich Co., St. Louis, MO), and tetrahydrofuran (THF; CAS# 109-99-9; Sigma-Aldrich Co.) were purchased and used as received for the preparation of EOC-loaded

* Reprinted with permission from "Development and characterization of geraniol loaded polymeric nanoparticles with antimicrobial activity against foodborne bacterial pathogens" by Yegin, Y., K. L. Perez-Lewis, M. Zhang, M. Akbulut, and T. M. Taylor, 2016, Journal of Food Engineering, 170, 64-71, Copyright 2016, with permission from Elsevier.

NPs. Nile Red (CAS# 7385-67-3) (Tokyo Kasei Kogyo Co., LTD, Tokyo, Japan) and poly-L-lysine (CAS# 25988-63-0) (Sigma-Aldrich Co.) were used for experiments determining nanoparticle adsorption to bacterial pathogen surfaces.

3.2.2 Preparation of Geraniol-Loaded Nanoparticles

Geraniol-loaded polymeric NPs were prepared with a rapid nano-precipitation method previously reported.[141,142] Briefly, geraniol and the amphiphilic triblock copolymer PF127 were dissolved in THF to differing ratios to determine impact of blending ratios on resulting geraniol-containing NP size. Then, THF solution was rapidly impinged against milli-Q water to produce polymer-encapsulated geraniol-bearing NPs. The flow rate of water was 50.0 mL/min, and the flow rate of the THF solution was 5.0 mL/min. Following impingement processing, the NP-contained solution was placed under a fume hood for 7.0 hr to remove THF (Figure 1).

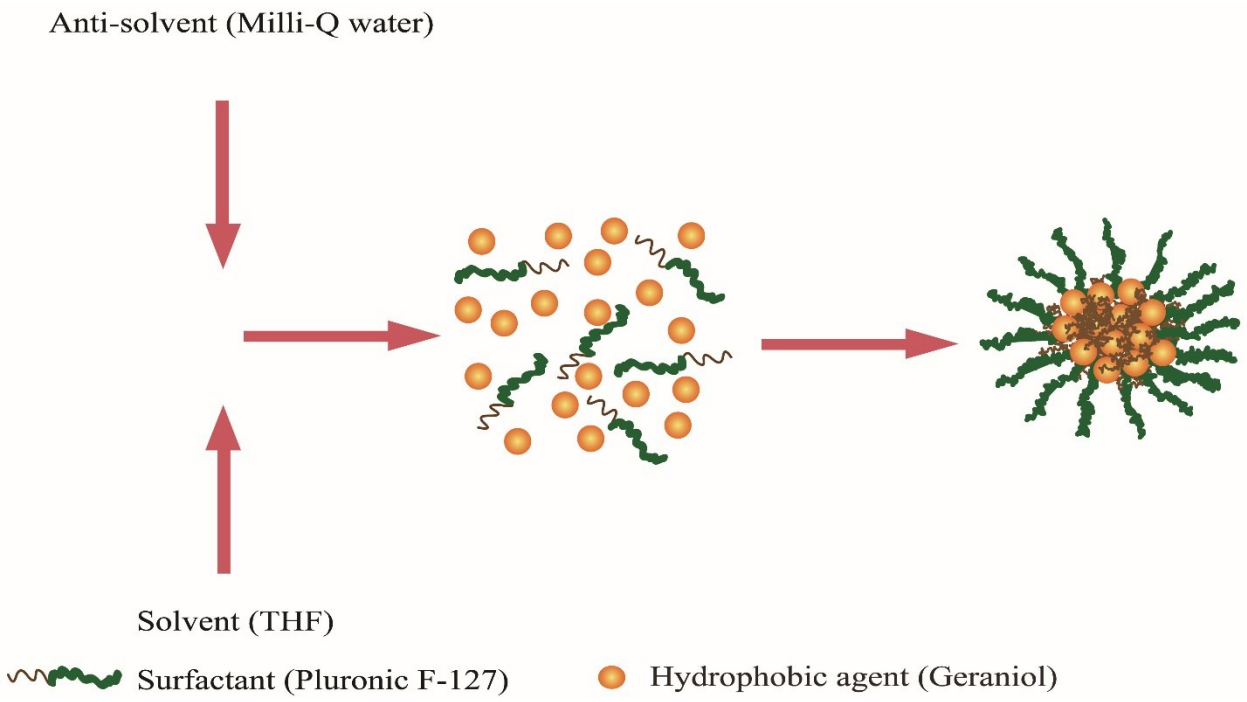

Figure 6: Process for preparation of geraniol-loaded Pluronic® F-127 polymeric nanoparticles.

3.2.3 Characterization of Nanoparticles

Particle size distribution of polymeric NPs was measured by dynamic light scattering (DLS) following four-fold dilution in milli-Q water using a Zetasizer ZS90 particle size and zeta potential analyzer (Malvern Instruments, Ltd., Westborough, MA). The measurements were carried out at a scattering angle of 90° at 25°C. Size and shape of individual NPs was characterized by use of transmission electron microscope (TEM; JEM-2010, Jeol USA, Inc., Peabody, MA) at the Microscopy Imaging Center at Texas A&M University (College Station, TX). Nanoparticle-containing solution was diluted four-fold in milli-Q water prior to drop-wise application of NP solution onto a copper grid (400 mesh) with carbon film (CF400-Cu, Electron Microscopy Sciences, Hatfield, PA). The NP sample was dried at ambient temperature prior to TEM analysis. Observations were performed at 200 kV accelerating voltage, $<2.5 \times 10^{-5}$ Pa, at ambient temperature (~25 °C).

3.2.4 Release Kinetics of Geraniol from Polymeric NPs

Geraniol-containing NPs (9.0 mL) were added into standard regenerated cellulose membrane (molecular weight cut-off 12,000-14,000 Da; approximately 2.0 nm diameter cut-off) (Spectrum Laboratories, Inc., Rancho Dominguez, CA); membranes were then placed into beakers containing 200.0 mL milli-Q water. Unencapsulated geraniol was expected to passively diffuse through dialysis membranes, while NPs were expected to be unable to diffuse through membranes, preventing entrapped geraniol from diffusion. Changes in concentration of free geraniol were tracked by spectroscopy using a UV-1800 UV/Visible scanning spectrophotometer (Shimadzu Corp., Columbia, MD), scanning all wavelengths from 190 to 800 nm (geraniol maximal absorption: 240 nm). UV measurements were performed at ambient temperature at 1, 2, 4, 8, 24, 48, 96, and 144 h. Four independent replications were completed for each measurement.

3.2.5 Encapsulation Efficiency (EE) of Nanoparticles

Geraniol loading and EE was determined by mass spectrometry (MS). Nanoparticles were added to hexane at 1:10 NP: hexane (calculated as weight NP:weight hexane) to degrade NPs and release geraniol into the solvent phase. Following geraniol release from NPs, hexane was used to complete MS analysis of geraniol at the Laboratory for Biological Mass Spectrometry (Department of Chemistry, Texas A&M University). A reference/standard solution of 0.08 wt. % geraniol was prepared to calibrate the concentration of geraniol obtained from degraded NPs in mass spectra. Ten µl of 0.5 mg/ml of hexadecanol was added as internal standard to 50 µL of sample. 100 µL of N,O-Bis(trimethylsilyl)trifluoroacetamide (BSTFA) with trimethylchlorosilane (TMCS) was added into this solution. The mixture was heated at 60 °C for 1 h. The compounds of interest were detected as trimethylsilyl (TMS) derivatives using GC/MS. Ultra GC/DSQ (Thermo-Electron, Waltham, MA) was used for GC-MS. Chromatography was carried out using an Rxi-5ms column (60 m x 0.25 mm with 0.25 µm film thickness) (Restek, Bellefonte, PA). Helium was used as a carrier gas at constant flow of 1.5 mL/min. GC inlet was held at 225 °C while transfer line and ion source temperatures were held at 250 °C. An aliquot of 1.0 µL of sample was injected in splitless mode. The oven temperature was maintained at 50 °C for 5 min, then raised to 320°C at 20°C/min. Electron impact ionization at 70 eV was used for ionization and mass spectra were acquired in full scan mode in the range of 30-500 m/z. Three replications were completed for MS analysis of NP EE; EE was determined as:

$$EE\ (\%) = (\textit{Weight of drug in NPs / Initial weight of drug}) \times 100\% \qquad \text{(Eq. 1)}$$

3.2.6 Stability of NPs to Storage at Differing Environmental Temperature and Acidity Conditions

In order to determine the stability of NPs to exposure to conditions of storage abuse, NPs were prepared and stored at differing temperature (4, 25, 37, and 50 °C) at pH 7.0. In a separate experiment, NPs were prepared and loaded into reaction vessels pre-conditioned to pH 4.0, or 10.0 at ambient temperature; storage solutions were diluted and pH-adjusted to desired pH with either HCl or NaOH (0.133 mM ea.). In both experiments, NPs subjected to temperature- or pH-abuse conditions were sampled at 0, 1, 2, 4, 7, 14, 30, and 60 days of storage and subjected to size analysis via DLS as described above. Hydrochloric acid (HCl; 36.5-38.0 %) (VWR, Inc., Radnor, PA), and NaOH (≥98.0 %; Sigma-Aldrich Co.) were purchased for use in reaction pH adjustment and were used as received.

3.2.7 Microorganisms and Inoculum Preparation

Salmonella Typhimurium LT2 (American Type Culture Collection [ATCC] No. 700720) (Manassas, VA) and *E. coli* O157:H7 (ATCC No. 700728) were obtained from the Food Microbiology Laboratory (Department of Animal Science, Texas A&M University) culture collection and revived according to previously published methods.[143] Working cultures were obtained by aseptically scraping a loopfull (10 μL) of culture from tryptic soy agar (TSA; Becton, Dickinson and Co., Sparks, MD) slant surfaces into 9.0 mL sterile tryptic soy broth (TSB; Becton, Dickinson and Co.), followed by incubation at 35°C for 24 h. A second passage was completed in identical fashion, with subsequent incubation at 35°C for 24 h prior to antimicrobial assay completion.

3.2.9 Interaction of Fluorescent NPs with Bacterial Pathogen Cells by Confocal Microscopy

For confocal microscopy analysis of NP/bacterial cell interaction, Nile Red (0.001 wt. %) was co-entrapped with geraniol to produce fluorescing NPs. Poly-L-lysine was used to provide cell immobilization on glass cover slides to immobilize bacterial cells while taking confocal images. Glass cover slides were coated by dipping into poly-L-lysine solution (0.1 mg/mL) for 5 min. Excess poly-L-lysine was removed and slides were dried completely under a fume hood. A 1.0 mL suspension of *E. coli* O157:H7 cells, prepared as described in Section 2.6, was mixed with 1.0 ml Nile Red-containing NPs and incubated 2 h; samples were then washed once in 0.1% peptone water. For the control, Nile Red was prepared to 0.001%; a 1.0 mL suspension of *E. coli* O157:H7 was similarly mixed with 1.0 ml Nile Red, incubated 2 h, and then samples were washed once in 0.1% peptone water. One drop of sample was then placed in the middle of the poly-L-lysine coated glass cover slides. The images were obtained using a confocal microscope (Zeiss LSM 780 NLO Multiphoton Microscope) using an excitation wavelength of 561 nm to determine the distribution of nanoparticles; fluorescence emission was detected at 579-624 nm. Confocal microscopy was conducted at the Image Analysis Laboratory, College of Veterinary Medicine & Biomedical Sciences at Texas A&M University (College Station, TX).

3.2.10 Statistical Analysis of Data

Data analysis was completed using ORIGIN® v.8 software (OriginLab Corp., Northampton, MA). One-way analysis of variance (ANOVA) was used to test the differences between treatments and Tukey's Honestly Significant Differences (HSD) test was performed to separate means differing at $p<0.05$.

3.3 Results and Discussion

3.3.1 Characterization of Nanoparticles and Encapsulation Efficiency

Figure 7A depicts the intensity-weighted size distribution for one of such NPs as obtained by DLS analysis. Hydrodynamic NP size ranged from 200 to 1000 nm, with an average diameter of 412 + 25 nm for particles constructed from a 1:1 ratio geraniol:PF127 (Table 1); polydispersity index (PDI) values approximated 0.19 for freshly prepared NPs at ambient temperature. Transmission electron microscopy analysis revealed NPs were spherically shaped, as well as agreeing with particle size estimates obtained by DLS (Figure 7B). It was also possible to obtain EOC-loaded NPs of differing mean hydrodynamic sizes by altering geraniol:PF127 mixing ratio (Table 1). Among different drug:polymer ratios 1.0:1.0 ratio gave the highest size as 412 nm. Geraniol-loaded polymeric nanoparticle size increased by increasing drug amount for 0.25:1.0, 0.6:1.0, and 1.0:1.0. When the drug amount was the same and only the polymer amount was different for 1.0:0.25 and 1.0:1.0, size of the nanoparticles increased from 290 nm to 412 nm. The mean particle size shifted towards a higher particle size for increased polymer amount. Even though the drug:polymer ratios are the same for 2.0:0.5 and 1.0:0.25 ratios, the mean particle sizes were different due to the use of different amount of drug and polymer. Kohli et. al (2017)[144] investigated the effect of drug:polymer ratios on the mean particle size of zidovudine-loaded polylactide-co-glycolide (PLGA) microspheres. They also observed the increased mean particle size shift towards a higher particle size by increasing drug:polymer ratios. Encapsulation efficiency analysis can indicate the percent of drug entrapped within a polymeric matrix from the amount of drug applied during NP formulation and manufacture. The mean EE for geraniol in PF127 NPs was 57.5 $\pm$ 5.5 %; non-entrapped geraniol was removed during THF evaporation. The EOC loading ratio (wt. of drug divided by wt. of whole particles) was 0.365. Manaspon et al.[145] reported

Pluronic® F127/chitosan NPs containing doxuribicin entrapped between 58.1 and 51.2% when PF127 was loaded at 5 and 10% (w/v), respectively, similar to the EE obtained in the current study.

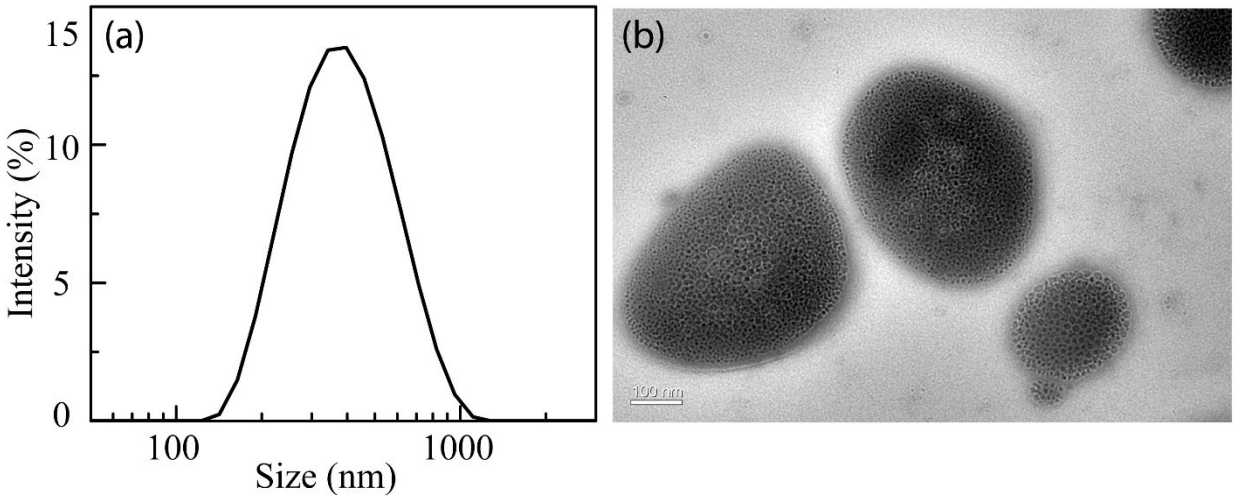

Figure 7: Size distribution for geraniol-loaded nanoparticles obtained by dynamic light scattering (DLS) analysis (a), and TEM micrograph of typical geraniol-loaded nanoparticles (b). DLS analysis was carried out at 25°C with 4X-diluted nanoparticles in milli-Q water; a 90° incident angle was used for application of light.

Table 1: Impact of nanoparticle formulation on resulting particle size.

Geraniol: PF127 ratio	Geraniol: PF127 amount (g)	Particle size[a] (nm)
0.25: 1.0	0.08: 0.32	25 ± 2A
2.0: 0.5	0.64: 0.16	155 ± 3B
1.0: 0.25	0.32: 0.08	290 ± 6CD
0.6: 1.0	0.192: 0.32	315 ± 6D
1.0: 1.0	0.32: 0.32	412 ± 25E

[a] Values are means from three identically completed replicates (n= 3) ± one standard deviation from mean. Means not sharing letters (A, B, C) differ, determined by analysis of variance (ANOVA) and Tukey's Honestly Significant Differences (HSD) test at p = 0.05.

3.3.2 Release of Geraniol from PF127 Nanoparticles

The release of geraniol from NPs into water was observed by the spectroscopic determination of geraniol concentration as a function of incubation at 25°C for 144 h (Figure 8). Early in the experiment, the concentration of geraniol diffusing across the dialysis membrane increased significantly from 0 to 8 h, as well as from 8 to 24 h ($p<0.05$). The concentration of geraniol diffusing across the membrane appeared to be maximal at 24 h, with a plateau observed in geraniol content in dialysis water from 24 until 144 h of storage. The resulting diffusion curve was fitted with an exponential regression curve ($R^2= 0.9994$), with a half-release occurring within 7.25 h. Drug release properties from nanoparticles in the current study are similar to that reported previously for PF127 micelles constructed in pharmaceutic and antimicrobial drug delivery applications.[146,147] Nonetheless, NPs in the current study outperformed PF127 micelles encapsulating the plant oil curcumin with respect to release profile where 80% drug release was observed to occur within 6 h at 37°C.[148]

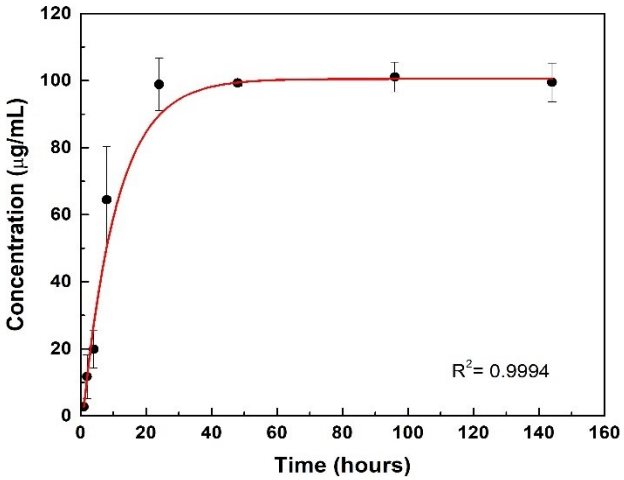

Figure 8: Geraniol release from nanoparticles stored at 25°C as a function of time. Symbols depict means from four independent replications while error bars depict one sample standard deviation (n=4).

3.3.3 Stability of NPs to Temperature- and pH-Abuse Storage

Hydrodynamic size measurement results are measured at DLS up to 60 days shown at Figure 9-15. The effect of NP storage under extremes of environmental temperature and acidity/alkalinity are depicted in Figures 9 and 10, respectively. At 25 °C, particle size did not change as a function of storage period, demonstrating good storage stability at ambient temperature ($p \geq 0.05$). Conversely, mean diameters of NPs stored at 4 °C differed at $p=0.05$ from NP diameters of 25 °C-stored NPs up to day 14 (Fig. 9). Mean diameters of NPs at 4 °C were 392.93±19.88 nm, 331.45±8.76 nm, 342.95±37.57 nm, 302.33±21.19 nm, 292.05±6.08 nm, 250.5±45.75 nm (94.65%) and 34.97±3.78 nm (5.35%), 315.58±26.38 nm (97.4%) and 35.99±4.79 nm (2.6%), 347.5±50.16 nm (97.45%) and 41.84±1.09 nm (2.55%) for day 0, 1, 2, 4, 7, 14, 30, and 60 respectively. Conversely, at 37 °C, although the size of NPs did not change during storage for the majority of particles, a second population of particles with a mean diameter of approximately 37.36±25.57 nm was detected at day 14 of storage; this second population of NPs was also identified at 30 days of storage, but by 60 days the diameter of both populations of NPs were nearly identical (Fig. 9). This trend may be explained as empty NPs that released EO early on into the storage period, with subsequent aggregation of polymer into larger complexes over the course of sample storage. Samples taken from NPs stored at 50 °C also revealed a second population of smaller NPs that initially decreased in diameter through 14 days of storage without further decrease in diameter thereafter through the end of the experimental period (Fig. 9). Given the results obtained with NPs stored at 37 °C, results from 50 °C-stored samples are not surprising and indicate the expulsion of geraniol early on with a likely reassembly of micellar structures. Prud'homme et al.[149] reported that micelles of PF127 in aqueous solution were favored as incubation temperature was increased over 30 °C due to disappearance of large domains as

poly(oxyethylene) chains were increasingly dehydrated and repulsive interactions were decreased. The NPs stored at 50 °C showed a second peak detected at the second day of storage. However, unlike those samples taken from NPs held at 37 °C, the second population of NPs from 50 °C incubation did not increase in size during storage, but rather remained constant up to day 14. It has been observed previously that elevated temperature storage can assist the release of entrapped drug, resulting in NP degradation.[150] Surprisingly, a second population of NPs with smaller diameter was also determined to exist in NP solution stored at 4 °C. As with samples stored at 37 °C, the mean diameter of this second population of NPs was initially observed at 14 days of storage, though it behaved more like NPs stored at 50 °C in that its mean diameter did not increase over storage but rather decreased until a point at which it remained static thereafter. This may have been the result of reduced hydrophobicity of the poly(oxypropylenes) at the reduced storage temperature, which may have led to loss of emulsification of the hydrophobic oil and breakdown of the micelles, as well as the potential for unimers of PF127 to exist at temperatures below the micellization temperature at the concentration used in the present study (8.0 wt.%; ~24 °C).[54,151]

Nanoparticles were loaded into solutions adjusted to pH 4.0, 7.0, or 10.0 and then stored at 25 °C (Fig. 10). No differences in NP mean diameter were observed for samples taken from the three storage conditions through the first 14 days (Fig. 10). However, evidence of NP degradation was detected at day 30 for pH 4.0-stored samples as compared to NPs held under neutral and alkaline pH conditions, with the detection of a second population of smaller NPs with a mean diameter of approximately 79.05±35.86 nm ($p<0.05$). The release of drug was faster at pH 4.0 than the release of drug at neutral pH conditions, a response to environmental storage conditions previously reported for drug-delivering NPs.[152] Interestingly, in NPs stored at pH 10.0, evidence of NP breakdown and development of a bimodal distribution of NPs was not observed until day

60 of the incubation period, indicating that polymeric capsules are not long-term stable to acid hydrolysis but bear moderate stability to hydroxide attack.

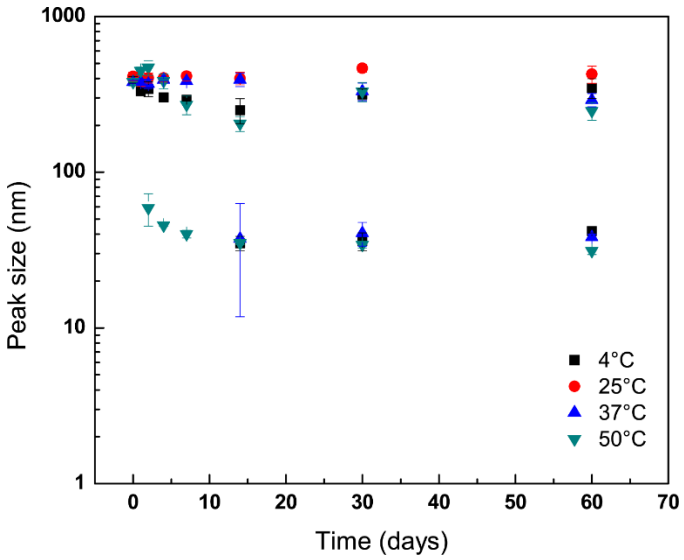

Figure 9: Stability of geraniol-loaded nanoparticles over 60 days of storage in milli-Q water (pH 7) as a function of storage temperature. Particle size and polydispersity was determined by dynamic light scattering. Symbols reflect sample means taken from two identical independent replications, with duplicate readings taken per sample and then averaged (n=4); error bars indicate one sample standard deviation.

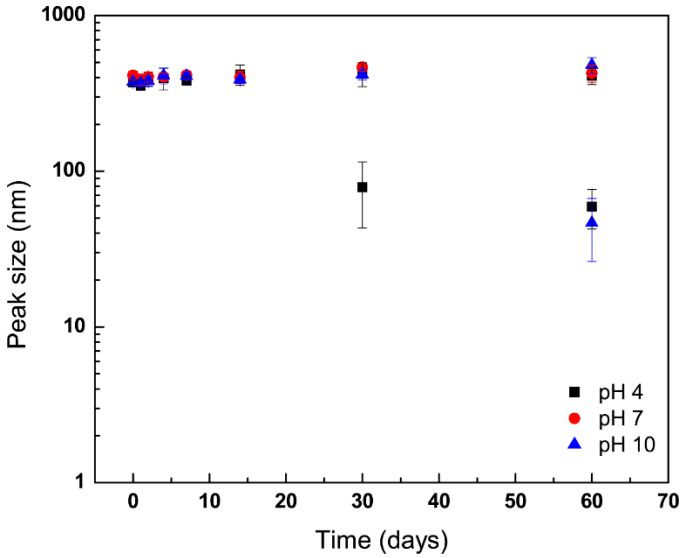

Figure 10: Stability of geraniol-loaded nanoparticles over 60 days of storage in milli-Q water (25 °C) as a function of storage pH. Storage solution pH was modified by controlled addition of 0.133 mM HCl or NaOH. Particle size and polydispersity was determined by dynamic light scattering. Symbols reflect sample means taken from two identical independent replications, with duplicate readings taken per sample and then averaged (n=4); error bars indicate one sample standard deviation.

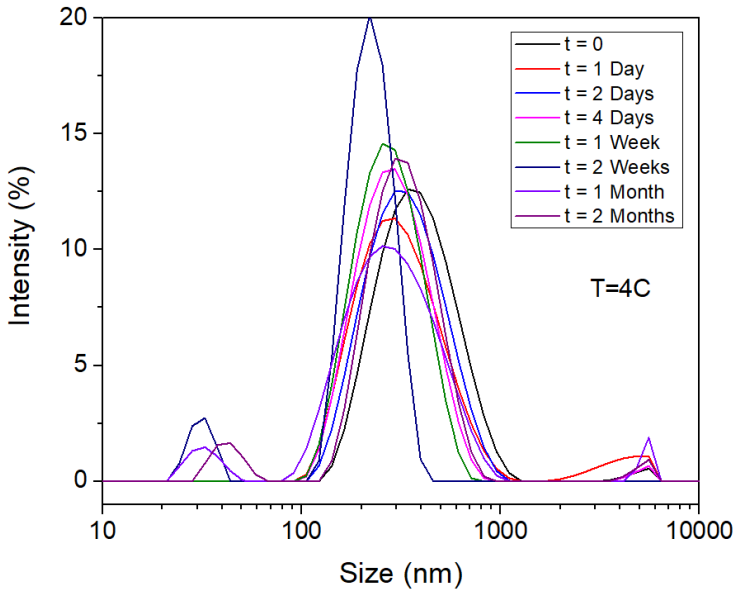

Figure 11: Particle size distributions of geraniol-loaded nanoparticles at 4˚C over 60 days.

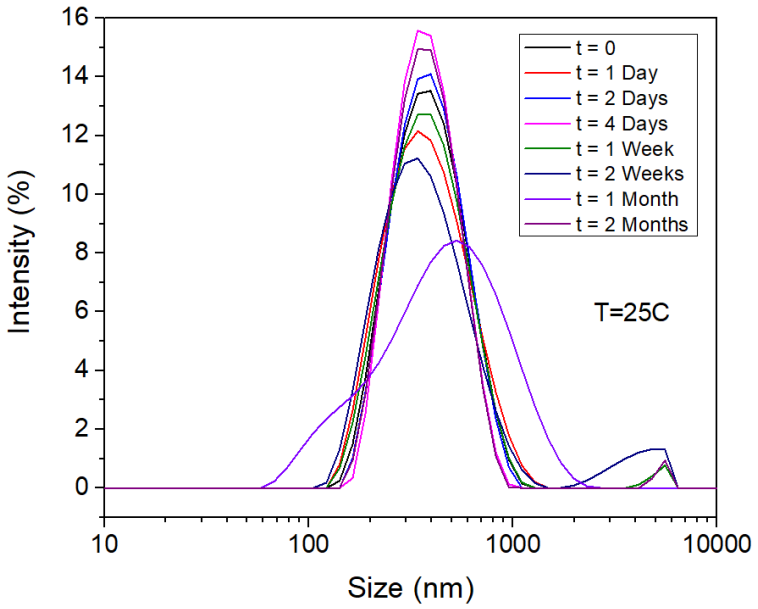

Figure 12: Particle size distributions of geraniol-loaded nanoparticles at 25˚C over 60 days.

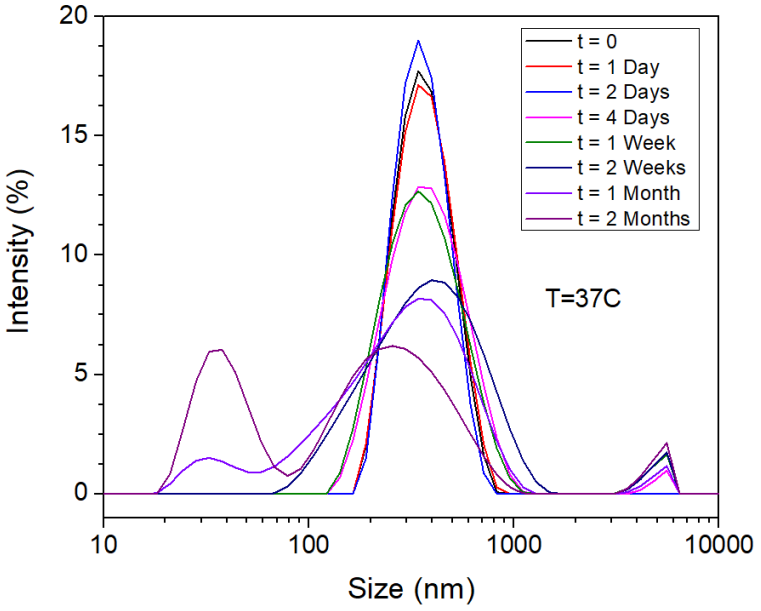

Figure 13: Particle size distributions of geraniol-loaded nanoparticles at 37˚C over 60 days.

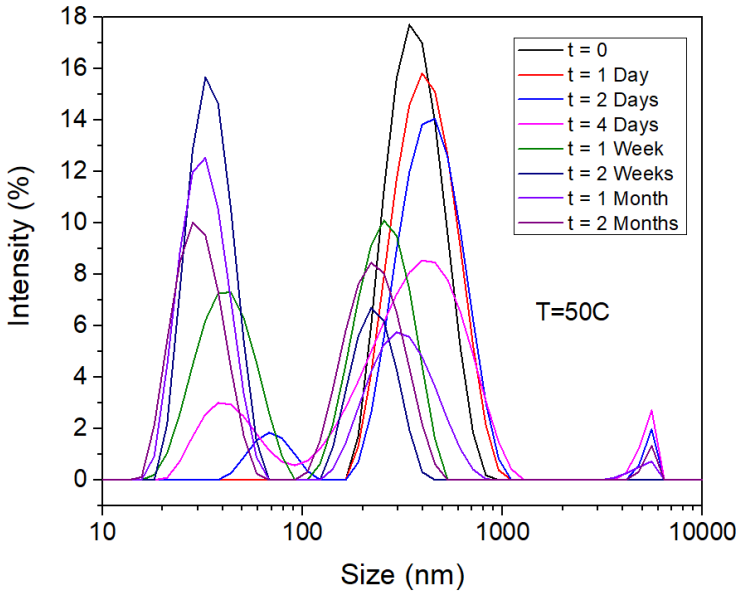

Figure 14: Particle size distributions of geraniol-loaded nanoparticles at 50˚C over 60 days.

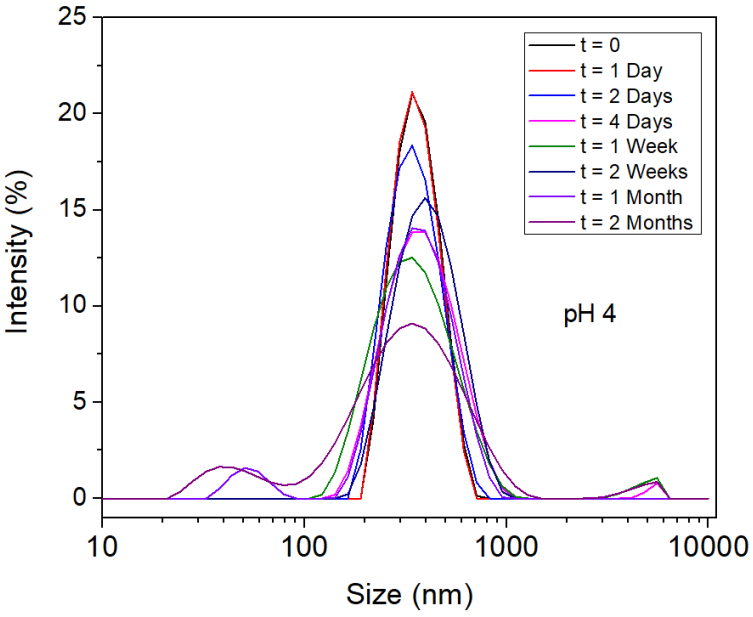

Figure 15: Particle size distributions of geraniol-loaded nanoparticles at pH 4 over 60 days.

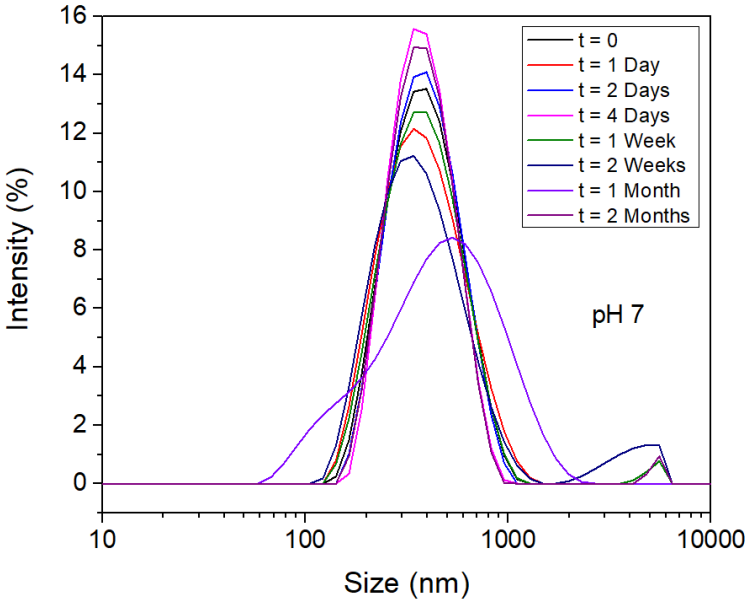

Figure 16: Particle size distributions of geraniol-loaded nanoparticles at pH 7 over 60 days.

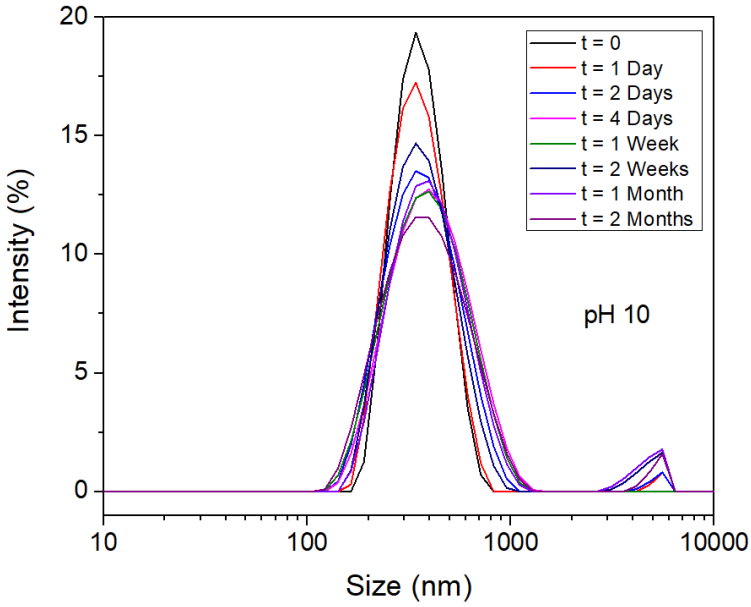

Figure 17: Particle size distributions of geraniol-loaded nanoparticles at pH 10 over 60 days.

3.3.4 Antimicrobial Activity of Geraniol NPs against Foodborne Bacterial Pathogens

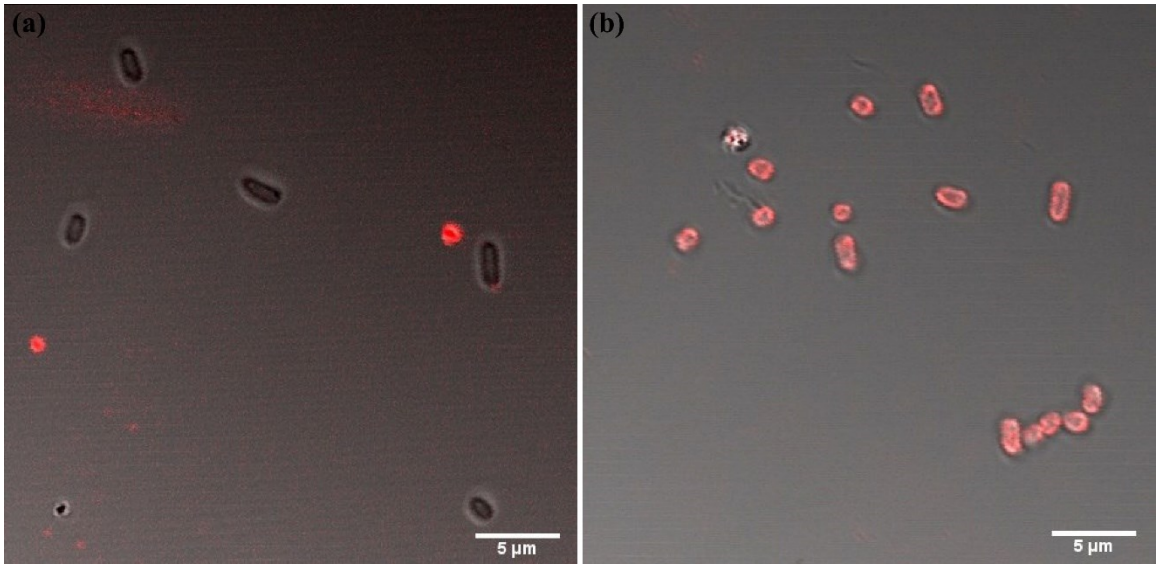

Figure 18: Exposure of *E. coli* O157:H7 cells to 0.001% free (a) or nanoparticle-loaded Nile Red (b). Fluorophore excitation was at 561 nm, with emission scanned from 579-624 nm.

E. coli O157:H7 cells were exposed to fluorescent geraniol-loaded NPs to characterize nanoparticle absorption and interaction with bacterial membrane lipids by confocal microscopy. Fluorescence was detected in cells incubated with NPs, while no fluorescent signal was detected from cells incubated with free Nile Red (Figure 18). Non-entrapped Nile Red was not absorbed into cell membranes and showed aggregation (Fig. 18A). However, NP-encapsulated Nile Red and geraniol was taken up into the internal compartments of *E. coli* O157:H7 cells (Fig. 18B). These results suggest that encapsulation of plant-derived EOC such as geraniol can indeed enhance their bioavailability and the transport of EOC. Our findings are also in accord with others reporting greater susceptibility of *E. coli* O157:H7 to free and nano-encapsulated plant phenolic acids as compared to *Salmonella*.[9,153] Other authors have previously theorized that nano-entrapment within

polymeric nanocapsules of plant-derived antimicrobials (including geraniol) enhances their interaction with pathogenic cells through allowing greater suspension of active compound(s) in aqueous medium as well as limiting interactions with medium components that would degrade antimicrobial activity (e.g., partitioning within fat phases in emulsified foods, oxidation, etc.).[154,155]

3.4. Conclusions

A rapid nano-precipitation method for encapsulating the plant-derived terpene geraniol in the polymer Pluronic® F-127 was demonstrated to produce a unimodal population of NPs, with variable particle hydrodynamic size that differed according to PF127: geraniol mixing ratio. Geraniol release against dialysis water followed an exponential release kinetic, with 50% of drug being released within the first 7.25 h of storage at 25 °C. Storage stability of NPs decreased upon exposure and during storage at both decreased and elevated temperatures (4, 37, 50 °C) as well as acidic and alkaline pH conditions (pH 4.0, 10.0). Whereas NPs stored at pH 7.0 did not undergo any significant change in mean particle diameter, samples of NPs stored at pH 4.0 and 10.0 became bimodal during storage, with the development of a sub-population of particles with mean diameter approximating 35-37 nm over 60 days of storage at 25 °C. Geraniol release followed an exponential release kinetic, with 50 % of drug being released within the first 24 h of storage at 25 °C. Nano-encapsulation of geraniol enhanced antimicrobial activity against the enteric pathogens *S.* Typhimurium and *E. coli* O157:H7 by lowering the required amount of EOC necessary for inhibition through improved transport of EOC to pathogen membranes. Further, release profile analysis indicates that reduced temperature storage of EO-loaded NPs during distribution will slow the rates of NP degradation and EO loss. These data were collected so as to characterize the physico-chemical, loading, and antibacterial properties of Pluronic® F-127 NPs containing the

plant EO geraniol prior to the determination of their pathogen decontamination capacity on food surfaces.

4. GROWTH BEHAVIOR OF MICROORGANISMS USING UV-VIS SPECTROSCOPY AFTER NP AND FREE DRUG TREATMENTS

4.1. Overview

Antibacterial properties of prepared nanoparticles and non-encapsulated geraniol were tested on different bacterial species, *S.* Typhimurium, *S. aureus*, *E. coli*, and *L. innocua* at different concentrations, measured by using UV-Vis spectroscopy. Geraniol-loaded NPs and geraniol effectively reduce the concentrations Optical density as a function of time up to 24 h was determined for each type of bacteria. Geraniol NPs showed better efficacy at inhibiting the growth of bacteria than non-encapsulated geraniol.

4.2. Introduction

Bacteria grow by a process known as binary fission. The growth rate of bacteria population depends on the cell type and bacterial growth conditions such as growth media composition and temperature. Bacteria growth curve can be divided into different phases as lag phase, log phase, stationary phase, and death phase.[156] In the lag phase, microorganisms adapt to their environment and get prepared for growth or cell division. Cells start to recover from damages and synthesize enzymes during this stage. During log phase (exponential phase), cells actively divide and grow. During this stage biomass, DNA, RNA, protein, viable count of the population significantly increases.[157] In the stationary stage, the number of dying bacteria cells and growing bacteria cells are in balance. At the final phase (death phase), the number of dying cells are more than the number of growing cells.

UV-Vis spectroscopy is a reliable and rapid instrument that can be used for the quantification of microorganisms.[158] Spectroscopic analysis of a sample can be determined with

the measurement of a big range of wavelengths. UV-Vis spectroscopy provides beneficial information about a sample concentration while it is easy to operate and fast.

Changes in number of bacteria cells can be detected through spectroscopy measurements. Spectral changes during bacterial growth can be used to attain quantitative information on the growth behavior of bacteria cells. UV-Vis spectroscopy is an advantages tool to monitor real-time cell growth monitoring.

This study demonstrates that geraniol-loaded polymeric nanoparticles can be used to control growth rate of pathogenic bacteria at different concentrations after 24 h incubation and act as an antimicrobial agent. UV-Vis spectrophotometry measured the growing bacteria cells absorbance and the inhibition rate of their growth after the treatment with nanoparticles in various concentrations.

4.3. Materials and Methods

Salmonella, *Escherichia coli*, *S. aureus*, and *Listeria* cells was obtained by aseptically scraping a loopful (10 mL) of culture from tryptic soy agar (TSA; Becton, Dickinson and Co., Sparks, MD) slants into 9.0 mL sterile tryptic soy broth (TSB; Becton, Dickinson and Co.). After that, the cultures were incubated at 35 °C for 24 h. A second transfer was completed in identical fashion. Revived bacteria cells will be centrifuged at 4,000 rpm on a bench-top mini-centrifuge for 15 min at ambient condition (25 °C) to produce a bacterial pellet. Following centrifugation, the supernatant was poured off and cell pellets were suspended in one volume of sterile phosphate buffered saline (PBS; Thermo-Fisher Scientific, Waltham, MA, USA). Three identically completed centrifugation and washing procedures will be completed. Geraniol-loaded polymeric nanoparticles were diluted with sterilized deionized water to obtain the concentrations of NPs (0.1, 0.2, 0.4, 0.6, and 0.8%). Non-encapsulated geraniol solutions were prepared to deliver increased

concentrations of geraniol. Geraniol was diluted in sterilized deionized water to produce various concentrations of geraniol (0.0625, 0.125, 0.25, 0.375, and 0.5 %). Then, bacteria cells were added in prepared antimicrobial solutions (NPs or geraniol solutions) and vortexed for few seconds. The cells were homogenously mixed with differing concentrations of geraniol NPs and non-encapsulated geraniol. After that they were added in sterile TSB and placed in an incubator at 35 ˚C. The samples were collected up to 24 h. Duplicate samples were also taken from the incubator at the determined time and then washed with sterilized deionized water prior to UV-Vis spectroscopy measurements. The collected samples were centrifuged at 4,000 rpm on a centrifuge for 15 min to produce a bacterial pellet. The supernatant was slowly drawn off and removed. A small amount of the fluid was left in each centrifuge tube without disturbing the pellet. The remaining pellets were resuspended in sterilized deionized water and then vortexed. The washing process was repeated three times. After the final washing step, the pellet of clean cells was resuspended in sterilized deionized water. Bacterial growth was tracked by using a UV-1800 UV/Visible scanning spectrophotometer, scanning from 200 to 800 nm. UV measurements was performed at ambient temperature at 2, 4, 8, 12, 18, and 24 h.

The number of bacteria cells after the treatment of various concentrations of geraniol-loaded polymeric nanoparticles and non-encapsulated geraniol was enumerated on 3M™ Petrifilm™ Aerobic Count Plate films to verify the number of bacteria cells. Inoculated films were incubated 24 h at 36±1 °C prior to colony counting.

4.4. Results and Discussion

The antibacterial activities of geraniol-loaded nanoparticles were measured at different concentrations of nanoparticles (0.1, 0.2, 0.4, 0.6, and 0.8%). UV-Vis absorbance values which mean that the growth or growth inhibition of bacteria are illustrated in Figs. 18-21. It was observed

that NPs showed effective antibacterial activity against all the targeted bacteria species in our study. The antibacterial action of nanoparticles and non-encapsulated drug was concentration dependent as shown in Figs. 19-22. Figures prove that the geraniol-loaded nanoparticles show better antibacterial activity than non-encapsulated geraniol. Figures show the optical density measured at 260 nm as a function of time for four different bacteria. The number of particles/mL depending on the incubation time for different pathogenic bacteria is shown through Figure 19 and 22. Tables 2-5 show the values for UV-Vis spectroscopy measurements to illustrate the curves especially for not-growing bacteria cells. In this study, peak was observed at 260 nm during scanning from 800 nm to 200 nm wavelength. No other peak was observed at other wavelengths. Different absorbances were observed at 260 nm wavelength depending on the increases at bacterial concentrations. Nucleic acids absorb UV light at 260 nm.[159]Alupoaei et al.[160] also observed a peak at 260 nm for their study since at 260 nm wavelength changes on cell concentrations and nucleotide concentrations were obtained depending on the bacteria growth.

Target bacteria cells were treated with 0, 0.0625 (F1), 0.125 (F2), 0.25 (F3), 0.375 (F4), and 0.5 % (F5) geraniol and 0.1 (N1), 0.2 (N2), 0.4 (N3), 0.6 (N4), and 0.8% (N5) geraniol-loaded NPs. N1 and F1; N2 and F2; N3 and F3; N4 and F4; and N5 and F5 include same amount of geraniol.

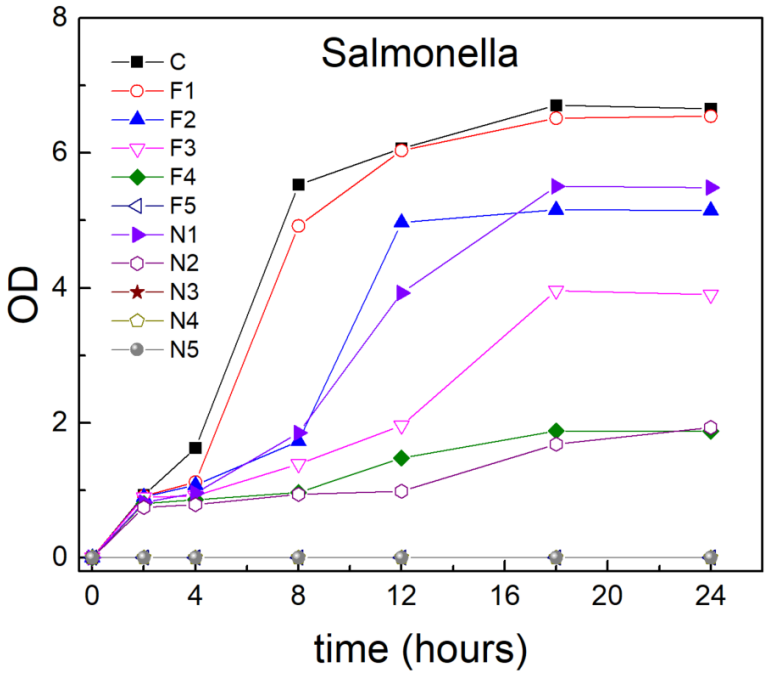

Figure 19: Optical density at 260 nm as a function of time (hr) for *Salmonella* Typhimirium.

Table 2: Optical density measurement values at 260 nm as a function of time (hr) for *Salmonella* Typhimirium.

Salmonella	time (hr)						
	0	2	4	8	12	18	24
Control	0	0.926	1.624	5.53	6.07	6.71	6.66
F1	0	0.912	1.119	4.92	6.04	6.52	6.55
F2	0	0.898	1.075	1.726	4.97	5.16	5.15
F3	0	0.891	0.916	1.388	1.958	3.96	3.9
F4	0	0.802	0.857	0.965	1.476	1.877	1.876
F5	0	0	0	0	0	0	0
N1	0	0.819	0.957	1.849	3.926	5.507	5.49
N2	0	0.744	0.785	0.938	0.984	1.683	1.931
N3	0	0	0	0	0	0	0
N4	0	0	0	0	0	0	0
N5	0	0	0	0	0	0	0

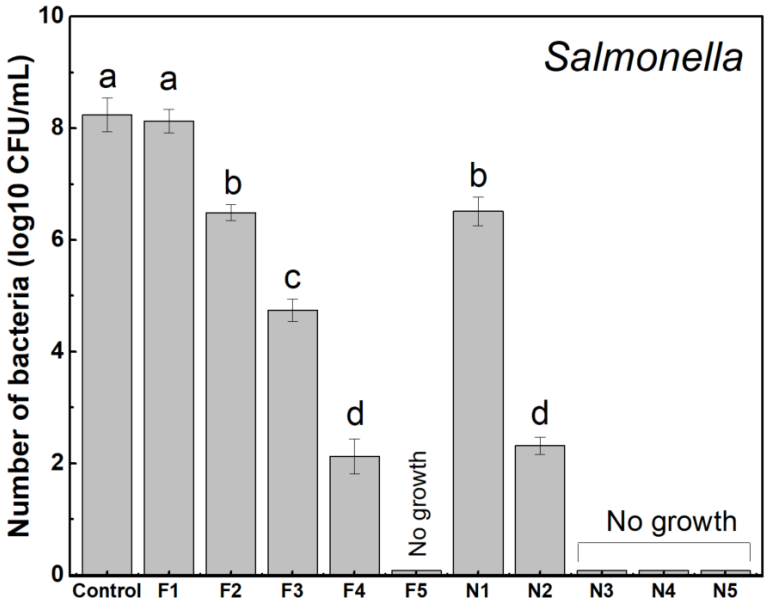

Figure 20: Number of *Salmonella* Typhimirium after the treatment of different concentrations of geraniol-loaded polymeric nanoparticles and non-encapsulated geraniol. Means with the same letter are not significantly different ($p \geq 0.05$).

Optical density at 260 nm as a function of time up to 24 h for ST was shown in Figure 19. Increased concentrations of geraniol NPs and non-encapsulated geraniol either decreased or inhibited the growth of the bacteria cells. Control (without any geraniol) showed the highest growth as expected. F5 (0.5% geraniol) treated *Salmonella* did not show any growth while lower concentrations of non-encapsulated geraniol (0.375, 0.25, 0.125, and 0.0625%) showed growth of ST. N3, N4, and N5-treated bacteria cells didn't show any growth. 0.5% (F5) or more non-encapsulated geraniol should be applied to inhibit the growth while 0.4% geraniol-loaded NPs (N3) (including 0.25% geraniol) or more NPs should be applied to inhibit ST cells. Table 3 shows the number of ST cells after the treatment of NPs and non-encapsulated geraniol. No growth was observed for F5, N3, N4, and N5-treated cells. Higher concentrations of NPs and non-encapsulated

drugs decreased the number of cells. NPs show better efficacy compared to non-encapsulated geraniol depending on both UV-vis spectroscopy measurements and plating results (Fig. 20).

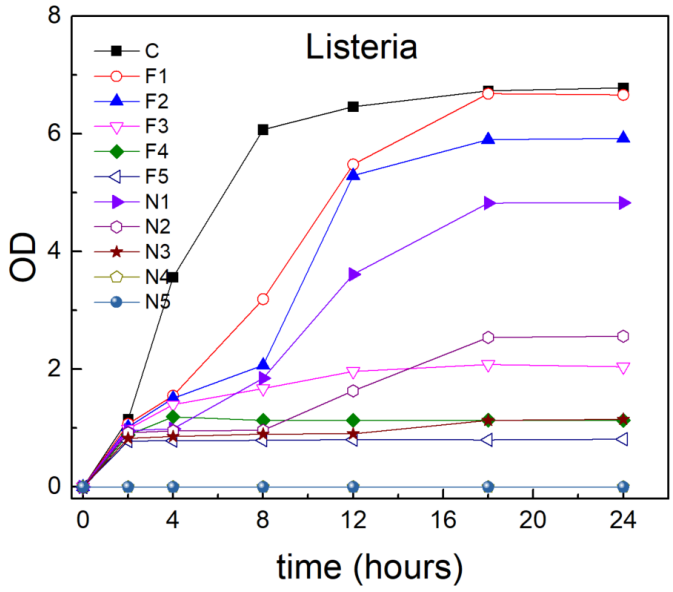

Figure 21: Optical density at 260 nm as a function of time (hr) for *Listeria innocua*.

Optical density at 260 nm as a function of time up to 24 h for *Listeria innocua* was done as shown in Fig 21. Five different concentrations of geraniol applied and none of them was high enough to inhibit the growth of the *Listeria* cells. The lowest two concentrations of geraniol-loaded NPs (N4 and N5) were able to inhibit the growth of the cells. Final bacteria concentration showed a high dependency on drug concentration. Higher concentrations of non-encapsulated or encapsulated geraniol resulted in reduced growth of the bacteria cells. Table 5 shows the number of *L. innocua* cells after the treatment of NPs and non-encapsulated geraniol. No growth was observed for N4 and N5-treated cells for both UV-Vis spectroscopy measurements and plating results. Higher concentrations of NPs and non-encapsulated drugs decreased the number of cells as shown in Table 5. However, even the highest concentration of non-encapsulated geraniol (F5)

was not high enough to stop the growth of *L. innocua* cells. Higher concentrations of geraniol should be applied.

Table 3: Optical density measurement values at 260 nm as a function of time (hr) for *Listeria innocua*.

Listeria	time (hr)						
	0	2	4	8	12	18	24
Control	0	1.147	3.562	6.07	6.46	6.73	6.78
F1	0	1.072	1.551	3.19	5.478	6.68	6.66
F2	0	1.019	1.506	2.068	5.29	5.9	5.92
F3	0	0.985	1.397	1.672	1.962	2.08	2.04
F4	0	0.882	1.191	1.131	1.134	1.135	1.134
F5	0	0.782	0.785	0.792	0.803	0.8	0.81
N1	0	0.958	0.989	1.847	3.611	4.823	4.827
N2	0	0.921	0.953	0.964	1.634	2.54	2.56
N3	0	0.828	0.857	0.899	0.902	1.13	1.15
N4	0	0	0	0	0	0	0
N5	0	0	0	0	0	0	0

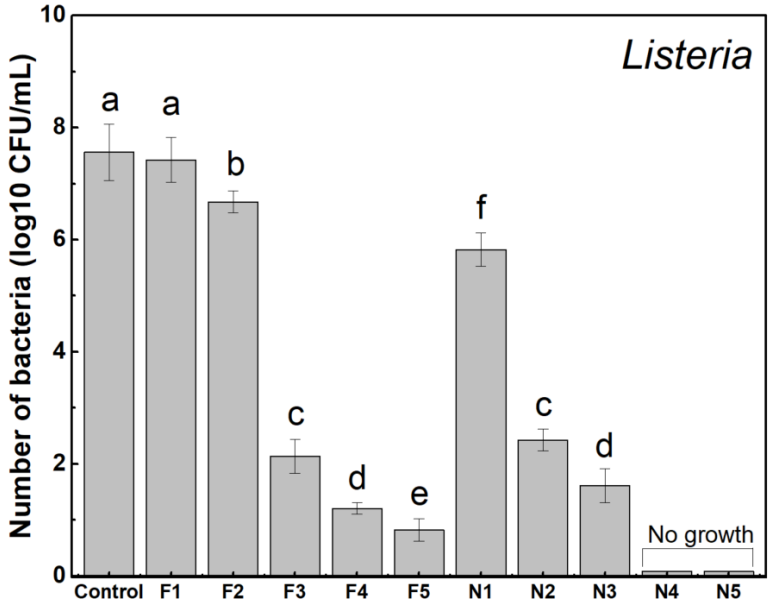

Figure 22: Number of *Listeria innocua* after the treatment of different concentrations of geraniol-loaded polymeric nanoparticles and non-encapsulated geraniol. Means with the same letter are not significantly different ($p \geq 0.05$).

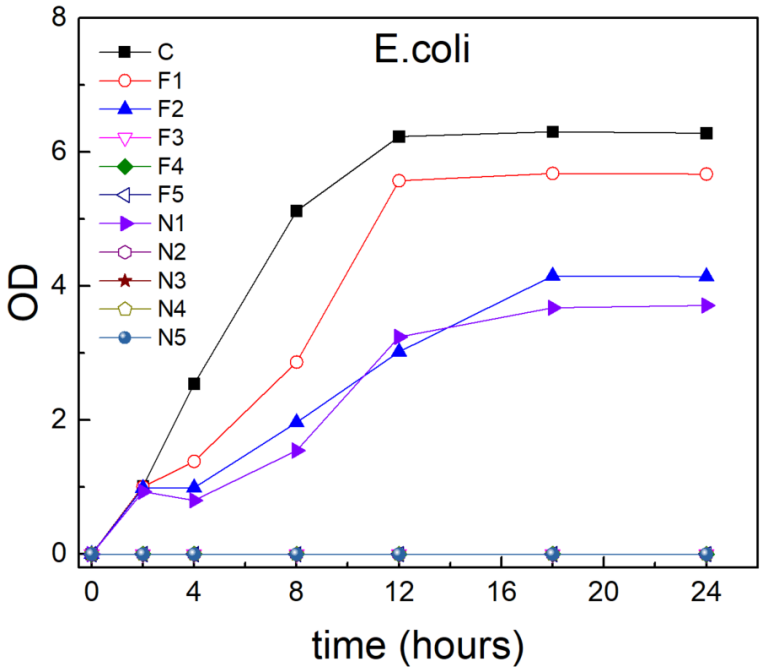

Figure 23: Optical density at 260 nm as a function of time (hr) for *E. coli*.

Figure 23 shows optical density at 260 nm as a function of time up to 24 h for *E. coli*. The bacterial cell inhibition depends on the drug concentration. F3, F4, and F4 concentrations of non-encapsulated geraniol and N2, N3, N4, and N5 concentrations of geraniol-loaded NPs inhibited the growth of the bacteria cells. NPs showed better efficacy at inhibiting the growth of bacteria than non-encapsulated drug. The number of *E. coli* cells after the treatment of NPs and non-encapsulated geraniol as shown at Table 7. No growth was observed for F3, F4, F5, N2, N3, N4 and N5-treated cells for both UV-Vis spectroscopy measurements and plating results. Higher concentrations of NPs and non-encapsulated drugs decreased the number of cells as shown in Table 4. For example, for the same concentration of geraniol-containing F1 and N1-treated *E. coli*, the number of cells were 7.2±0.2 $\log_{10}$ CFU/mL for F1 treatment while the number of cells were

4.3±0.5 $\log_{10}$ CFU/mL for N1 treatment. The efficacy of both geraniol-loaded nanoparticles and non-encapsulated geraniol were higher for *E. coli* than *L. innocua* and ST.

Table 4: Optical density measurement values at 260 nm as a function of time (hr) for *Escherichia coli*.

E. coli	time (hr)						
	0	2	4	8	12	18	24
Control	0	1.011	2.54	5.12	6.23	6.3	6.28
F1	0	1.005	1.385	2.864	5.57	5.68	5.67
F2	0	0.987	0.99	1.965	3.02	4.15	4.14
F3	0	0	0	0	0	0	0
F4	0	0	0	0	0	0	0
F5	0	0	0	0	0	0	0
N1	0	0.932	0.801	1.545	3.24	3.675	3.71
N2	0	0	0	0	0	0	0
N3	0	0	0	0	0	0	0
N4	0	0	0	0	0	0	0
N5	0	0	0	0	0	0	0

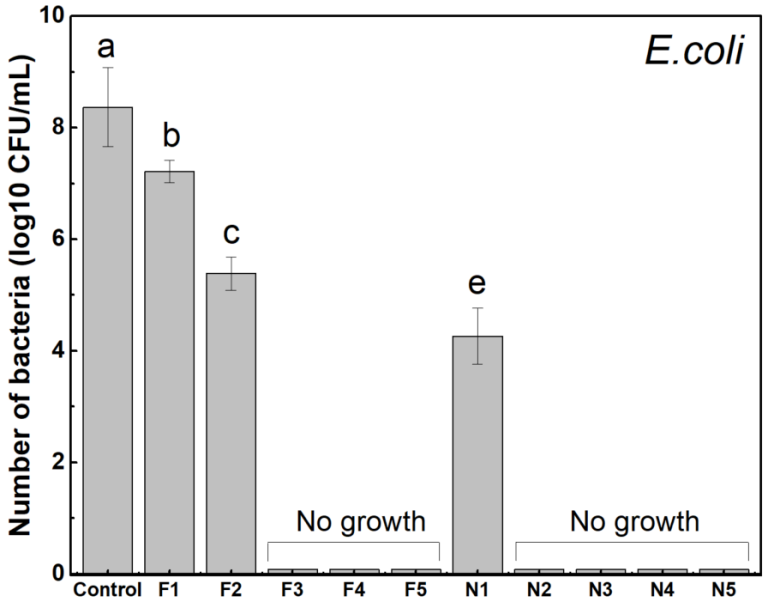

Figure 24: Number of *Escherichia coli* after the treatment of different concentrations of geraniol-loaded polymeric nanoparticles and non-encapsulated geraniol. Means with the same letter are not significantly different ($p \geq 0.05$).

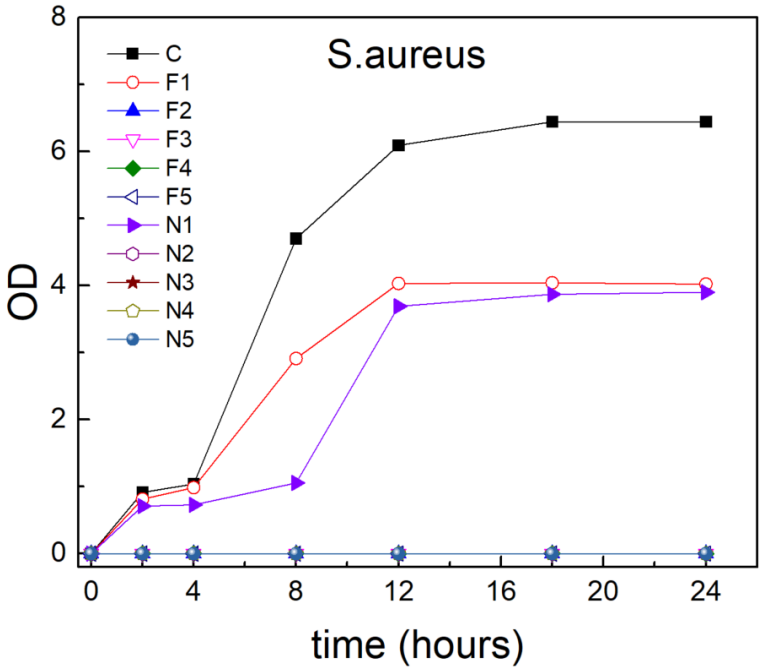

Figure 25: Optical density at 260 nm as a function of time (hr) for *S. aureus*.

Non-encapsulated and NP-treated *S. aureus* growth was also measured at UV/Visible scanning spectrophotometer as a function of time (Fig. 25). Geraniol in both encapsulated and non-encapsulated showed a very high efficacy at the inhibition of *S. aureus*. Only control (0% geraniol-treated), F1, and N1 -treated bacteria cells showed growth while the rest of the treated bacteria cells were inhibited, and no growth were observed. The number of *S. aureus* cells after the treatment of NPs and non-encapsulated geraniol is shown at Table 5. No growth was observed for F2, F3, F4, F5, N2, N3, N4 and N5-treated cells for both UV-Vis spectroscopy measurements and plating results. Only N1 and F1-treated *S. aureus* cells showed growth both at UV-Vis measurements and plating results. The efficacy of both geraniol-loaded nanoparticles and non-encapsulated geraniol were highest for *S. aureus* than *E. coli*, *L. innocua* and ST.

Table 5: Optical density measurement values at 260 nm as a function of time (hr) for *Staphylococcus aureus*.

S. aureus	time (hr)						
	0	2	4	8	12	18	24
Control	0	0.914	1.04	4.7	6.09	6.44	6.44
F1	0	0.813	0.985	2.91	4.03	4.04	4.02
F2	0	0	0	0	0	0	0
F3	0	0	0	0	0	0	0
F4	0	0	0	0	0	0	0
F5	0	0	0	0	0	0	0
N1	0	0.71	0.728	1.055	3.69	3.87	3.9
N2	0	0	0	0	0	0	0
N3	0	0	0	0	0	0	0
N4	0	0	0	0	0	0	0
N5	0	0	0	0	0	0	0

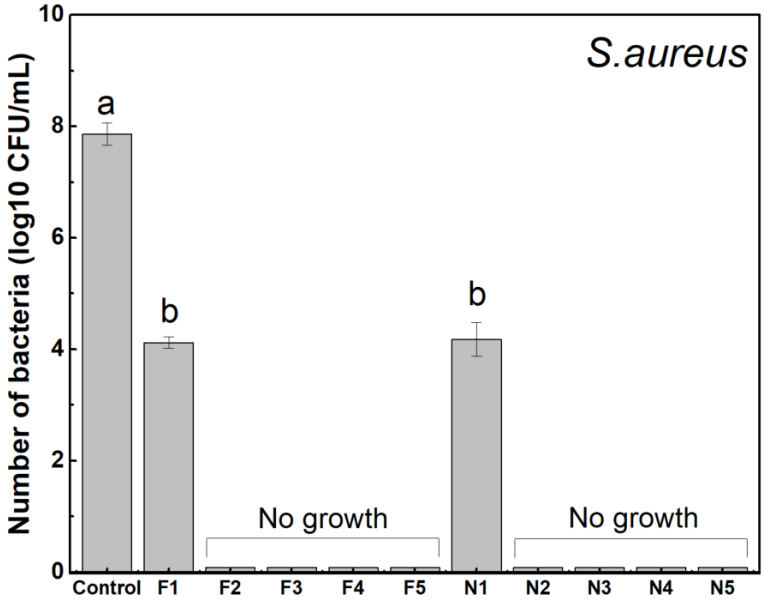

Figure 26: Number of *Staphylococcus aureus* after the treatment of different concentrations of geraniol-loaded polymeric nanoparticles and non-encapsulated geraniol. Means with the same letter are not significantly different ($p \geq 0.05$).

Like our study, Wahab et. al.[161] studied antibacterial activity of nanostructures using UV-Vis spectrophotometry. They synthesized peanut-shaped ZnO nanostructures (ZnO-PNTs) and tested their bacteriostatic properties on *S.* Typhimurium, *E. coli*, *S. aureus*, and *Klebsiella*

pneumoniae at different concentrations. The absorbance of growing bacteria cells and the inhibition rate of these bacteria after ZnO-PNTs addition at various concentrations were measured by UV-vis spectrophotometry. Their study showed that ZnO-PNTs at low concentrations inhibit the growth of the tested bacteria species (decreased their concentration). Depending on their findings, UV-vis spectrophotometry is a very useful tool to investigate the antibacterial activities of nanostructures by measuring the absorbance of growing bacteria and the growth inhibition rates at different concentrations.

Alupoaei and Garcia-Rubio[160] also studied the growth behavior of *E. coli* using UV-Vis spectroscopy. They also measured optical density at 260 nm recorded as a function of time for the bacteria cells. They recorded bacteria growth up to 6 hr, shorter than our recordings. When the bacteria cells incubated longer in an incubator, the higher the optical density was measured at UV-Vis spectroscopy due to the increase in the turbidity.

Zanetti et al.[162] studied bactericidal activity of geraniol in Gram-Positive and Gram-Negative bacteria. Antimicrobial activity of geraniol against various bacteria cells including *Escherichia coli*, *Staphylococcus aureus*, *Salmonella enterica*, and *Listeria monocytogenes*. Agar diffusion test was used to determine the antimicrobial activity of geraniol for the four types of bacteria. Average diameter of the inhibition zone was measured to determine antimicrobial activity, therefore larger the inhibition zone in petri dish means better antimicrobial bactericidal activity. Largest inhibition zone from largest to smallest was obtained in order *Staphylococcus aureus*, *Escherichia coli*, *Salmonella enterica*, and *Listeria monocytogenes*. It means that geraniol showed the most antimicrobial activity against *S. aureus* while geraniol showed the least antimicrobial activity against *L. monocytogenes*. Our UV-Vis spectroscopy results after the treatment with geraniol-loaded nanoparticles or non-encapsulated geraniol showed similar

antimicrobial activity against pathogens like their results. Both geraniol NPS and free geraniol exhibited the most antibacterial activity against *S. aureus* and *E. coli* while they exhibited the least antibacterial activity against *L. innocua*. There is a high correlation between UV-Vis spectrophotometer measurement and plating results. Depending on bacteria growth curves obtained at UV-Vis measurements, number of bacteria cells can be predicted.

4.5. Conclusion

The results in this study shows that UV-Vis spectroscopy measurements at 260 nm wavelength are useful for the determination of the real-time analysis of bacterial populations. If the antimicrobial concentration was high enough to inhibit the bacterial cells, no peak was observed during the measurements. If not, bacteria cells continue to grow until the plateau. Both non-encapsulated geraniol and geraniol-loaded NPs were able to either decrease or inhibit the growth of bacteria cells. Geraniol was least effective on the inhibition of *L. innocua* cells while it was most effective on the inhibition of *S. aureus*. cells. According to this study, inhibitory effect of geraniol-loaded nanoparticles was concentration dependent. The higher concentration of the applied NPs, the higher the antimicrobial activity would be. Geraniol nanoparticles exhibit excellent inhibition of pathogenic bacterial growth at low concentrations especially against three of the four bacteria tested. Geraniol-loaded polymeric nanoparticles should get more interest from the industry due to their superior antimicrobial activity.

5. ALTERATION OF ZETA POTENTIAL AND SIZE CHANGES OF BACTERIA DEPENDING ON TREATMENT WITH GERANIOL-LOADED NP OR NON-ENCAPSULATED GERANIOL

5.1. Overview

The interactions between pathogenic bacteria (*S.* Typhimurium, *E. coli* O157:H7, *L. innocua*, and *S. aureus*) and geraniol-loaded polymeric nanoparticles/non-encapsulated geraniol were investigated to gain new insight into their mechanisms of action against bacteria cells. Pathogenic bacteria cells were treated with increasing concentrations of nanoparticles and free drug. Zeta (ζ) potential of bare bacteria cells were increased depending on the antimicrobial concentration. ζ-potential increased from negative to positive values. NP-treated and non-encapsulated geraniol-treated bacteria cells showed a significant difference on their ζ-potential. ζ-potential values of NP-treated bacteria cells increased sharper towards negative to positive as compared ζ-potential values of geraniol-treated bacteria cells. Upon geraniol NPs treatment, cell structure of bacteria cells was disrupted, and the size of the treated bacteria cells decreased. Size of the bacteria cells were increased after non-encapsulated geraniol treatment. Overall, this study contributes to understanding the mechanisms of geraniol NPs and non-encapsulated geraniol.

5.2. Materials and Methods

5.2.1. Microorganisms and inoculum preparation

*Salmonella enteric*a subsp. *enterica* serovar Typhimurium str. LT2 (ATCC 700720), *Listeria innocua* (NADC 2841), *E. coli* O157:H7 (ATCC No. 700728), and *Staphylococcus aureus* (ATCC 13368) were used for the testing of the antimicrobials (geraniol nanoparticles and non-encapsulated geraniol). The microorganisms were obtained from the Food Microbiology

Laboratory (Department of Animal Science, Texas A&M University) culture collection and revived according to previously published methods[143].

Briefly, the microorganisms were revived from cryo-storage (-80 °C) from the culture collection by aseptically inoculating a loop of culture into 10.0 mL steam sterilized (at 121°C for 15 min) tryptic soy broth (TSB; Becton, Dickinson and Co., Sparks, MD, USA), and incubating statically for 24 h at 35 °C. After that, working cultures were obtained by aseptically scraping a loopful (10 mL) of culture from tryptic soy agar (TSA) slants into 9.0 mL sterile tryptic soy broth (TSB), followed by incubation at 35 ˚C for 24 h. A second passage was completed in identical fashion, with subsequent incubation at 35˚C for 24 h prior to antimicrobial assay completion.

5.2.2. Preparation of geraniol-loaded NPs and non-encapsulated geraniol reagents

Geraniol-loaded NPs and non-encapsulated geraniol were diluted in sterile distilled, deionized water to produce desired concentrations of antimicrobials for experimentation. Geraniol-loaded NPs was diluted to produce the concentrations of NPs (0.1, 0.2, 0.4, 0.6, and 0.8%) upon addition to reaction tubes containing targeted bacterial cells. Geraniol was diluted in sterile deionized water to produce the concentrations of geraniol (0.0625, 0.125, 0.25, 0.375, and 0.5%).

5.2.3. Visualization of geraniol-loaded NPs and non-encapsulated geraniol-treated cells

Microscopic images were obtained by scanning electron microscopy (SEM) using a JSM-7500F electron microscope (JEOL, Tokyo, Japan), in order to visualize any changes in *S.* Typhimurium, *L. innocua*, *E. coli*, and *S. aureus* cells shape and morphology as a function of geraniol-loaded NPs and non-encapsulated geraniol treatments. The samples were coated with 15 nm platinum/palladium (Pt/Pd) to eliminate any positive charging effects. The SEM was operated at an accelerating voltage of 1.0 kV and emission current of 20 μA. SEM images were taken of the

cells after treatment with 0.8% non-encapsulated geraniol and geraniol-loaded NPs. After the treatment cells were thoroughly rinsed in sterile milli-Q water.

5.2.4. Light scattering analysis of bacteria cells treated by geraniol NPs and non-encapsulated geraniol

Revived bacteria cells were centrifuged at 4,000 rpm on a bench-top mini-centrifuge for 15 min at ambient condition (25 °C) to produce a bacterial pellet. Following centrifugation, the supernatant was poured off and cell pellets were suspended in one volume of sterile phosphate buffered saline (PBS; Thermo-Fisher Scientific, Waltham, MA, USA). Three identically completed centrifugation and washing procedures were completed, after which cells were serially diluted in PBS and enumerated on 3M™ Petrifilm™ Aerobic Count Plate films to verify the number of bacteria cells in the reaction tube will be approximately 7.0-8.0 $\log_{10}$ CFU/mL. Inoculated films were incubated 24 hr at 36±1 °C prior to colony counting. Following enumeration of cells, reaction tubes containing bacteria cells were mixed with geraniol-loaded NPs and non-encapsulated geraniol-containing solution prepared to deliver 0.1, 0.2, 0.4, 0.6, and 0.8% antimicrobial upon addition to the culture-containing tube. Immediately thereafter, cells were loaded into a ZS90 Zetasizer Instrument (Malvern Instruments, Ltd., Westborough, MA, USA) for dynamic light scattering (DLS) analysis of cell size. The measurements were carried out at a scattering angle of 90º at 25 ºC.

5.2.5. Surface ζ-potential changes by NPs and non-encapsulated geraniol exposure

Following the initial DLS measurements of bacterial cells, analyses were made to verify the impact of different concentrations of geraniol-loaded NPs (0.0, 0.002, 0.005, 0.006, 0.013, 0.025, 0.05, 0.1, 0.2, 0.4, 0.6, and 0.8%) on outer surface ζ-potential (electrophoretic mobility) of

bacteria cells. Cell surface ζ-potential was measured at ambient temperature using a Zeta-Sizer ZS90 Instrument after the treatment of bacterial cells.

5.3. Results and Discussion

5.3.1. Alteration of ζ-potential in Bacteria Depending on Treatment with Geraniol-Loaded NP or Geraniol (Free Drug)

Zeta potential values of free drug, polymer in milli-q water, and geraniol-loaded nanoparticles are shown in Figure 27. Mean ζ-potential of non-encapsulated geraniol was 9.53 ± 0.20 mV. The polymer zeta potential was electro-negative, with a ζ-potential of −3.76 ± 0.33 mV. Similarly, geraniol-loaded polymeric NPs was also electro-negative, with a ζ-potential of −0.34 ± 0.10 mV.

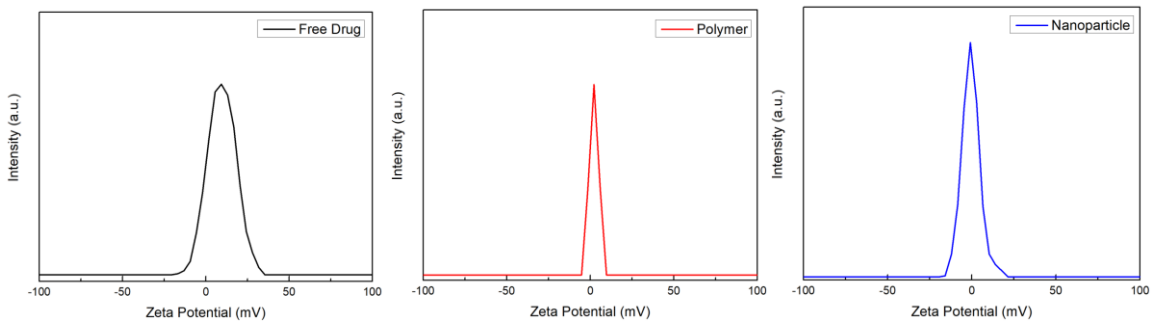

Figure 27: Zeta potential of free drug (geraniol in milli-q water), polymer (PF127) in milli-q water, and geraniol-loaded nanoparticles.

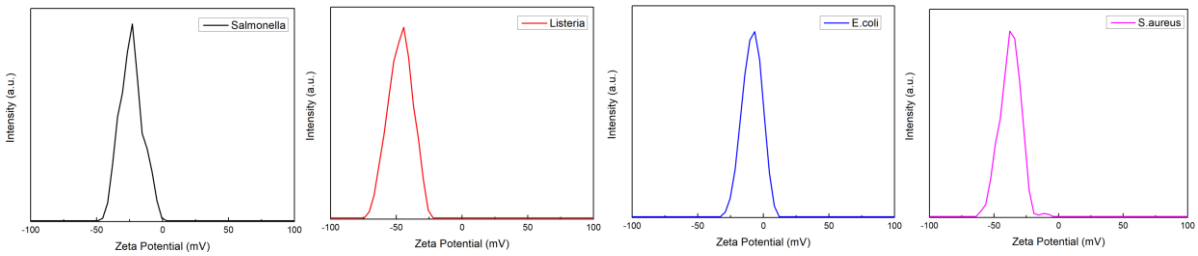

Figure 28: Zeta potential of *Salmonella*, *Listeria innocua*, *E. coli*, and *S. aureus* without any treatment

Mean ζ-potential of *Salmonella* cells without any treatment was electro-negative (–23.60 ± 0.14 mV) in milli-q water (Fig. 28). After the bacterial cells were treated with different concentrations of geraniol-loaded NPs, ζ-potential increased from –23.60 ± 0.14 mV (0% NPs) to -4.08 ± 0.35 mV (0.8% NPs) (Fig. 30). Mean ζ-potential of *Salmonella* cells increased depending on the concentration of geraniol-loaded NPs. ζ-potential values of NP-treated *Salmonella* cells were -18.25 ± 0.78 mV (0.1%), -16.90 ± 0.71 mV (0.2%), -11.85 ± 0.64 mV (0.4%), -5.22 ± 0.07 mV (0.1%), and -4.08 ± 0.35 mV (0.8%). Figure 30 depicts the impact of 0.1 to 0.8% NP addition on the resulting mean ζ-potential of *Salmonella* cells. ζ-potential shift of *Salmonella* cells was shown in Figure 30.

After the *Salmonella* cells were treated with different concentrations of non-encapsulated geraniol, ζ-potential increased from –23.60 ± 0.14 mV (0% geraniol) to -8.1 ± 0.49 mV (0.5% geraniol) (Fig. 29). However, the increase is not as high compared to the same concentrations of NP-treated bacteria cells (Fig. 30). Mean ζ-potential of *Salmonella* cells also increased depending on the concentration of geraniol. ζ-potential values of geraniol-treated cells were -22.6 ± 0.44 mV (0.0625%), -21.1 ± 0.46 mV (0.125%), -14.5.85 ± 0.28 mV (0.25%), -12.2 ± 0.14 mV (0.375%), and -8.1 ± 0.49 mV (0.5%). Table 6 shows the corresponding zeta potential values for Fig. 29 and 30. Depending on our plating results for *Salmonella* Typhimurium (Fig. 20), bacteria growth was not observed for F5, N3, N4, and N5. Zeta potential values and plating results may provide information about the threshold zeta potential for inhibition of bacterial growth. Zeta potential value of -8.1 mV for F5-treated cells, and -11.9 mV for N3-treated bacteria cells can be considered as threshold. For example, when zeta potential value for non-encapsulated *Salmonella* Typhimurium was more positive than -8.1 mV, no growth is expected.

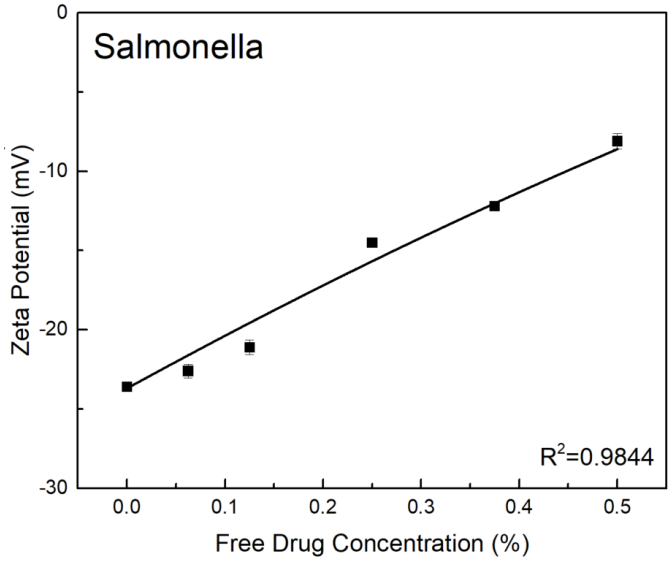

Figure 29: Zeta potential changes of *Salmonella* depending on concentrations of FD.

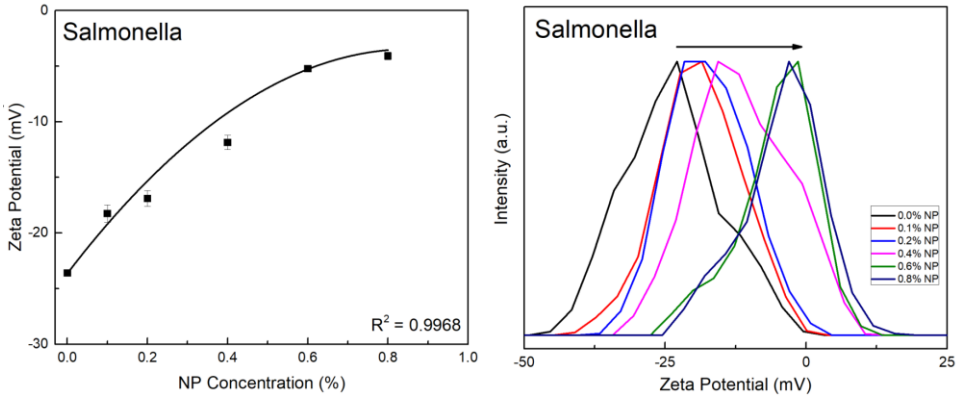

Figure 30: ζ-potential shifts *of Salmonella* depending on geraniol-loaded nanoparticles concentrations.

Table 6: Zeta potential values for *Salmonella* Typhimurium.

FD Concentration		ζ-potential
Notation	%	mV
Control	0	-23.6 ± 0.1
F1	0.0625	-22.6 ± 0.4
F2	0.125	-21.1 ± 0.5
F3	0.25	-14.5 ± 0.3
F4	0.375	-12.2 ± 0.1
F5	0.5	-8.1 ± 0.5

NP Concentration		ζ-potential
Notation	%	mV
Control	0	-23.6 ± 0.1
N1	0.1	-18.3 ± 0.8
N2	0.2	-16.9 ± 0.7
N3	0.4	-11.9 ± 0.6
N4	0.6	-5.2 ± 0.1
N5	0.8	-4.1 ± 0.3

Mean ζ-potential of Listeria cells without any treatment was electro-negative (–47.20 ± 0.53 mV) in milli-q water (Fig. 28). After the bacterial cells were treated with different concentrations of geraniol-loaded NPs, ζ-potential increased from –47.20 ± 0.53 mV (0% NPs) to -4.92 ± 0.43 mV (0.8% NPs) (Fig. 32). Mean ζ-potential of *Listeria* cells increased depending on the concentration of geraniol-loaded NPs. ζ-potential values of NP-treated *Salmonella* cells were -40.7 ± 0.17 mV (0.1%), -31.3 ± 0.27 mV (0.2%), -12 ± 0.60 mV (0.4%), -6.66 ± 0.26 mV (0.1%), and -4.92 ± 0.43 mV (0.8%). Figure 32 depicts the impact of 0.1 to 0.8% NP addition on the resulting mean ζ-potential of listeria cells. ζ-potential shift of listeria cells was shown in Figure 32.

After the *Listeria* cells were treated with different concentrations of non-encapsulated geraniol, ζ-potential increased from –47.20 ± 0.53mV (0% geraniol) to -23.65 ± 0.21 mV (0.5% geraniol) (Fig. 31). However, the increase is not as high compared to the same concentrations of NP-treated bacteria cells (Fig. 32). Mean ζ-potential of *Listeria* cells also increased depending on the concentration of geraniol. ζ-potential values of geraniol-treated cells were -45.95 ± 1.34 mV (0.0625%), -44.55 ± 0.07 mV (0.125%), -42.4 ± 0.42 mV (0.25%), -39.65 ± 0.35 mV (0.375%), and -23.65 ± 0.21 mV (0.5%). The corresponding zeta potential values for *L. innocua* after the treatment of various concentrations of geraniol-loaded NPs and non-encapsulated geraniol is shown in Table 11. Depending on our plating results for *L. innocua* (Fig. 22), bacterial growth was not observed for only N4 and N5. Zeta potential value for N4-treated bacteria cells was -6.7 mV which can be considered as threshold. N5-tretated cells showed less negative zeta potential compared to N4-treated *L. innocua* cells. Zeta potential values less negative than -6.7 mV may indicate corresponding NP concentration enough to inhibit bacterial growth.

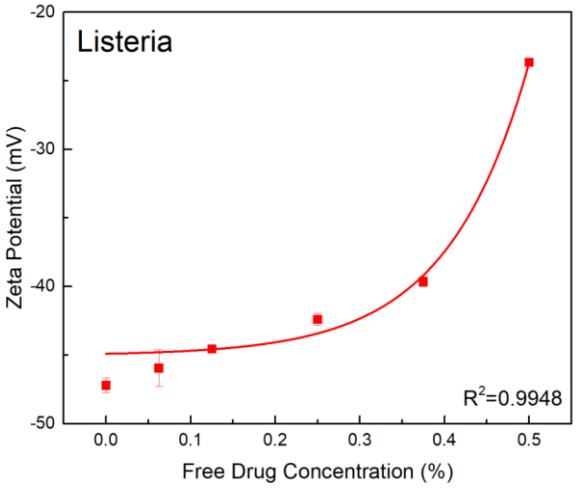

Figure 31: Zeta potential changes of *Listeria* depending on concentrations of FD.

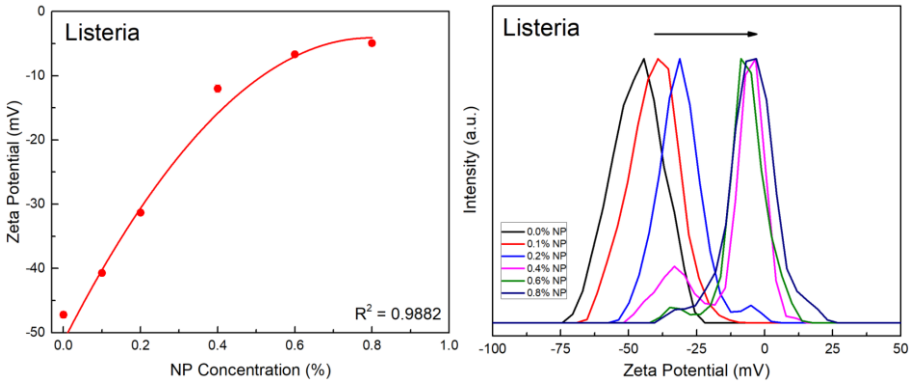

Figure 32: ζ-potential shifts *of Listeria* depending on geraniol-loaded nanoparticles concentrations.

Table 7: Zeta potential values for *Listeria innocua*.

FD Concentration		ζ-potential	NP Concentration		ζ-potential
Notation	%	mV	Notation	%	mV
Control	0	-47.2 ± 0.5	Control	0	-47.2 ± 0.5
F1	0.0625	-46.0 ± 1.3	N1	0.1	-40.7 ± 0.2
F2	0.125	-44.6 ± 0.1	N2	0.2	-31.3 ± 0.3
F3	0.25	-42.4 ± 0.4	N3	0.4	-12.0 ± 0.6
F4	0.375	-39.7 ± 0.4	N4	0.6	-6.7 ± 0.3
F5	0.5	-23.7 ± 0.2	N5	0.8	-4.9 ± 0.4

Mean ζ-potential of *E. coli* cells without any treatment was electro-negative (-8.95 ± 0.52 mV) in milli-q water (Fig. 28). After the bacterial cells were treated with different concentrations of geraniol-loaded NPs, ζ-potential increased from (-8.95 ± 0.52 mV (0% NPs) to -3.48 ± 0.37 mV (0.8% NPs) (Fig. 34). Mean ζ-potential of *E. coli* cells increased depending on the concentration of geraniol-loaded NPs. ζ-potential values of NP-treated *E. coli* cells were -8.93 ± 0.12 mV (0.1%), -7.63 ± 0.49 mV (0.2%), -7.22 ± 0.25 mV (0.4%), -4.45 ± 0.17 mV (0.6%), and -3.48 ± 0.37 mV (0.8%). Figure 34 depicts the impact of 0.1 to 0.8% NP addition on the resulting mean ζ-potential of *E. coli* cells. ζ-potential shift of *E. coli* cells was also shown in Figure 34.

After the *E. coli* cells were treated with different concentrations of non-encapsulated geraniol, ζ-potential increased from -8.95 ± 0.52 mV (0% geraniol) to -4.6 ± 0.26 mV (0.5% geraniol) (Fig. 33). However, the increase is not as high compared to the same concentrations of NP-treated bacteria cells (Fig. 34). Mean ζ-potential of E. coli cells also increased depending on the concentration of geraniol. ζ-potential values of geraniol-treated cells were -8.94 ± 0.40 mV (0.0625%), -8.94 ± 0.30 mV (0.125%), -7.7 ± 0.10 mV (0.25%), -5.97 ± 0.15 mV (0.375%), and -4.6 ± 0.26 mV (0.5%). The corresponding zeta potential values for *E. coli* after the treatment of various concentrations of geraniol-loaded NPs and non-encapsulated geraniol is shown at Table 12. Increase in zeta potential of non-encapsulated geraniol-treated cells was not high as NP-treated cells. Depending on our plating results for *E. coli* (Fig. 25), bacteria growth was not observed for F3, F4, F5, N2, N3, N4 and N5. Zeta potential value for F3-treated bacteria cells was -7.7 mV and N2-treated bacteria cells was -7.6 mV. Zeta potentials for higher concentrations of non-encapsulated geraniol for F4 and F5-treated cells were less negative, and no bacteria growth was observed. Zeta potential values for N3, N4, and N5-treated cells were also less negative, and no

bacteria growth was observed. Therefore, zeta potential values where we did not observe bacteria growth can be considered as threshold values.

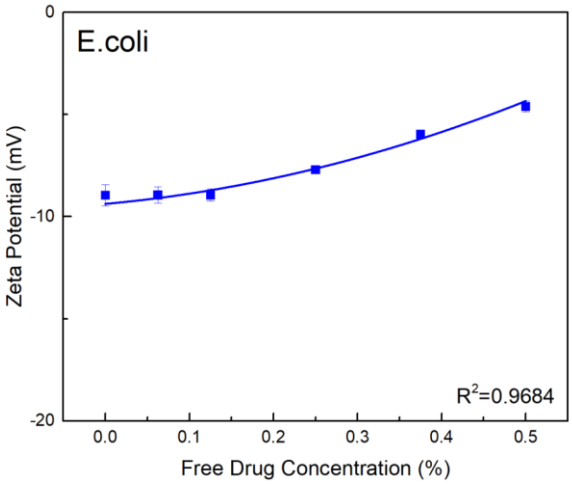

Figure 33: Zeta potential changes of *E. coli* depending on concentrations of FD.

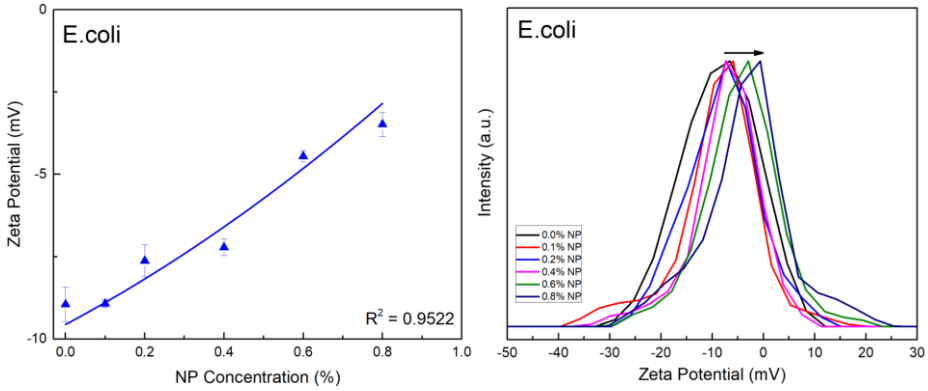

Figure 34: ζ-potential shifts *of E. coli* depending on geraniol-loaded nanoparticles concentrations.

Table 8: Zeta potential values for *Escherichia coli*.

FD Concentration		ζ-potential	NP Concentration		ζ-potential
Notation	%	mV	Notation	%	mV
Control	0	-9.0 ± 0.5	Control	0	-9.0 ± 0.5
F1	0.0625	-8.9 ± 0.4	N1	0.1	-8.9 ± 0.1
F2	0.125	-8.9 ± 0.3	N2	0.2	-7.6 ± 0.5
F3	0.25	-7.7 ± 0.1	N3	0.4	-7.2 ± 0.2
F4	0.375	-6.0 ± 0.2	N4	0.6	-4.5 ± 0.2
F5	0.5	-4.6 ± 0.3	N5	0.8	-3.5 ± 0.4

Mean ζ-potential of *S. aureus* cells without any treatment was electro-negative -37.70 ± 0.49 mV) in milli-q water (Fig. 28). After the bacterial cells were treated with different concentrations of geraniol-loaded NPs, ζ-potential increased from -37.70 ± 0.49 mV (0% NPs) to -6.49 ± 0.26 mV (0.8% NPs) (Fig. 35). Mean ζ-potential of *S. aureus* cells increased depending on the concentration of geraniol-loaded NPs. ζ-potential values of NP-treated *S. aureus* cells were -32.75 ± 0.35 mV (0.1%), -31.3 ± 0.85 mV (0.2%), -15.5 ± 0.14 mV (0.4%), -8.99± 0.15 mV (0.6%), and -6.49 ± 0.26 mV (0.8%). Figure 31 depicts the impact of 0.1 to 0.8% NP addition on the resulting mean ζ-potential of *E. coli* cells. ζ-potential shift of *E. coli* cells was shown in Figure 31.

After the *S. aureus* cells were treated with different concentrations of non-encapsulated geraniol, ζ-potential increased from -37.70 ± 0.49 mV (0% geraniol) to -19 ± 0.86 mV (0.5% geraniol) (Fig. 35). However, the increase is not as high compared to the same concentrations of NP-treated bacteria cells (Fig. 36). Mean ζ-potential of *S. aureus* cells also increased depending on the concentration of geraniol. ζ-potential values of geraniol-treated cells were -33.5 ± 0.10 mV (0.0625%), -32 ± 0.36 mV (0.125%), -25.4 ± 0.15 mV (0.25%), -23.1 ± 0.49 mV (0.375%), and -19 ± 0.86 mV (0.5%). Zeta potential values for *S. aureus* after the treatment of various concentrations of geraniol-loaded NPs and non-encapsulated geraniol were shown (Table 9).

Increase in zeta potential of non-encapsulated geraniol-treated cells was not high as NP-treated cells. The highest concentration of NPs increased the zeta potential of the cells up to -6.5 mV while the highest concentration of non-encapsulated geraniol increased the zeta potential of the cells up to -19.0 mV. Magnitude of the zeta potential changes was higher for NP-treated cells. Plating results were shown at Fig. 26 for *S. aureus*. Table 9 shows number of bacteria for S. aureus after the treatment of NPs and non-encapsulated geraniol. Bacteria growth was not observed for F2, F3, F4, F5, N2, N3, N4 and N5. Geraniol-loaded polymeric nanoparticles and non-encapsulated geraniol showed high antibacterial efficacy on S. aureus. The same concentrations of both F2 and N2 did not allow the growth of the cells. Zeta potential value for F2-treated bacteria cells was -32.0 mV and N2-treated bacteria cells was -31.3 mV. Zeta potentials for higher concentrations of both NP-treated non-encapsulated geraniol-treated cells were less negative, and no bacteria growth was observed.

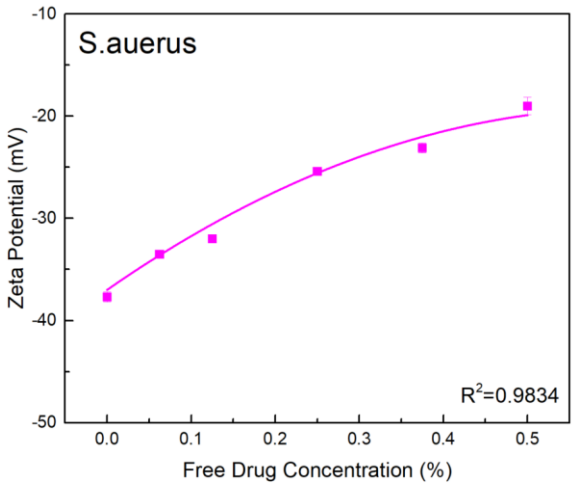

Figure 35: Zeta potential changes of *S. aureus* depending on concentrations of FD.

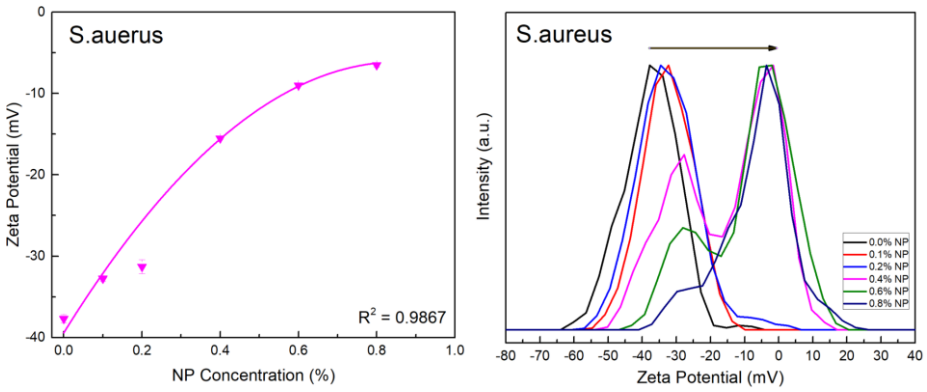

Figure 36: ζ-potential shifts *of S. aureus* depending on geraniol-loaded nanoparticles concentrations.

Table 9: Zeta potential values for *Staphylococus aureus*.

FD Concentration		ζ-potential	NP Concentration		ζ-potential
Notation	%	mV	Notation	%	mV
Control	0	-37.7 ± 0.5	Control	0	-37.7 ± 0.5
F1	0.0625	-33.5 ± 0.1	N1	0.1	-32.8 ± 0.4
F2	0.125	-32.0 ± 0.4	N2	0.2	-31.3 ± 0.8
F3	0.25	-25.4 ± 0.2	N3	0.4	-15.5 ± 0.1
F4	0.375	-23.1 ± 0.5	N4	0.6	-9.0 ± 0.1
F5	0.5	-19.0 ± 0.9	N5	0.8	-6.5 ± 0.3

The ζ-potential values of ST, *E. coli*, *L. innocua*, and *S. aureus* became less negative after treatment with different concentrations of geraniol-loaded NPs and non-encapsulated geraniol. However, NP-treated bacteria cells showed more alteration on their surface charges compared to non-encapsulated geraniol-treated bacteria cells. Lopez-Romero et al.[163] investigated antibacterial effects and mode of action of some of the essential oil components against *E. coli* and *S. aureus*. Changes in surface charge of both types of bacterial cells were observed after exposure to essential oil components. Zeta potential value changes depending on the type of essential oil components were measured for both bacteria. Greater alteration on the surface charges of bacteria cells was observed for the applied essential oil component having significant antibacterial activity against

the bacteria cells tested. Depending on our study, greater alteration on the surface charges of the cells were measured for the NP-treatment having stronger antimicrobial properties than free geraniol-treatment.

The cell surface charges have an importance in the keeping microbial balance and antimicrobial resistance[164]. Bacterial cells have a negative surface charge due to the anionic groups such as phosphate and carboxyl in their membranes[165]. Surface charge values of bacteria cells depends on species of bacteria, pH, ionic strength, and age of the culture[165]. In our study, ζ-potentials of ST, *E. coli*, *L. innocua*, and *S. aureus* increased after exposured to geraniol-loaded polymeric nanoparticles and non-encapsulated geraniol (ζ-potential shifted towards positive charges and less negative charge values). Alteration of zeta potential beyond a critical point can be correlated to the bacteria cell death for both Gram-positive and Gram-negative bacteria depending on our results.

5.3.2. Alteration of Size in Bacteria Depending on Treatment with Geraniol-Loaded NP or Geraniol

Size changes on various types of pathogenic bacteria were investigated depending on the treatment with geraniol-loaded nanoparticles and non-encapsulated geraniol. Figure 37, 38, 39, and 40 show the impact of 0.1 to 0.8% geraniol-loaded NP addition and 0.0625 to 0.5% geraniol addition on the resulting size of *S.* Typhimurium, *L. innocua*, *E. coli*, and *S. aureus* cells.

Figure 37 depicts the impacts of various concentration of nanoparticles and free drug addition on the resulting sizes of *S.* Typhimurium cells. The mean hydrodynamic radius of untreated (control) ST cells was 1.53 ± 0.06 μm in diameter. The addition non-encapsulated geraniol (free drug) broadened the size distribution of ST cells, producing a mean size of 2.03 ± 0.2 μm for 0.5 % geraniol. Geraniol caused the aggregation of the cells and produced broadened

size distribution. Addition of 0.8 % geraniol-loaded nanoparticles (including 0.5 % geraniol) decreased the size distribution of *Salmonella* cells to a mean size of 0.67 ± 0.02 µm. Linear decrease on the cell size were observed for nanoparticle-treated cells. The higher the nanoparticle concentration lower the size of ST cells. However, the size of bacteria cells increases as the concentration of non-encapsulated geraniol increased.

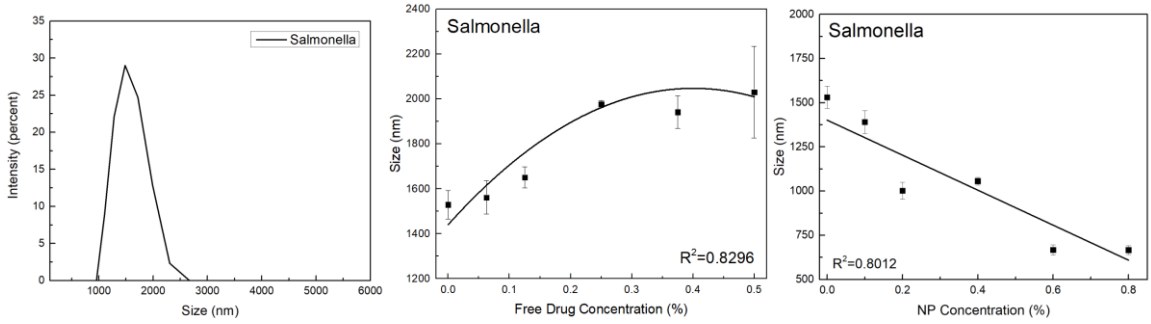

Figure 37: Size of *Salmonella* Typhimurium without any treatment, hydrodynamic size (intensity averaged) of ST as a function of concentration of concentration of geraniol and geraniol-loaded nanoparticles.

Various concentrations of geraniol NPs and free drug treatments on the sizes of *L. innocua* cells were shown in Figure 38. The mean size of control *Listeria* cells was 0.96 ± 0.01 µm in diameter. The addition free drug sharply increased the size distribution of *Listeria* cells. The mean size was 2.05 ± 0.08 µm for 0.5 % geraniol-treated bacteria. However, mean size showed slight decrease for nanoparticle-treated cells. The mean size of the cells was 0.94 ± 0.1 µm after the treatment with the highest concentration of geraniol-loaded nanoparticles. Size of the *Listeria* cells did not decrease as significantly as other pathogenic cells after the treatment with geraniol-loaded polymeric nanoparticles.

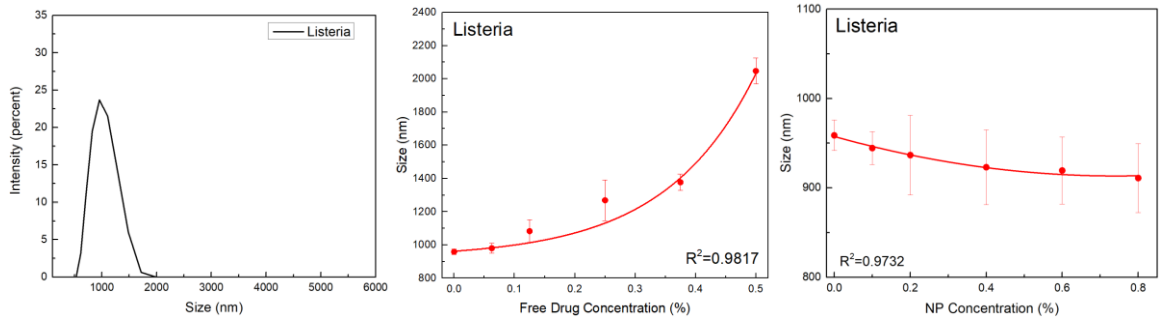

Figure 38: Size of *Listeria innocua* without any treatment, hydrodynamic size (intensity averaged) of *L. innocua* as a function of concentration of concentration of geraniol and geraniol-loaded nanoparticles.

Figure 39 shows the impact of nanoparticle and free drug addition on the resulting sizes of *E. coli* cells. Control *E. coli* cells have a mean size of 1.7 ± 0.04 µm in diameter. Addition of free drug increased the size up to 2.2 ± 0.07 µm. Size of the cells after the treatment of geraniol-loaded nanoparticles (0.8 %) decreased to 0.72 ± 0.03 µm. Size of the *E. coli* cells decreased sharply for 0.1 and 0.2 % NP-treated bacteria, then the size reached to plateau and did not show a significant change up to the highest NP concentration (0.8%).

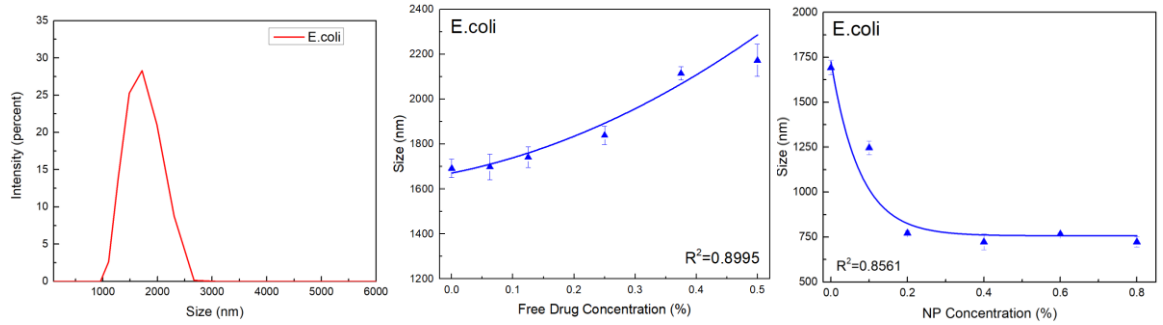

Figure 39: Size of *E. coli* without any treatment, hydrodynamic size (intensity averaged) of *E. coli* as a function of concentration of concentration of geraniol and geraniol-loaded nanoparticles.

Addition of free drug and nanoparticle on the changes of size of *S. aureus* was investigated (Figure 40). Size of the untreated (control) cells were 1.7 ± 0.05 µm in diameter. Similar to the other bacteria tested in this study, *S. aureus* cells also showed similar trend after the treatments. Size of the bacteria cells were decreased for NP-treated bacteria while size increased for non-encapsulated drug treated bacteria. Mean size significantly increased to 2.21 ± 0.06 µm. Size of the *S. aureus* cells decreased to 1.06 ± 0.05 µm for 0.6 % geraniol-loaded nanoparticle-treated bacteria and reached to plateau.

Based on our results, it can be suggested that treatment with non-encapsulated geraniol led to the increase on the mean size of both Gram-positive and Gram-negative bacteria cells while treatment with geraniol-loaded polymeric nanoparticles led to decrease on the mean size of both Gram-positive and Gram-negative bacteria cells. Nanoencapsulation of the drug improved homogenous distribution of the antimicrobial drug and made it much easier to reach out to the pathogenic bacteria cells. Antimicrobial drug was absorbed by cell membrane and taken internal comportments of the cell. After that, the drug caused the breaking of the cells. However, when the bacteria cells were treated with non-encapsulated drug, the drug caused the aggregation of the cells and increased the mean size due to the electrostatic attraction between the drug and the cells.

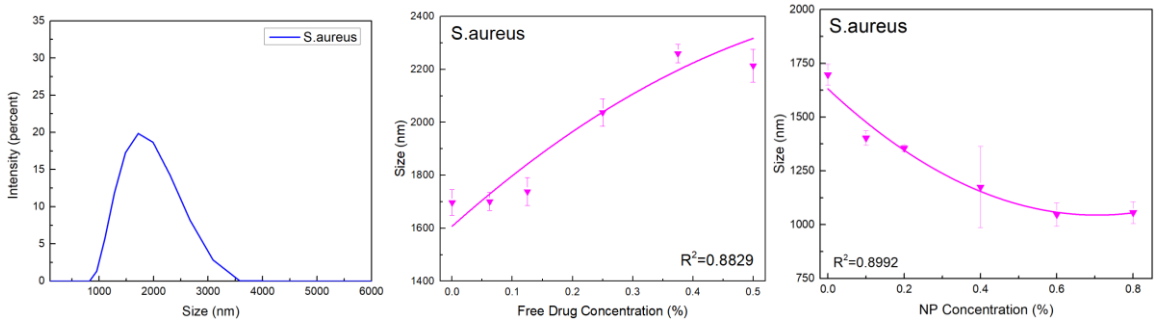

Figure 40: Size of *S. aureus* without any treatment, hydrodynamic size (intensity averaged) of *S. aureus* as a function of concentration of concentration of geraniol and geraniol-loaded nanoparticles.

5.3.3. Effect of Geraniol-loaded Polymeric Nanoparticles and Non-Encapsulated Geraniol on Morphological Change of Bacteria Cells

Bacteria cells without any treatment were set as bare or untreated bacteria. Morphological changes of both untreated and treated bacteria cells were visualized by SEM. The SEM images are shown in Figure 41. Bare ST, *E. coli*, *L. innocua*, and *S. aureus*, as shown in Figure 41A, D, G, and J showed the shape and intact surface of bacteria cells. In contrast, most of the FD and NP treated bacteria cells became irregular and showed differences as compared to bare bacteria. Figure 41B, E, H, and K show the bacteria cells after treatment with non-encapsulated geraniol. Bacteria cells did not show regular and smooth surface, bacterial cell aggregation was observed. Morphological changes of bacteria cells were due to the effect of geraniol, which caused the destruction of the cell membranes of tested bacteria and they lost their intracellular materials. When exposed to geraniol-loaded polymeric nanoparticles (NP), the cell membranes lost their regular and smooth surfaces and have a smaller size, as shown in Figure 41C, F, I, and L. SEM images show that geraniol-loaded NPs aggregates around the bacteria cells, and result in an alteration of the bacteria surfaces.

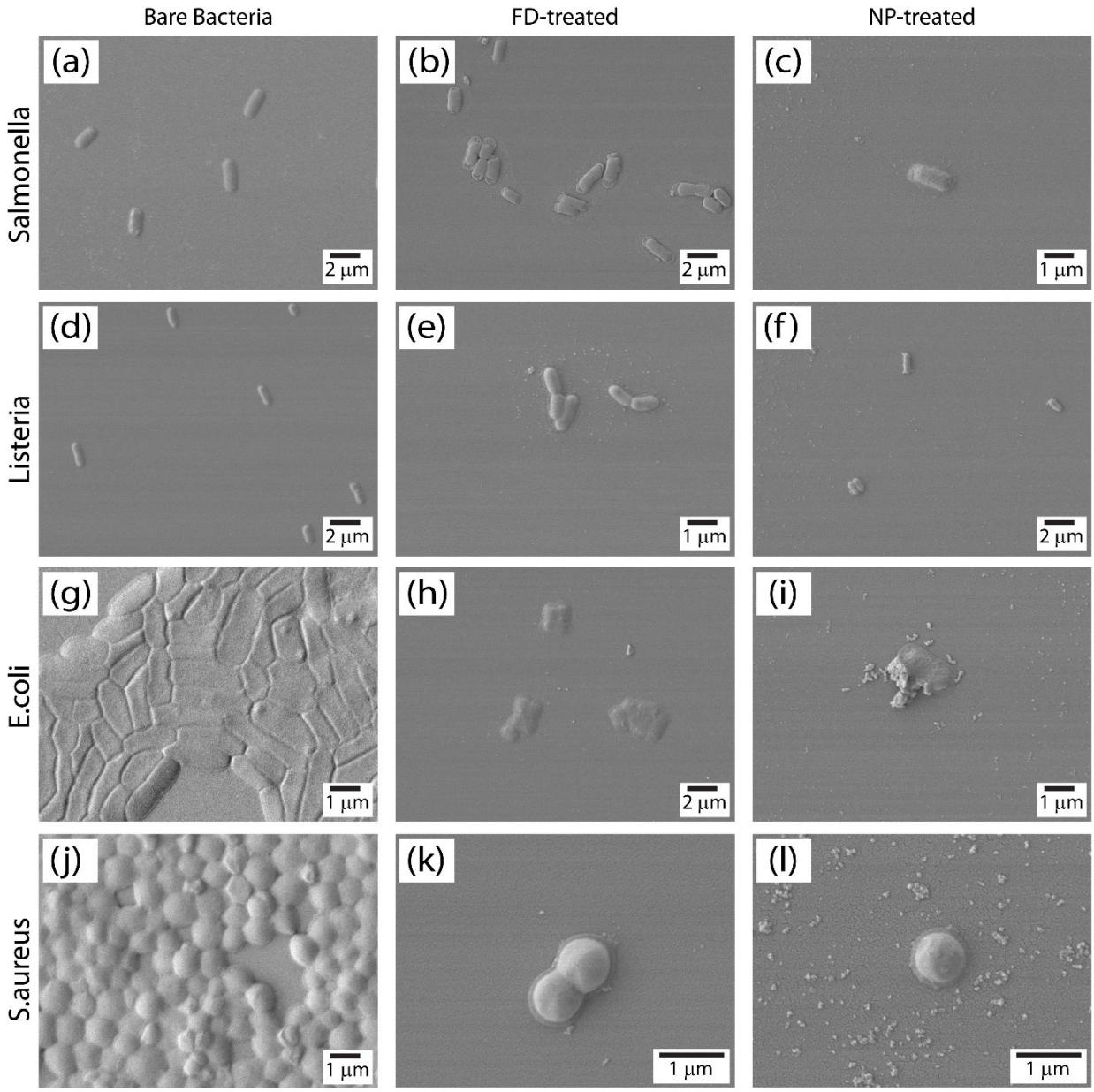

Figure 41: Effects of NPs and free drug treatments on morphological changes of pathogenic bacteria. a) untreated ST; b) ST treated with FD; c) ST treated with NP; d) untreated *L. innocua*; e) *L. innocua* treated with FD; f) *L. innocua* treated with NP; g) untreated *E. coli*; h) *E. coli* treated with FD; i) *E. coli* treated with NP; j) untreated *S. aureus*; k) *S. aureus* treated with FD; and l) *S. aureus* treated with NP.

5.4. Conclusions

In this study, the interactions between bacteria (*Salmonella* Typhimurium, *Escherichia coli* O157:H7, *Listeria innocua*, and *Staphylococcus aureus*) and geraniol-loaded polymeric nanoparticles/non-encapsulated geraniol were investigated to understand surface charge and size changes depending on the concentration of antimicrobial and type of bacteria. All four bacteria showed similar size changes depending on the type of antimicrobial treatment and concentration. In general, increased concentrations of non-encapsulated geraniol increased the mean size while increased concentrations of geraniol nanoparticles decreased the mean size. The addition of geraniol broadened the size distribution of the cells. Geraniol was not homogenously distributed in an aqueous environment since it is a hydrophobic drug. Therefore, geraniol was aggregated right after the mixing. The drug also has more positive charges compared to the bacteria cells and pulls the cells together. This would indicate that non-encapsulated geraniol antimicrobial resulted in aggregation of bacteria cells. Nano-entrapment within nanocapsules of geraniol antimicrobial improved its interaction with pathogenic bacteria cells through allowing better suspension of antimicrobial active compounds in liquid environment. When pathogenic bacteria cells were treated with geraniol-loaded polymeric, geraniol was taken up into internal compartments of the cells resulting breaking of the cells.

6. CONCLUSIONS

This research explored the inactivation of bacterial food pathogens with essential oil encapsulated nanoparticles and non-encapsulated geraniol. The following conclusions were reached:

1. Various sizes of geraniol nanoparticles can be synthesized by changing PF127: geraniol mixing ratio.
2. Nanoparticles stored at room temperature (25°C) and pH 7.0 showed stability.
3. Stability of NPs decreased at 4, 37, 50 °C temperatures and acidic (pH 4.0) and alkaline (pH 10.0).
4. Nanoencapsulation of geraniol showed better antimicrobial activity against both *S.* Typhimurium, *E. coli* O157:H7, *L. innocua*, and *S. aureus* compared to non-encapsulated geraniol.
5. Nanoencapsulation enhanced the transport of essential oil component to bacterial food pathogens membranes.
6. Increased concentration of geraniol-loaded polymeric nanoparticles and non-encapsulated geraniol antimicrobials resulted in increased inhibition of bacteria cells.
7. Both non-encapsulated and encapsulated geraniol damaged to cell shape and membrane integrity.
8. Zeta (ζ) potential of bare bacteria cells were increased depending on the antimicrobial concentration. ζ-potential increased from negative to positive values. NP-treated and non-encapsulated geraniol-treated bacteria cells showed a significant difference on their ζ-potential. ζ-potential values of NP-treated bacteria cells increased sharply towards negative to positive as compared ζ-potential values of geraniol-treated bacteria cells.

9. Treatment with increased concentrations of non-encapsulated geraniol increased the mean size while increased concentrations of geraniol nanoparticles decreased the mean size.
10. The addition of non-encapsulated geraniol broadened the size distribution of the cells.
11. Nano-entrapment within nanocapsules of geraniol antimicrobial improved its interaction with pathogenic bacteria cells through allowing better suspension of antimicrobial active compounds in liquid environment.

7. RECOMMENDATIONS FOR FURTHER STUDY

Recommendations for future research on mechanistic investigation of inactivating bacterial food pathogens with nanoparticles and change moieties to improve food safety:

1. Synthesize nanoparticles with other essential oils together with geraniol to create more effective antimicrobial nanoparticles with high level of bacterial pathogen inhibition.
2. Compare MIC values or bacteria inhibition at UV-Vis spectroscopy for different sizes of geraniol nanoparticles.
3. Compare antimicrobial release rates at different temperatures, pH, and release environments that reflect various storage conditions.
4. Incorporate geraniol-loaded nanoparticles in a superhydrophobic coating material to prevent bacterial attachment and growth.

REFERENCES

1. Scallan, E., Griffin, P. M., Angulo, F. J., Tauxe, R. V. & Hoekstra, R. Foodborne illness acquired in the United States-unspecified agents. *Emerg. Infect. Dis. Infect. Dis.* **17**, 16–22 (2011).
2. Scallan, E. *et al.* Foodborne Illness Acquired in the United States — Major Pathogens. *Emerg. Infect. Dis.* **17**, 7–15 (2011).
3. Scharff, R. L. Economic burden from health losses due to foodborne illness in the United States. *J. Food Prot.* **75**, 123–131 (2012).
4. Painter, J. A. *et al.* Attribution of foodborne illnesses, hospitalizations, and deaths to food commodities by using outbreak data, United States, 1998-2008. *Emerg. Infect. Dis.* **19**, 407–415 (2013).
5. Brul, S. & Coote, P. Preservative agents in foods. Mode of action and microbial resistance mechanisms. *Int. J. Food Microbiol.* **50**, 1–17 (1999).
6. Nychas, G. E., Skandamis, P. N. & Tassou, C. C. Antimicrobials from herbs and spices. in *Microbial Implication for Safe and Qualitative Food Products* 177–200 (2003). doi:10.1533/9781855737037.176.
7. Sofos, J., Beuchat, L. R., Davidson, P. M. & Johnson, E. A. *Naturally occurring antimicrobials in food*. (1998).
8. Davidson, P. M. & Naidu, A. S. Phyto-Phenols. in *Natural Food Antimicrobial Systems* 265–294 (2000).
9. Gutierrez, J., Barry-Ryan, C. & Bourke, P. The antimicrobial efficacy of plant essential oil combinations and interactions with food ingredients. *Int. J. Food Microbiol.* **124**, 91–97 (2008).

10. Smith-Palmer, A., Stewart, J. & Fyfe, L. Antimicrobial properties of plant essential oils and essences against five important food-borne pathogens. *Lett. Appl. Microbiol.* **26**, 118–122 (1998).

11. Locher, C. P., Burch, M. T., Mower, H. F., Berestecky, J. & Davis, H. Anti-microbial activity and anticomplement activity of extracts obtained from selected Hawaiian medicinal plants. *J. Ethnopharmacol.* **49**, 23–32 (1995).

12. Kramer, P. R., Hindorf, H., Jha, C. H., Kallage, J. & Zilliken, F. Antifungal activity of soybean and chickpea isoflavones and their reduced derivatives. *Phytochemistry* **23**, 2203–2205 (1984).

13. Hassan, S. M., Byrd, J. A., Cartwright, A. L. & Bailey, C. A. Hemolytic and antimicrobial activities differ among saponin-rich extracts from guar, quillaja, yucca, and soybean. *Appl. Biochem. Biotechnol.* **162**, 1008–1017 (2010).

14. Jadhav, S. J., Sharma, R. P. & Salunkhe, D. K. Naturally occurring toxic alkaloids in foods. *Crit. Rev. Toxicol.* **9**, 21–104 (1981).

15. Cicio, B. *et al.* Antimicrobial Activity and Chemical Composition of Some Essential Oils. **25**, 860–864 (2002).

16. Singh, D., Kumar, T. R. S., Gupta, V. K. & Chaturvedi, P. Antimicrobial activity of some promising plant oils , molecules and formulations. **50**, 714–717 (2012).

17. Si, W., Gong, J., Tsao, R., Zhou, T. & Yu, H. Antimicrobial activity of essential oils and structurally related synthetic food additives towards selected pathogenic and beneficial gut bacteria. *J. Appl. Mibrobiology* **100**, 296–305 (2005).

18. Inouye, S., Takizawa, T. & Yamaguchi, H. Antibacterial activity of essential oils and their major constituents against respiratory tract pathogens by gaseous contact. *J. Antimicrob. Chemother.* **47**, 565–573 (2001).

19. Pattnaik, S., Subramanyam, V. R., Bapji, M. & Kole, C. R. Antibacterial and antifungal activity of aromatic constituents of essential oils. *Microbios.* **89**, 39–46 (1997).

20. Kim, J., Marshall, M. R. & Wei, C. I. Antibacterial activity of some essential oil components against five foodborne pathogens. *J. Agric. Food Chem.* **43**, 2839–2845 (1995).

21. Friedman, M., Henika, P. R., Levin, C. E. & Mandrell, R. E. Antibacterial activities of plant essential oils and their components against Escherichia coli O157:H7 and Salmonella enterica in apple juice. *J. Agric. Food Chem.* **52**, 6042–6048 (2004).

22. Knight, K. P. & McKellar, R. C. Influence of cinnamon and clove essential oils on the D- and z-values of Escherichia coli O157:H7 in apple cider. *J. Food Prot.* **70**, 2089–2094 (2007).

23. Burt, S. Essential oils: their antibacterial properties and potential applications in foods-a review. *Int. J. Food Microbiol* **94**, 223–253 (2004).

24. Knobloch, K., Weis, N. & Weigand, H. Mechanism of antimicrobial activity of essential oils. *Planta Med.* **1**, 556–556 (1986).

25. Faleiro, M. L. The mode of antibacterial action of essential oils. *Sci. against Microb. Pathog. Commun. Curr. Res. Technol. Adv. A. Méndez-Vilas* **177**, 1143–1156 (2011).

26. Greathead, H. Plants and plant extracts for improving animal productivity. *Proc. Nutr. Soc.* **62**, 279–290 (2003).

27. Hart, K. J., Yanez-Ruiz, D. R., Duval, S. M., McEwan, N. R. & Newbold, C. J. Plant extracts to manipulate rumen fermentation. *Anim. Feed Sci. Technol.* **147**, 8–35 (2008).

28. Kim, B. H. & Gadd, G. M. *Bacterial Physiology and Metabolism*. (Cambridge University Press, 2008).

29. Sikkema, J., De Bont, J. A. & Poolman, B. Mechanisms of membrane toxicity of hydrocarbons. *Microbiol. Rev.* **59**, 201–222 (1995).

30. Parveen, S. M. S., Misra, R. M. S. & Sahoo, S. K. P. Nanoparticles: a boon to drug delivery, therapeutics, diagnostics and imaging. *Nanomedicine Nanotechnology, Biol. Med.* **8**, 147–166 (2012).

31. Danhier, F., Feron, O. & Préat, V. To exploit the tumor microenvironment: passive and active tumor targeting of nanocarriers for anticancer drug delivery. *J. Control. Release* **148**, 135–146 (2010).

32. Van Eerdenbrugh, B. *et al.* Solubility increases associated with crystalline drug nanoparticles: methodologies and significance. *Mol. Pharm.* **7**, 1858–1870 (2010).

33. Wang, X.-Q. & Zhang, Q. pH-sensitive polymeric nanoparticles to improve oral bioavailability of peptide/protein drugs and poorly water-soluble drugs. European Journal of. *Pharm. Biopharm.* **82**, 219–229 (2012).

34. Monsky, W. L. *et al.* Augmentation of transvascular transport of macromolecules and nanoparticles in tumors using vascular endothelial growth factor. *Cancer Res.* **59**, 4129–4135 (1999).

35. Weiss, J., Gaysinksy, S., Davidson, M. & McClements, J. *Nanostructured encapsulation systems: food antimicrobials, IUFoST world congress book: Global issues in food science and technology*. (Elsevier Inc., 2009).

36. McClements, D. J. *Food emulsions: Principles, practices and techniques*. (CRC Press, Inc., 1999).

37. Robach, M. C. Use of preseratives to control microorganisms in food. *Food Technol.* **34**, 81–84 (1980).

38. Hammer, K. A. & Carson, C. F. *Antibacterial and Antifungal Activities of Essential Oils: Lipids and Essential Oils as Antimicrobial Agents*. (Wiley Online Library, 2011).

39. Kalemba, D., and Kunicka, A. Antibacterial and Antifungal Properties of Essential Oils. *Curr. Med. Chem.* **10**, 813–829 (2003).

40. Kuan, C., Yee-Fung, W., Yuen, K. & Liong, M. Nanotech: propensity in foods and bioactives. *Crit. Rev. Food Sci. Nutr.* **52**, 55–71 (2012).

41. Acevedo-Fani, A., Salvia-Trujillo, L., Rojas-Graü, M. A. & Martín-Belloso, O. Edible films from essential-oil-loaded nanoemulsions: physicochemical characterization and antimicrobial properties. *Food Hydrocoll* **47**, 168–177 (2015).

42. Hamad, A. F., Han, J. H., Kim, B. C. & Rather, I. A. The intertwine of nanotechnology with the food industry. *Saudi J. Biol. Sci.* **25**, 27–30 (2018).

43. Jain, K. K. Nanodiagnostics: application of nanotechnology in medical diagnostics. *Inf. Heal. Care* **3**, 153–161 (2003).

44. Davidson, P. M., Critzer, F. J. & Taylor, T. M. Naturally occurring antimicrobials for minimally processed foods. Annu. Rev. *Food Sci. Technol.* 163–190 (2013).

45. Hill, L. E., Gomes, C. & Taylor, T. M. Characterization of beta-cyclodextrin inclusion complexes containing essential oils, trans-cinnamaldehyde, eugenol, cinnamon bark extract, and clove bud extracts for antimicrobial delivery applications. *LWT-Food Sci. Technol.* **51**, 86–93 (2013).

46. Sanguansri, P. & Augustin, M. A. Nanoscale materials development – a food industry perspective. *Trends Food Sci. Technol.* **17**, 547–556 (2006).

47. Gaysinsky, S., Davidson, P. M., Bruce, B. D. & Weiss, J. Stability and antimicrobial efficiency of eugenol encapsulated in surfactant micelles as affected by temperature and pH. *J. Food Prot.* **68**, 1359–1366 (2005).

48. Gaysinsky, S., Davidson, P. M., Bruce, B. D. & Weiss, J., 2005a. Growth inhibition of Escherichia coli O157:H7 and Listeria monocytogenes by carvacrol and eugenol encapsulated in surfactant micelles. *J. Food Prot.* **68**, 2559–2566 (2005).

49. Gomes, C. *et al.* E-Beam Irradiation of Bagged, Ready-to-Eat Spinach Leaves (Spinacea oleracea): An Engineering Approach. *J. Food Sci.* **73**, E95–E102 (2008).

50. Gomes, C., Moreira, R. G. & Castell-Perez, E. Microencapsulated antimicrobial compounds as a means to enhance electron beam irradiation treatment for inactivation of pathogens on fresh spinach leaves. *J. Food Sci.* E479–E488 (2011).

51. Bodratti, A. M. & Alexandridis, P. Formulation of poloxamers for drug delivery. *J. Funct. Biomater.* **9**, (2018).

52. Zhang, W. *et al.* Synthesis and characterization of thermally responsive Pluronic F127chitosan nanocapsules for controlled release and intracellular delivery of small molecules. *ACS Nano* **4**, 6747–6759 (2010).

53. Kabanov, A. V, Batrakova, E. V & Alakhov, V. Y. Pluronic® block copolymers as novel polymer therapeutics for drug and gene delivery. *J. Control. Release* **82**, 189–212 (2002).

54. Pham Trong, L.C., Djabourov, M. & Ponton, A. Mechanisms of micellization and rheology of PEO-PPO-PEO triblock copolymers with various architectures. *J. Colloid Interface Sci.* **328**, 278–287 (2008).

55. Shi, C., Khan, S. A., Wang, K. & Schneider, M. Improved delivery of the natural anticancer drug tetrandrine. *Int. J. Pharm.* **479**, 41–51 (2015).

56. Tilley, A. J., Drummond, C. J. & Boyd, B. J. Disposition and association of the steric stabilizer Pluronic® F-127 in lyotropic liquid crystalline nanostructured particle dispersions. *J. Colloid Interface Sci.* **392**, 288–296 (2013).

57. Dorn, K., Hoerpel, G. & Ringsdorf, H. In Bioactive Polymeric Systems: An Overview. in (ed. Gebelein, C. G., Carraher Jr., C. E., E.) 531 (Plenum: New York, 1985).

58. Torchilin, V. P. Structure and design of polymeric surfactantbased drug delivery systems. *J. Control. Release* **73**, 137 (2001).

59. Harrison, R. G., Todd, P., Rudge, S. R. & Petrides, D. P. *Bioseparations science and engineering*. *Oxford University Press.* (2003).

60. Liese, A. & Hilterhaus, L. Evaluation of immobilized enzymes for industrial applications. *Chem. Soc. Rev.* **42**, 6236–6249 (2013).

61. Clogston, J. D. & Patri, A. K. Zeta potential measurement. *Methods Mol. Biol.* **697**, 63–70 (2011).

62. Zeta potential; an introduction in 30 minutes. www.malvern.com. (2012).

63. Becker, W., Reece, J. & Poenie, M. *The world of the cell*. (Benjamin/Cummings Publishing Company, Inc., 1996).

64. Cieśla, J., Bieganowski, A., Janczarek, M. & Sypniewska, T. U. Determination of the electrokinetic potential of Rhizobium leguminosarum bv trifolii Rt24.2 using Laser Doppler Velocimetry—a methodological study. *J. Microbiol. Methods* **85**, 199–205 (2011).

65. Chang, H. *et al.* Electrical characterization of micro-organisms. *J. Vaccine Sci. Technol. B* **5**, 20 (2002).

66. Saito, T., Takatsuka, T., Kato, T., Ishihara, K. & Okuda, K. Adherence of oral streptococci to an immobilized antimicrobial agent. *Arch Oral Biol.* **42**, 539–545 (2001).

67. Tokumasu, F., Ostera, G. R., Amaratunga, C. & Fairhurst, R. M. Modifications in erythrocyte membrane zeta potential by Plasmodium falciparum infection. *Exp. Parasitol.* **131**, 245–251 (2012).

68. Wilson, W. W., Wade, M. M., Holman, S. C. & Champlin, F. R. Status of methods for assessing bacterial cell surface charge properties based on zeta potential measurements. *J. Microbiol. Methods* **43**, 153–164 (2001).

69. Montville, T. J. *Principles which influence microbial growth, survival, and death in foods: Food Microbiology, Fundamentals and Frontiers*. (1997).

70. Hong, Y. & Brown, D. G. Cell surface acid – base properties of Escherichia coli and Bacillus brevis and variation as a function of growth phase, nitrogen source and C:N ratio. *Colloids Surfaces B Biointerfaces* **50**, 112–119 (2006).

71. Yongsuk, H. & Brown, D. G. Electrostatic behavior of the charge-regulated bacterial cell surface. *Langmuir* **24**, 5003–5009 (2008).

72. Jun Kyun Oh *et al.* The influence of surface chemistry on the kinetics and thermodynamics of bacterial adhesion. *Sci. Rep.* **8**, 17247 (2018).

73. Sharma, P. K. & Rao, K. H. Adhesion of Paenibacillus polymyxa on chal copyrite and pyrite: surface thermodynamic and extended DLVO approaches. *Colloids Surfaces B Biointerfaces* **29**, 21–38 (2003).

74. Chen, G. & Walker, S. L. Role of solution chemistry and ion valence on the adhesion kinetics of groundwater and marine bacteria. *Langmuir* **23**, 7162–7171 (2007).

75. Yoshinari, M., Oda, Y., Kato, T., Oukda, K. & Hirayama, A. Influence of surface modifications to titanium on oral bacterial adhesion in vitro. *J. Biomed. Mater. Res.* **52**, 388–394 (2000).

76. Mills, A. L., Herman, J. S., Hornberger, G. M. & DeJesus, T. H. Effect of ionic strength and iron coatings on mineral grains on sorption of bacterial cells to quartz sand. *Appl. Environ. Microbiol.* **60**, 3300–3306 (1994).

77. Yee, N., Fein, J. B. & Daughney, C. J. Experimental study of the pH, ionic strength, and reversibility behavior of bacteria – mineral adsorption. *Geochim. Cosmochim. Acta* **64**, 609–617 (2000).

78. Beveridge, T. J. & Graham, L. L. Surface layers of bacteria. *Microbiol. Rev.* **55**, 684–705 (1991).

79. Lytle, D. A., Rice, E. W., Johnson, C. H. & Fox, K. R. Electrophoretic mobilities of Escherichia coli 0157:H7 and wild-type Eschericia coli strains. *Appl. Environ. Microbiol.* **65**, 3222–3225 (1999).

80. Brinton Jr., C. C. & Lauffer, M. A. *The electrophoresis of viruses, bacteria, and cells and the microscope of electrophoresis*. (Academis Press, Inc., 1959).

81. Dyar, M. T. & Ordal, E. J. Electrokinetic studies on bacterial surfaces, I. The effects of surface-active agents on the electrophoretic mobilities of bacteria. *J. Bacteriol.* **51**, 149–167 (1945).

82. Reynolds, E. C. & Wong, A. Adherence, Effect of adsorbed protein on hydroxyapatite zeta potential and Streptococcus mutans. *Infect. Immun.* **39**, 1285–1290 (1983).

83. Gilbert, P., Evans, D. J., Evans, E., Duguid, I. G. & Brown, M. R. W. Surface characteristics and adhesion of Eschericia coli and Staphylococcus epidermidis. *J. Appl. Bacteriol.* **71**, 72–77 (1991).

84. van der Mei, H. C., van de Belt-Gritter, B. & Busscher, H. J. Implications of microbial adhesion to hydrocarbons for evaluating cells surface hydrophobicity. *Colloids Surfaces B* **5**, 117–129 (1995).

85. Mangia, A. H. R., Teixeira, L. M. & Filho, F. C. E. S. The electrokinetic surface of five enteropathogenic Eschericia coli serogroups. *Cell Biophys.* **26**, 45–55 (1995).

86. Pedersen, K. Electrostatic interaction chromatography, a method of assaying the relative surface charges of bacteria. *FEMS Microbiol. Lett.* **12**, 365–367 (1981).

87. Magnussion, K.-E., Stendahl, O., Tagesson, C., Edebo, L. & Johansson, G. The tendency of smooth and rough Salmonella typhimurium bacteria and lipopolysaccaharide to hyrdophobic and ionic interaction, as studied in aqueous polymer two-phase systems. *Acta Pathol. Microbiol. Sect. B* **85**, 212–218 (1977).

88. Liang, O. D., Ascencio, F., Vazquez-Juarez, R. & Wadstrom, T. Binding of collagen fibronectin, lactoferrin, laminin, vitrobectin and heparin sulphate to Staphylococcus aureus strain V8 at various growth phases and under nutrient stress conditions. *Zentralblatt für Bakteriol.* **279**, 180–190 (1993).

89. Wood, J. M. *The interaction of micro-organisms with ion-exchange resins: Microbial adhesion to surfaces*. (Ellis Harwood, 1980).

90. Wong, J. D., Miller, M. A. & Janda, J. M. Surface properties and ultrastructure of Edwardsiella species. *J. Clin. Microbiol.* **27**, 1797–1801 (1989).

91. Flint, S. H., Brooks, J. D. & Bremer, P. J. The influence of cell surface properties of thermophilic streptococci on attachment to stainless steel. *J. Appl. Mibrobiology* **83**, 508–517 (1997).

92. Sherbet, G. V, Lakshmi, M. S. & Rao, K. V. Characterization of ionogenic groups and estimation of the net negative electric charge on the surface of cells using natural pH ingredients. *Exp. Cell Res.* **70**, 113–123 (1972).

93. Vanhaecke, E. *et al.* Kinetics of Pseudomonas aeruginosa adhesion to 3014 and 316-L stainless stee: role of cell surface hydrophobicity. *Appl. Environ. Microbiol.* **56**, 788–795 (1990).

94. Blake, I. R. C., Shute, E. A. & Howard, G. T. Solubilization of minerals by bacteria: electrophoretic mobility of Thiobacillus ferrooxidans in the presence og iron, pyrite and sulfur. *Appl. Environ. Microbiol.* **60**, 3349–3357 (1994).

95. Morris, C. M., George, A., Wilson, W. W. & Champlin, F. R. Effect of polymyxin B nanopeptide on daptomycin permeability and cell surface properties in Pseudomonas aeruginosa, Eschericia coli, and Pasteurella multocida. *J. Antibiot. (Tokyo).* **48**, 67–72 (1995).

96. Swanson, J., Dorward, D., Lubke, L. & Kao, D. Porin polypeptide contributes to surface charge of gonococci. *J. Bacteriol.* **179**, 3541–3548 (1997).

97. Cabeen, M. T. . & Jacobs-Wagner, C. Bacterial cell shape. *Nat Rev Microbiol* **3**, 601–610 (2005).

98. Holtje, J. V. Growth of the stress-bearing and shape-maintaining murein sacculus of Escherichia coli. *Microbiol Mol Biol Rev* **62**, 181–203 (1998).

99. Scheffers, D. J. . & Pinho, M. G. Bacterial cell wall synthesis: New insights from localization studies. *Microbiol Mol Biol Rev* **69**, 585–607 (2005).

100. Trombetta, D. . *et al.* Mechanisms of antibacterial action of three monoterpenes. *Antimicrob. Agents Chemother.* **49**, 2474–2478 (2005).

101. C, W., CM, S. & M, A. Essentials of Glycobiology. in (Cold Spring Harbor Laboratory Press, 2015).

102. Tiwari, B. K. ., Valdramidis, V. P. ., O'Donnel, C.P.; Muthukumarappan, K.; Bourke, P. . & Cullen, P. J. Application of natural antimicrobials for food preservation. *J. Agric. Food Chem.* **57**, 5987–6000 (2009).

103. Nikaido, H. Prevention of drug access to bacterial targets: Permeability barriers and active efflux. *Science (80-.).* **264**, 382–388 (1994).

104. Vaara, M. Agents that increase the permeability of the outer membrane. *Microbiol. Rev.* **56**, 395–411 (1992).

105. Plesiat, P. . & Nikaido, H. Outer membranes of Gram-negative bacteria are permeable to steroid probes. *Mol. Microbiol.* **6**, 1323–1333 (1992).

106. Soon, R. L. *et al.* Different surface charge of colistin-susceptible and -resistant Acinetobacter baumannii cells measured with zeta potential as a function of growth phase and colistin treatment. *J. Antimicrob. Chemother.* **66**, 126–133 (2011).

107. D'Aoust, J. . & Maurer, J. Food microbiology fundamental and frontiers. in (eds. Doyle, M. P. . & Beuchat, L. R.) 187–236 (ASM Press, Washington, D.C., 2007).

108. Daoust, J. Y. Pathogenicity of foodborne Salmonella. *Int. J. Food Microbiol.* **12**, 17–40 (1991).

109. FDA. *Analysis and evaluation of preventive control measures for the control and reduction/elimination of microbial hazards on fresh and fresh-cut produce*. http://www.fda.gov/Food/FoodScienceResearch/SafePracticesforFoodProcesses/ucm091%0A016.htm (2015).

110. Jay, J. M. . & Loessner, M. J.; Golden, D. A. . *Modern food microbiology*. (Springer Science+Business Media, LLC, 2005).

111. CDC. *Multistate outbreak of Salmonella Typhimurium infections linked to tomatoes (final update)*. http://www.cdc.gov/salmonella/typh2006/index.html (2006).

112. Raybaudi-Massilia R.M.; Mosqueda-Melgar, J. ., Soliva-Fortuny, R. . & Martín-Belloso, O. Control of pathogenic and spoilage microorganisms in fresh-cut fruits and fruit juices by traditional and alternative natural antimicrobials. *Compr. Rev. Food Sci Food Saf.* **8**, 157–180 (2009).

113. D'Aoust, J.-Y. Salmonella. p. 1233-1299. In B.M. Lund, T.C. BairdParker, and G.W. Gould (ed.), Microbiological Safety and Quality of Food, vol. 1-2. Springer-Verlag, New York. in (2000).

114. Bell, C. . & Kyriakides, A. *Salmonella a practical approach to the organism and its control in foods*. (Blackwell Science, Ames, Iowa, 2002).

115. Goepfert, J. M. . & Biggie, R. A. Heat resistance of Salmonella typhimurium and Salmonella senftanberg 775W in milk chocolate. *Appl. Micro.* **16**, 1939–1940 (1968).

116. Greenwood, M. H. ., Roberts, D. . & Burden, P. The occurrence of Listeria species in milk and dairy products: a national survey in England and Wales. *Int J Food Microbiol.* **12**, 197–206 (1991).

117. Abdollahzadeh, E. ., Rezaei, M. . & Hosseini, H. Antibacterial activity of plant essential oils and extracts: the role of thyme essential oil, nisin, and their combination to control Listeria monocytogenes inoculated in minced fish meat. *Food Control* **35**, 177–183 (2014).

118. Shamloo, E. . & Jalali, M. Prevalence of Listeria species in raw milk and traditional dairy products in Isfahan, Iran. *Int. J. Environ. Heal. Eng* **4**, (2015).

119. Rabiey, S. ., Hosseini, H. . & Rezaei, M. The Hurdle effect of B unium persicum essential oil, smoke and NaCl for controlling the Listeria monocytogenes growth in fish model systems. *J. Food Saf.* **33**, 137–144 (2013).

120. Liu, D. ., Lawrence, M. L. ., Ainsworth, A. J. . & Austin, F. W. Isolation and PCR amplification of a species-specific oxidoreductase-coding gene region in Listeria grayi. *Can. J. Microbiol.* **51**, 95–98 (2005).

121. Cox, L. J. . *et al.* Listeria spp. in food processing, non-food and domestic environments. *Food Microbiol.* **6**, 49–61 (1989).

122. Wilson, I. G. Occurrence of Listeria spp. in ready to eat foods. *Epidemiol. Inf.* **115**, 519–526 (1995).

123. Jemmi, T. Listeria monocytogenes in smoked fish: an overview. *Arch. Leb.* **44**, 10–13 (1993).

124. Farber, J. M. . & Daley, E. Presence and growth of Listeria monocytogenes in naturally contaminated meats. *Int. J. Food Microbiol.* **22**, 33–42 (1994).

125. Loncarevic, S. . & Danielsson-Tham, M.L.; Tham, W. Occurrence of Listeria monocytogenes in soft and semi-soft cheeses in retail outlets in Sweden. *Int. J. Food Microbiol.* **26**, 245–250 (1995).

126. Scallan, E. *et al.* Foodborne Illness Acquired in the United States—Major Pathogens. *Emerg. Infect. Dis.* **17**, 7–15 (2011).

127. Buzby, J. C. Children and microbial foodborne illness. *FoodReview* **24**, (2001).

128. Neill, M. A. ., Tarr, P. I. ., Clausen, C. R. ., Christie, D. L. . & Hickman, R. O. Escherichia coli O157:H7 as the predominant pathogen associated with the hemolytic uremic syndrome: a prospective study in the Pacific Northwest. *Pediatrics* **80**, 37–40 (1987).

129. Kader, A. A. Postharvest technology of horticultural crops. in (University of California, Oakland, Calif, 2002).

130. Meng, J. ., Doyle, M. P. ., Zhao, T. . & Zhao, S. *Enterohemorrhagic Escherichia coli*. (Food microbiology fundamental and frontiers, ASM press, Washington, D.C., 2007).

131. Nataro, J. P. . & Kaper, J. B. Diarrheagenic Escherichia coli. *Clin. Microbiol Rev.* **11**, 142–201 (1998).

132. Orskov, I. ., Orskov, F. ., Jann, B. . & Jann, K. Serology, chemistry, and genetics of O and K antigens of Escherichia coli. *Bacteriol. Rev.* **41**, 667–710 (1977).

133. FDA. Chapter IV. Outbreaks associated with fresh and fresh-cut produce. Incidence, growth, and survival of pathogens in fresh and fresh-cut produce. http://www.fda.gov/Food/FoodScienceResearch/SafePracticesforFoodProcesses/%0Aucm091265.htm. (2013).

134. Tilden, J. . *et al.* A new route of transmission for Escherichia coli: infection from dry fermented salami. *Am. J. Public Heal.* **86**, 1142–1145 (1996).

135. Buzby, J. C. & Roberts, T. The Economics of Enteric Infections: Human Foodborne Disease Costs. *Gastroenterology* **136**, 1851–1862 (2009).

136. Schelin, J. . *et al.* The formation of Staphylococcus aureus enterotoxin in food environments and advances in risk assessment. *Virulence* **2**, 580–592 (2011).

137. Genigeorgis, C. ., Foda, M. S. ., Mantis, A. . & Sadler, W. W. Effect of sodium chloride and pH on enterotoxin C production. *Appl. Microbiol.* **21**, 862 (1971).

138. Scott, W. J. Water relations of Staphylococcus aureus at 30°C. *Aust. J. Biol. Sci.* **6**, 549 (1953).

139. Troller, J. A. Effect of water activity on enterotoxin B production and growth of Staphylococcus aureus. *Appl. Microbiol.* **21**, 435 (1971).

140. Rodriguez-Caturla, M. Y. ., Díaz, A. V. ., Vallejo, J. L. R. ., García-Gimeno, R. M. . & Cosano, G. Z. Effect of pre-incubation conditions on growth and survival of Staphylococcus aureus in sliced cooked chicken breast. *Meat Sci.* **92**, 409–416 (2012).

141. Akbulut, M. *et al.* Generic Method of Preparing Multifunctional Fluorescent Nanoparticles Using Flash NanoPrecipitation. *Adv. Funct. Mater.* **19**, 718–725 (2009).

142. Zhang, M. & Akbulut, M. Adsorption, desorption, and removal of polymeric nanomedicine on and from cellulose surfaces: Effect of size. *Langmuir* **27**, 12550–12559 (2011).

143. Perez, K. L., Lucia, L. M., Cisneros-Zevallos, L., Castillo, A. & Taylor, T. M. Efficacy of antimicrobials for the disinfection of pathogen contaminated green bell pepper and of consumer cleaning methods for the decontamination of knives. *Int. J. Food Microbiol.* **156**, 76–82 (2012).

144. Kohli, S., Pal, A. & Jain, S. PREPARATION , CHARACTERIZATION AND EVALUATION OF POLY (LACTIDE – CO – GLYCOLIDE) MICROSPHERES FOR THE CONTROLLED RELEASE OF ZIDOVUDINE. **9**, (2017).

145. Manaspon, C., Viravaidya-Pasuwat, K., Pimpha, N. Preparation of folate-conjugated Pluronic F127/chitosan core-shell nanoparticles encapsulation doxuribicin for breast cancer. *J. Nanomater.* 593878 (2012).

146. Kelishady, P.D., Saadat, E., Ravar, F., Akbari, H., Dorkoosh, F. Pluronic F127 polymeric micelles for co-delivery of paclitaxel and lapatinib against metastatic breast cancer: preparation, optimization and in vitro evaluation. *Pharm. Dev. Technol.* **29**, 1–9 (2014).

147. Taha, E.I., Badran, M.M., El-Anazi, M.H., Bayomi, M.A., El-Bagory, I. M. Role of Pluronic F127 micelles in enhancing ocular delivery of ciprofloxacin. *J. Mol. Liq.* **199**, 251–256 (2014).

148. Peng, S., Hung, W.-L., Peng, Y.-S., Chu, I.-M. Oligoalanine-modified Pluronic-F127 nanocarriers for the delivery of curcumin with enhanced entrapment efficiency. *J. Biomater. Sci. Polym. Ed.* **25**, 1225–1239 (2014).

149. Prud'homme, R. K., Wu, G. & Schneider, D. K. Structure and rheology studies of poly(oxyethylene-oxypropylene-oxyethylene) aqueous solution. *Langmuir* **12**, 4651–4659 (1996).

150. Hill, L. E. & Gomes, C. L. Optimization of synthesis process of thermally-responsive poly-n-isopropylacrylamide nanoparticles for controlled release of antimicrobial hydrophobic compounds. *Mater. Res. Express* **1**, 045404 (2014).

151. Wanka, G., Hoffman, H. & Ulbricht, W. Phase diagrams and aggregation behavior of poly(oxyethylene)-poly(oxypropylene)-poly(oxyethylene) triblock copolymers in aqueous solutions. *Macromolecules* **27**, 4145–4159 (1994).

152. Wuang, S. C., Neoh, K. G., Kang, E.-T., Leckband, D. E. & Pack, D. W. Acid-sensitive magnetic nanoparticles as potential drug depots. *AIChE J.* **57**, 1638–1645 (2011).

153. Ravichandran, M., Hettiarachchy, N., Ganesh, V., Ricke, S., Singh, S. Enhancement of antimicrobial activities of naturally occurring phenolic compounds by nanoscale delivery against Listeria monocytogenes, Escherichia coli O157:H7, and Salmonella Typhimurium in broth and chicken meat system. *J. Food Saf.* **31**, 462–471 (2011).

154. Liolios, C.C., Gortzi, O., Lalas, S., Tsaknis, J., Chinou, I. Liposomal incorporation of carvacrol and thymol isolated from the essential oil of Origanum dictamnus L. and in vitro antimicrobial activity. *Food Chem.* **112**, 77–83 (2009).

155. Mourtzinos, I., Kalogeropoulos, N., Papadakis, S.E., Konstantinou, K., Karathanos, V. T. Encapsulation of nutraceutical monoterpenes in β-cyclodextrin and modified starch. *J. Food Sci.* **73**, S89–S94 (2008).

156. D.V., L. *Microbiology*. (St. Paul, MN: West Publishing, 1989).

157. Park, C. W., Yoon, K. Y., Byeon, J. H., Kim, K. & Hwang, J. Development of Rapid Assessment Method to Determine Bacterial Viability Based on Ultraviolet and Visible (UV-Vis) Spectroscopy Analysis Including Application to Bioaerosols. 399–408 (2012) doi:10.4209/aaqr.2011.08.0129.

158. Alupoaei, C. E., Olivares, J. A. & Garcia-Rubio, L. H. *Quantitative analysis of prokaryotic cells: vegetative cells and spores. Report No LAUR026586. Los Alamos, NM: Los Alamos National Laboratory*. (2002).

159. Wilfinger, W. W., Mackey, K. & Chomczynski, P. *In: DNA sequencing II optimizing preparation and cleanup. Assessing the quantity, purity and integrity of RNA and DNA following nucleic acid purification*. (MA: Jones and Bartlett Publishers., 2006).

160. Alupoaei, C. E. & García-Rubio, L. H. Growth Behavior of Microorganisms Using UV-Vis Spectroscopy: Escherichia coli. *Biotechnol. Bioeng.* **86**, 163–167 (2004).

161. Wahab, R., Khan, F. & Al-Khedhairy, A. A. Peanut-shaped ZnO nanostructures: A driving force for enriched antibacterial activity and their statistical analysis. *Ceram. Int.* **46**, 307–316 (2020).

162. Ternus ZR, Z. M. Microbiological Characterization of Pure Geraniol and Comparison with Bactericidal Activity of the Cinnamic Acid in Gram-Positive and Gram-Negative Bacteria. *J. Microb. Biochem. Technol.* **07**, 186–193 (2015).

163. Lopez-Romero, J. C., González-Ríos, H., Borges, A. & Simões, M. Antibacterial Effects and Mode of Action of Selected Essential Oils Components against Escherichia coli and Staphylococcus aureus. *Evidence-based Complement. Altern. Med.* **2015**, (2015).

164. Borges, A., Ferreira, C., Saavedra, M. J. & Simoes, M. Antibac terial activity and mode of action of ferulic and gallic acids against pathogenic bacteria. *Microb. Drug Resist.* **19**, 256–265 (2013).

165. Palmer, J., Flint, S. & Brooks, J. Bacterial cell attachment, the beginning of a biofilm. *J. Ind. Microbiol. Biotechnol.* **34**, 577–588 (2007).

166. USDA (United States Department of Agriculture) Economic Research Service. (2015).

167. Gould, L. H. *et al. Surveillance for Foodborne Disease Outbreaks — United States , 1998 – 2008*. vol. 62 (2013).

168. Shi, Z. *et al.* Comparison of methods for quantitating Salmonella enterica Typhimurium and Heidelberg strain attachment to reusable plastic shipping container coupons and preliminary assessment of sanitizer efficacy and preliminary assessment of sanitizer ef fi cacy. *J. Environ. Sci. Heal. Part B* **51**, 602–608 (2016).

169. Anumolu, V. K. & Lakkineni, V. R. Screening of poultry samples for Salmonella Typhimurium by PCR assay. *Vet. World* **5**, 169–172 (2012).

170. *Serotypes Profile of Salmonella Isolates from Meat and Poultry Products January 1998 through December 2014*. (2014).

171. *Safe and suitable ingredients used in the production of meat, poultry, and egg products*. (2018).

172. Brannon, D. K. Cosmetic microbiology: a practical handbook. in *Cosmetic microbiology: a practical handbook* (CRC Press, Inc., 1997).

173. Shimizu, M. *et al.* In Vitro Antiseptic Susceptibility of Clinical Isolates from Nosocomial Infections. *Dermatology* **204**, 21–27 (2002).

174. Gilbert, P. & Al-Taae, A. Antimicrobial Activity of Some Alkyltrimethylammonium Bromides. *Lett. Appl. Microbiol.* **1**, 101–104 (1985).

175. Salton, M. R. J. Lytic Agents , Cell Permeability , and Monolayer Penetrability. *J. Gen. Physiol.* **52**, 227–252 (1968).

176. Lambert, P. A. & Hammond., S. M. Potassium Fluxes. First Indications of Membrane Damage in Micro-Organisms. *Biochem. Biophys. Res. Commun.* **54**, 796–799 (1973).

177. Chaidez, C., Lopez, J. & Castro-del Campo, N. Quaternary ammonium compounds: an alternative disinfection method for fresh produce wash water. *J. Water Health* **5**, 329–333 (2007).

178. US Food and Drug Administration. *Cetylpyridinium chloride: as an antimicrobial in poultry processing*. (2004).

179. Russell, A. D. Mechanisms of Bacterial Resistance to Antibiotics and Biocides. *Prog. Med. Chem.* **35**, 133–197 (1998).

180. Cutter, C. N. *et al.* Antimicrobial Activity of Cetylpyridinium Chloride Washes against Pathogenic Bacteria on Beef Surfaces†. *J. Food Prot.* **63**, 593–600 (2000).

181. Kim, J. & Slavik, M. F. Cetylpyridinium Chloride (CPC) Treatment on Poultry Skin To Reduce Attached Salmonella. *J. Food Prot.* **59**, 322–326 (1996).

182. Breen, P. J., Salari, H. & Compadre, C. M. Elimination of Salmonella Contamination from Poultry Tissues by Cetylpyridinium Chloride Solutions. *J. Food Prot.* **60**, 1019–1021 (1997).

183. Xiong, H. U. A., Li, Y., Slavik, I. M. F. & Walkeri, J. T. Spraying Chicken Skin with Selected Chemicals to Reduce Attached Salmonella typhimurium. *J. Food Prot.* **61**, 272–275 (1998).

184. Li, Y., Slavik, M. F., Walker, J. T. & Xiong, H. Pre-Chill Spray of Chicken Carcasses to Reduce Salmonella typhimurium. *J. Food Sci.* **62**, 605–607 (1997).

185. Zhang, L. E. I., Garner, L. J. & Kee, S. R. M. C. Effectiveness of Several Antimicrobials Used in a Postchill Decontamination Tank against Salmonella and Campylobacter on Broiler Carcass Parts. *J. Food Prot.* **81**, 1134–1141 (2018).

186. Camesano, T. A. Role of Lipopolysaccharides in the Adhesion, Retention, and Transport of Escherichia coli JM109. *Environ. Sci. Technol.* **37**, 2173–2183 (2003).

187. Poortinga, A. T., Bos, R., Norde, W. & Busscher, H. J. Electric double layer interactions in bacterial adhesion to surfaces. *Surf. Sci. Rep.* **47**, 1–32 (2002).

188. Wal, A. van der, Norde, W., Zehnder, A. J. B. & Lyklema, J. Determination of the total charge in the cell walls of Gram-positive bacteria. *Colloids Surfaces B Biointerfaces* **9**, 81–100 (1997).

189. Hamouda, T. & Baker, J. R. Antimicrobial mechanism of action of surfactant lipid preparations in enteric Gram-negative bacilli. *J. Appl. Microbiol.* **89**, 397–403 (2000).

190. Zhang, L., Jiao, L., Zhong, J., Guan, W. & Lu, C. Lighting up the interactions between bacteria and surfactants with aggregation-induced emission characteristics. *Mater. Chem. Front.* **1**, 1829–1835 (2017).

191. Wessels, S. & Ingmer, H. Modes of action of three disinfectant active substances : A review. *Regul. Toxicol. Pharmacol.* **67**, 456–467 (2013).

192. Nikitina, E. V *et al.* Antibacterial effects of quaternary bis-phosphonium and ammonium salts of pyridoxine on Staphylococcus aureus cells: A single base hitting two distinct targets? *World J. Microbiol. Biotechnol.* **32**, 5–12 (2016).

193. *U.S. Department of Agriculture - Food Safety and Inspection Service. Directive 7120.1, Rev. 49: Safe and suitable ingredients used in the production of meat, poultry, and egg products.* https://www.fsis.usda.gov/wps/wcm/connect/bab10e09-aefa-483b-8be8-%0A809a1f051d4c/7120.1.pdf?MOD=AJPERES%0A (2019).

194. Chen, X. *et al.* Efficacy of various antimicrobials on reduction of Salmonella and Campylobacter and quality attributes of ground chicken obtained from poultry parts treated in a postchill decontamination tank. *J. Food Prot.* **77**, 1882–1888 (2014).

195. Chylkova, T., Cadena, M., Ferreiro, A. & Pitesky, M. Susceptibility of Salmonella biofilm and planktonic bacteria to common disinfectant agents used in poultry processing. *J. Food Prot.* **80**, 1072–1079 (2017).

196. Gamble, G. R. *et al.* Effect of simulated sanitizer carryover on recovery of Salmonella from broiler carcass rinsates. *J. Food Prot.* **79**, 710–714 (2016).

197. Gamble, G. R. *et al.* Neutralization of bactericidal activity related to antimicrobial carryover in broiler carcass rinse samples. *J. Food Prot.* **80**, 685–691 (2017).

198. *U.S. Department of Agriculture - Food Safety and Inspection Service. New performance standards for Salmonella and Campylobacter in not-ready-to-eat comminuted chicken and turkey products and raw chicken parts and changes to related agency verification pro*. (2016).

199. U.S. Department of Agriculture - Food Safety and Inspection Service. Notice 41-16: New neutralizing buffered peptone water to replace current buffered peptone water for poultry verification sampling. (2016).

200. Dey, B. P. & Engley Jr., F. B. Methodology for recovery of chemically treated Staphylococcus aureus with neutralizing medium. *Appl. Environ. Microbiol.* **45**, 1533–1537 (1983).

201. Mohammad, Z. H., Hasan, A. A., Kerth, C. R., Riley, D. G. & Taylor, T. M. Increased effectiveness of microbiological verification by concentration-dependent neutralization of sanitizers used in poultry slaughter and fabrication allowing Salmonella enterica survival. *Foods* (2018) doi:10.3390/foods7030032.

202. Ioannou, C. J., Hanlon, G. W. & Denyer, S. P. Action of disinfectant quaternary ammonium compounds against Staphylococcus aureus. *Antimicrob. Agents Chemother. Chemother.* **51**, 296–306 (2007).

203. Hwang, Y. Y. *et al.* Antimicrobial activity of nanoemulsion in combination with cetylpyridinium chloride in multidrug-resistant Acinetobacter baumanii. *Antimicrob. Agents Chemother.* **57**, 3568–3575 (2013).

204. Breen, P. J. *et al.* Quaternary ammonium compounds inhibit and reduce the attachment of viable Salmonella typhimurium to poultry tissues. *J. Food Sci.* **60**, 1191–1196 (1995).

205. Ma, Y.-L., Yang, B., Guo, T. & Xie, L. Antibacterial mechanism of Cu2+-ZnO/cetylpyridinium-montmorillonite in vitro. *Appl. Clay Sci.* **50**, 348–353 (2010).

206. *U.S. Department of Agriculture - Food Safety and Inspection Service. Neutralizing buffered peptone water (nBPW) in poultry carcass and parts sampling*.

https://askfsis.custhelp.com/app/answers/detail/a_id/2007/~/neutralizing-buffered peptone-water-%28nbpw%29-in-poultry-carcass-and-parts-sampling (2016).

207. Bhattarai, A., Yadav, A. K., Sah, S. K. & Deo, A. Influence of methanol and dimethyl sulfoxide and temperature on the micellization of cetyl pyridinium chloride. *J. Mol. Liq.* **242**, 831–837 (2017).

208. Wang, W. C., Li, Y., Slavik, M. F. & Xiong, H. Trisodium phosphate and cetylpyridinium chloride spraying on chicken skin to reduce attached Salmonella typhimurium. *J. Food Prot.* **60**, 992–994 (1997).

209. Gerba, C. P. Quaternary ammonium biocides: efficacy in application. *Appl. Environ. Microbiol.* **81**, 464–469 (2015).

210. McDonnell, G. & Russell, D. Antiseptics and Disinfectants : Activity , Action , and Resistance. *Clin. Microbiol. Rev.* **12**, 147–179 (1999).

211. Gunther, I., N.W., Abdul-Wakeel, A., Reichenberger, E. R., Al-Khalifa, S. & Minbiole, K. P. C. Quaternary ammonium compounds with multiple cationic moieties (multaQACs) provide antimicrobial efficacy against Campylobacter jejuni. *Food Control* **94**, 187–194 (2018).

212. Abbasnezhad, H., Gray, M. R. & Foght, J. M. Two different mechanisms for adhesion of Gram-negative bacterium, Pseudomonas fluorescens LP6a, to an oil-water interface. *Colloids Surfaces B* **62**, 36–41 (2008).

213. Quisno, R., Gibby, I. W. & Foter, M. J. A neutralizing medium for evaluating the germicidal potency of the quaternary ammonium salts. *Am. J. Pharm.* **118**, 320–323 (1946).

214. Vuia-Riser, J., Hieke, A.-S. C., Athrey, G., Kerth, C. R. & Taylor, T. M. Comparison of buffered peptone water to neutralizing buffered peptone water for Salmonella detection from

commercially slaughtered whole chicken carcasses and cut chicken parts. *Food Prot. trends* **38**, 410–420 (2018).

215. De-Wei, L. & Yang, C. S. Fungal Contamination as a Major Contributor to Sick Building Syndrome. *Adv. Appl. Microbiol.* **55**, 31–112 (2004).
216. Rocha, M. E. B., Freire, F. C. O., Maia, F. E. F., Guedes, M. I. F. & Rodina, D. Mycotoxins and their effects on human and animal health. *Food Control* **36**, 159–165 (2014).
217. Anfossi, L., Giovannoli, C. & Baggiani, C. Mycotoxin detection. *Curr. Opin. Biotechnol.* **37**, 120–126 (2016).
218. Njobeh, B. P., Dutton, F. M. & Makun, H. A. *Mycotoxins and human health: Significance, prevention and control*. (In: Mishra, A.K., Tiwari, A., Mishra, S.B. (Eds.), Smart Biomolecules in Medicine, 2010).
219. Terzi, V., Tumino, G. & MicheleStanca, A. M., Morcia, C. Reducing the incidence of cereal head infection and mycotoxins in small grain cereal species. *J. Cereal Sci.* **59**, (2014).
220. Makun, H. A., Dutton, M. F., Njobeh, P. B., Gbodi, T. M. & Ogbadu, G. H. Aflatoxin contamination in foods and feeds: A special focus on Africa. In: Eissa, Ayman Amer (Ed.). *Trends Vital Food Control Eng. InTech ISBN 978-953-51-0449-0* (2012).
221. Stoloff, L. *Aflatoxins-an overview. In: Mycotoxins in human and animal health, edited by Rodricks, J.V.; Hesseltine C.W.; Mehlman, M.A.* (Pathotox Publishers Inc., 1977).
222. Pitt, J. I. *Toxigenic Aspergillus and Penicillium Species. A paper presented on the International Training Course on Mycotoxin Prevention and Control*. (1989).
223. Hahn, M. The rising threat of fungicide resistance in plant pathogenic fungi: Botrytis as a case study. *J. Chem. Biol.* **7**, 133–141 (2014).

224. Kim, K. J. *et al.* Antifungal effect of silver nanoparticles on dermatophytes. *J. Microbiol. Biotechnol.* **8**, 1482–1484 (2008).

225. Reis, C. P., Neufeld, R. J., Ribeiro, A. J. & Veiga, F. Nanoencapsulation I. Methods for preparation of drug-loaded polymeric nanoparticles. *Nanomedicine* **2**, 8–21 (2006).

226. Kowalczuk, A. et al. Loading of polymer nanocarriers: Factors, mechanisms and applications. *Prog. Polym. Sci.* **39**, 43–86 (2014).

227. Wagner, V., Dullaart, A., Bock, A.-K. & Zweck, A. The emerging nanomedicine landscape. *Nat. Biotechnol.* **24**, 1211–1218 (2006).

228. Merisko-Liversidge, E., Liversidge, G. G. & Cooper, E. R. Nanosizing: a formulation approach for poorly-water-soluble compounds. *Eur. J. Pharm. Sci.* **18**, 113–120 (2003).

229. Steichen, S. D., Caldorera-Moore, M. & Peppas, N. A. A review of current nanoparticle and targeting moieties for the delivery of cancer therapeutics. *Eur. J. Pharm. Sci.* **48**, 416–427 (2013).

230. Bertrand, N., Wu, J., Xu, X., Kamaly, N. & Farokhzad, O. C. Cancer nanotechnology: the impact of passive and active targeting in the era of modern cancer biology. *Adv. Drug Deliv. Rev.* **66**, 2–25 (2014).

231. Etheridge, M. L. *et al.* The big picture on nanomedicine : the state of investigational and approved nanomedicine products. *Nanomedicine Nanotechnology, Biol. Med.* **9**, 1–14 (2013).

232. Highsmith, J. Nanoparticles in biotechnology, drug development and drug delivery. *Rep. No. BIO113A (BCC Res. Mark. Forecast. 2012)* (2012).

233. Transparency Market Research. *Biomaterials Market for Implantable Devices (Material Type — Metals, Polymers, Ceramics and Natural, Applications — Cardiology, Orthopedics,*

Dental, Ophthalmology and Others): Global Industry Analysis, Size, Share, Growth, Trends and Forecast 2013–2019. (2012).

234. Evers, P. Nanotechnology in Medical Applications: The Global Market. *BCC Res.* (2012).
235. He, X. *et al.* In Vivo Study of Biodistribution and Urinary Excretion of Surface-Modified Silica Nanoparticles. **80**, 9597–9603 (2008).
236. Minchin, R. Sizing up targets with nanoparticles Remote control of living cells. **3**, (2008).
237. Choi, H. S. *et al.* Renal clearance of quantum dots. **25**, 1165–1170 (2007).
238. Longmire, M., Choyke, P. L. & Kobayashi, H. Clearance Properties of Nano-sized Particles and Molecules as Imaging Agents: Considerations and Caveats. **3**, 703–717 (2012).
239. Misra, R., Acharya, S. & Sahoo, S. K. Cancer nanotechnology : application of nanotechnology in cancer therapy. *Drug Discov. Today* **15**, 842–850 (2010).
240. Kiser, M. A. *et al.* Titanium Nanomaterial Removal and Release from Wastewater Treatment Plants. **43**, 6757–6763 (2009).
241. Reijnders, L. Cleaner nanotechnology and hazard reduction of manufactured nanoparticles. *J. Clean. Prod.* **14**, 124–133 (2006).
242. Jones, O. A., Lester, J. N. & Voulvoulis, N. Pharmaceuticals: a threat to drinking water? *TRENDS Biotechnol.* **23**, 163–167 (2005).
243. Bruce, G. M., Pleus, R. C. & Snyder, S. A. Toxicological relevance of pharmaceuticals in drinking water. *Environ. Sci. Technol.* **44**, 5619–5626 (2010).
244. Zhang, Y., Geißen, S.-U. & Gal, C. Carbamazepine and diclofenac: removal in wastewater treatment plants and occurrence in water bodies. *Chemosphere* **73**, 1151–1161 (2008).
245. Rutsch, M. *et al.* Towards a better understanding of sewer exfiltration. *Water Res.* **42**, 2385–2394 (2008).

246. Wolf, L., Zwiener, C. & Zemann, M. Tracking artificial sweeteners and pharmaceuticals introduced into urban groundwater by leaking sewer networks. *Sci. Total Environ.* **430**, 8–19 (2012).

247. Buerge, I. J., Keller, M., Buser, H. R., Müller, M. D. & Poiger, T. Saccharin and other artificial sweeteners in soils: Estimated inputs from agriculture and households, degradation, and leaching to groundwater. *Environ. Sci. Technol.* **45**, 615–621 (2011).

248. McCormick, P. V & Cairns Jr, J. Algae as indicators of environmental change. *J. Appl. Phycol.* **6**, 509–526 (1994).

249. Ji, J., Long, Z. & Lin, D. Toxicity of oxide nanoparticles to the green algae Chlorella sp. *Chem. Eng. J.* **170**, 525–530 (2011).

250. González, S. O., Almeida, C. A., Calderón, M., Mallea, M. A. & González, P. Assessment of the water self-purification capacity on a river affected by organic pollution: application of chemometrics in spatial and temporal variations. *Environ. Sci. Pollut. Res.* **21**, 10583–10593 (2014).

251. Choi, C. J., Berges, J. A. & Young, E. B. Rapid effects of diverse toxic water pollutants on chlorophyll a fluorescence: variable responses among freshwater microalgae. *water Res.* **46**, 2615–2626 (2012).

252. González-Pleiter, M. *et al.* Toxicity of five antibiotics and their mixtures towards photosynthetic aquatic organisms: implications for environmental risk assessment. *water Res.* **47**, 2050–2064 (2013).

253. Ginebreda, A. *et al.* Assessment of multi-chemical pollution in aquatic ecosystems using toxic units: compound prioritization, mixture characterization and relationships with biological descriptors. *Sci. Total Environ.* **468**, 715–723 (2014).

254. Sáez, C. A., Roncarati, F., Moenne, A., Moody, A. J. & Brown, M. T. Copper-induced intra-specific oxidative damage and antioxidant responses in strains of the brown alga Ectocarpus siliculosus with different pollution histories. *Aquat. Toxicol.* **159**, 81–89 (2015).

255. Yu, X. *et al.* Toxicity evaluation of pharmaceutical wastewaters using the alga Scenedesmus obliquus and the bacterium Vibrio fischeri. *J. Hazard. Mater.* **266**, 68–74 (2014).

256. Johansson, C. H., Janmar, L. & Backhaus, T. Toxicity of ciprofloxacin and sulfamethoxazole to marine periphytic algae and bacteria. *Aquat. Toxicol.* **156**, 248–258 (2014).

257. Hoecke, K. V *et al.* Fate and Effects of CeO Nanoparticles in Aquatic Ecotoxicity Tests Fate and Effects of CeO 2 Nanoparticles in Aquatic Ecotoxicity Tests. *Environ. Sci. Technol.* **43**, 4537–4546 (2009).

258. Ma, X., Geiser-lee, J., Deng, Y. & Kolmakov, A. Science of the Total Environment Interactions between engineered nanoparticles (ENPs) and plants : Phytotoxicity , uptake and accumulation. *Sci. Total Environ.* **408**, 3053–3061 (2010).

259. Franklin, N. M. *et al.* Comparative toxicity of nanoparticulate ZnO , bulk ZnO and ZnCl 2 to a freshwater microalga (Pseudokirchnerilla subcapitata): the. **41**, 1–27 (2007).

260. Hoecke, K. V, De Schamphelaere, K. A. C., Der Meeren, P. V, Lucas, S. & Anssen, C. R. J. ECOTOXICITY OF SILICA NANOPARTICLES TO THE GREEN ALGA PSEUDOKIRCHNERIELLA SUBCAPITATA : IMPORTANCE OF SURFACE AREA. **27**, 1948–1957 (2008).

261. Navarro, E. *et al.* Toxicity of silver nanoparticles to Chlamydomonas reinhardtii. *Environ. Sci. Technol.* **42**, 8959–64 (2008).

262. Zounkova, R. *et al.* ECOTOXICITY AND GENOTOXICITY ASSESSMENT OF CYTOSTATIC PHARMACEUTICALS. **26**, 2208–2214 (2007).

263. Henschel, K.-P., Wenzel, A., Diedrich, M. & Fliedner, A. Environmental Hazard Assessment of Pharmaceuticals. *Regul. Toxicol. Pharmacol.* **25**, 220–225 (1997).

264. Sanderson, H., Johnson, D. J., Wilson, C. J., Brain, R. A. & Solomon, K. R. Probabilistic hazard assessment of environmentally occurring pharmaceuticals toxicity to fish, daphnids and algae by ECOSAR screening. *Toxicol. Lett.* **144**, 383–395 (2003).

265. Ivask, A. *et al.* Size-dependent toxicity of silver nanoparticles to bacteria, yeast, algae, crustaceans and mammalian cells in vitro. *PLoS One* **9**, e102108 (2014).

266. Quigg, A. *et al.* Direct and indirect toxic effects of engineered nanoparticles on algae: role of natural organic matter. *ACS Sustain. Chem. Eng.* **1**, 686–702 (2013).

267. Saison, C. *et al.* Effect of core–shell copper oxide nanoparticles on cell culture morphology and photosynthesis (photosystem II energy distribution) in the green alga, Chlamydomonas reinhardtii. *Aquat. Toxicol.* **96**, 109–114 (2010).

268. Leclerc, S. & Wilkinson, K. J. Bioaccumulation of Nanosilver by Chlamydomonas reinhardtii□ Nanoparticle or the Free Ion? *Environ. Sci. Technol.* **48**, 358–364 (2013).

269. Matorin, D. N., Todorenko, D. A., Seifullina, N. K., Zayadan, B. K. & Rubin, A. B. Effect of silver nanoparticles on the parameters of chlorophyll fluorescence and P700 reaction in the green alga Chlamydomonas reinhardtii. *Microbiology* **82**, 809–814 (2013).

270. Navarro, E., Wagner, B., Odzak, N., Sigg, L. & Behra, R. Effects of differently coated silver nanoparticles on the photosynthesis of Chlamydomonas reinhardtii. *Environ. Sci. Technol.* **49**, 8041–8047 (2015).

271. Ribeiro, F. *et al.* Silver nanoparticles and silver nitrate induce high toxicity to Pseudokirchneriella subcapitata, Daphnia magna and Danio rerio. *Sci. Total Environ.* **466**, 232–241 (2014).

272. Soenen, S. J. *et al.* Cellular toxicity of inorganic nanoparticles: common aspects and guidelines for improved nanotoxicity evaluation. *Nano Today* **6**, 446–465 (2011).

273. Gunawan, C., Sirimanoonphan, A., Teoh, W. Y., Marquis, C. P. & Amal, R. Submicron and nano formulations of titanium dioxide and zinc oxide stimulate unique cellular toxicological responses in the green microalga Chlamydomonas reinhardtii. *J. Hazard. Mater.* **260**, 984–992 (2013).

274. Wang, Z., Zhang, L., Zhao, J. & Xing, B. Environmental processes and toxicity of metallic nanoparticles in aquatic systems as affected by natural organic matter. *Environ. Sci. Nano* **3**, 240–255 (2016).

275. Schwab, F. *et al.* Barriers, pathways and processes for uptake, translocation and accumulation of nanomaterials in plants–critical review. *Nanotoxicology* **10**, 257–278 (2016).

276. Ivask, A. *et al.* Mechanisms of toxic action of Ag, ZnO and CuO nanoparticles to selected ecotoxicological test organisms and mammalian cells in vitro: A comparative review. *Nanotoxicology* **8**, 57–71 (2014).

277. Zhao, J. *et al.* Interactions of CuO nanoparticles with the algae Chlorella pyrenoidosa: Adhesion, uptake and toxicity. *Nanotoxicology* 1–31 (2016).

278. Melegari, S. P., Perreault, F., Costa, R. H. R., Popovic, R. & Matias, W. G. Evaluation of toxicity and oxidative stress induced by copper oxide nanoparticles in the green alga Chlamydomonas reinhardtii. *Aquat. Toxicol.* **142**, 431–440 (2013).

279. Röhder, L. A., Brandt, T., Sigg, L. & Behra, R. Influence of agglomeration of cerium oxide nanoparticles and speciation of cerium (III) on short term effects to the green algae Chlamydomonas reinhardtii. *Aquat. Toxicol.* **152**, 121–130 (2014).

280. Perreault, F., Oukarroum, A., Melegari, S. P., Matias, W. G. & Popovic, R. Polymer coating of copper oxide nanoparticles increases nanoparticles uptake and toxicity in the green alga Chlamydomonas reinhardtii. *Chemosphere* **87**, 1388–1394 (2012).

281. He, D., Dorantes-Aranda, J. J. & Waite, T. D. Silver nanoparticle□ algae interactions: oxidative dissolution, reactive oxygen species generation and synergistic toxic effects. *Environ. Sci. Technol.* **46**, 8731–8738 (2012).

282. Oukarroum, A., Bras, S., Perreault, F. & Popovic, R. Inhibitory effects of silver nanoparticles in two green algae, Chlorella vulgaris and Dunaliella tertiolecta. *Ecotoxicol. Environ. Saf.* **78**, 80–85 (2012).

283. Li, F. *et al.* Toxicity of nano-TiO 2 on algae and the site of reactive oxygen species production. *Aquat. Toxicol.* **158**, 1–13 (2015).

284. Fu, L., Hamzeh, M., Dodard, S., Zhao, Y. H. & Sunahara, G. I. Effects of TiO 2 nanoparticles on ROS production and growth inhibition using freshwater green algae pre-exposed to UV irradiation. *Environ. Toxicol. Pharmacol.* **39**, 1074–1080 (2015).

285. Escher, B. I., Bramaz, N., Eggen, R. I. L. & Richter, M. In vitro assessment of modes of toxic action of pharmaceuticals in aquatic life. *Environ. Sci. Technol.* **39**, 3090–3100 (2005).

286. Rosi-Marshall, E. J. *et al.* Pharmaceuticals suppress algal growth and microbial respiration and alter bacterial communities in stream biofilms. *Ecol. Appl.* **23**, 583–593 (2013).

287. Feng, L., van Hullebusch, E. D., Rodrigo, M. A., Esposito, G. & Oturan, M. A. Removal of residual anti-inflammatory and analgesic pharmaceuticals from aqueous systems by electrochemical advanced oxidation processes. A review. *Chem. Eng. J.* **228**, 944–964 (2013).

288. Maszkowska, J. *et al.* Beta-blockers in the environment: Part II. Ecotoxicity study. *Sci. Total Environ.* **493**, 1122–1126 (2014).

289. Watanabe, H. *et al.* Chronic toxicity of an environmentally relevant mixture of pharmaceuticals to three aquatic organisms (alga, daphnid, and fish). *Environ. Toxicol. Chem.* (2016).

290. Borecka, M. *et al.* The influence of salinity on the toxicity of selected sulfonamides and trimethoprim towards the green algae Chlorella vulgaris. *J. Hazard. Mater.* **308**, 179–186 (2016).

291. Minguez, L. *et al.* Toxicities of 48 pharmaceuticals and their freshwater and marine environmental assessment in northwestern France. *Environ. Sci. Pollut. Res.* **23**, 4992–5001 (2016).

292. Weissig, V., Pettinger, T. K. & Murdock, N. Nanopharmaceuticals (part 1): products on the market. *Int. J. Nanomedicine* **9**, 4357 (2014).

293. Booth, A. *et al.* Freshwater dispersion stability of PAA-stabilised cerium oxide nanoparticles and toxicity towards Pseudokirchneriella subcapitata. *Sci. Total Environ.* **505**, 596–605 (2015).

294. Piccapietra, F., Allué, C. G., Sigg, L. & Behra, R. Intracellular silver accumulation in Chlamydomonas reinhardtii upon exposure to carbonate coated silver nanoparticles and silver nitrate. *Environ. Sci. Technol.* **46**, 7390–7397 (2012).

295. Zhang, M., Soto-Rodríguez, J., Chen, I.-C. & Akbulut, M. Adsorption and removal dynamics of polymeric micellar nanocarriers loaded with a therapeutic agent on silica surfaces. *Soft Matter* **9**, 10155–10164 (2013).

296. Chen, I.-C. *et al.* Transport of Polymeric Nanoparticulate Drug Delivery Systems in the Proximity of Silica and Sand. *Environ. Sci. Technol.* **49**, 3575–3583 (2015).

297. OECD. *OECD guideline for the testing of chemicals-freshwater algae and cyanobacteria, growth inhibition test*. (2011).

298. Abouelmagd, S. A., Sun, B., Chang, A. C., Ku, Y. J. & Yeo, Y. Release kinetics study of poorly water-soluble drugs from nanoparticles: are we doing it right? *Mol. Pharm.* **12**, 997–1003 (2015).

299. Angel, B. M., Vallotton, P. & Apte, S. C. On the mechanism of nanoparticulate CeO2 toxicity to freshwater algae. *Aquat. Toxicol.* **168**, 90–97 (2015).

300. Moghimi, S. M., Hunter, A. C. & Murray, J. C. Long-circulating and target-specific nanoparticles: theory to practice. *Pharmacol. Rev.* **53**, 283–318 (2001).

301. Barbe, C. *et al.* Silica particles: a novel drug-delivery system. *Adv. Mater.* **16**, 1959–1966 (2004).

302. Zhang, M. *et al.* A Multifunctional Nanoparticulate Theranostic System with Simultaneous Chemotherapeutic, Photothermal Therapeutic, and MRI Contrast Capabilities. *RSC Adv.* **6**, 27798–27806 (2016).

303. Verma, A. & Stellacci, F. Effect of surface properties on nanoparticle–cell interactions. *Small* **6**, 12–21 (2010).

304. Chithrani, B. D., Ghazani, A. A. & Chan, W. C. W. Determining the size and shape dependence of gold nanoparticle uptake into mammalian cells. *Nano Lett.* **6**, 662–668 (2006).

305. Chithrani, B. D. & Chan, W. C. W. Elucidating the mechanism of cellular uptake and removal of protein-coated gold nanoparticles of different sizes and shapes. *Nano Lett.* **7**, 1542–1550 (2007).

306. Rogers, N. J. *et al.* Physico-chemical behaviour and algal toxicity of nanoparticulate CeO2 in freshwater. *Environmental Chemistry* vol. 7 50–60 (2010).

307. Franklin, N. M. *et al.* Comparative toxicity of nanoparticulate ZnO, bulk ZnO, and ZnCl2 to a freshwater microalga (Pseudokirchneriella subcapitata): the importance of particle solubility. *Environ. Sci. Technol.* **41**, 8484–8490 (2007).

308. Aruoja, V., Moosus, M., Kahru, A., Sihtmäe, M. & Maran, U. Measurement of baseline toxicity and QSAR analysis of 50 non-polar and 58 polar narcotic chemicals for the alga Pseudokirchneriella subcapitata. *Chemosphere* **96**, 23–32 (2014).

309. Yang, L. *et al.* Growth-inhibiting effects of 12 antibacterial agents and their mixtures on the freshwater microalga pseudokirchneriella subcapitata. *Environ. Toxicol. Chem.* **27**, 1201–1208 (2008).

310. James, G. O. *et al.* Fatty acid profiling of Chlamydomonas reinhardtii under nitrogen deprivation. *Bioresour. Technol.* **102**, 3343–3351 (2011).

311. Patil, V., Källqvist, T., Olsen, E., Vogt, G. & Gislerød, H. R. Fatty acid composition of 12 microalgae for possible use in aquaculture feed. *Aquac. Int.* **15**, 1–9 (2007).

312. Lavoie, M., Bernier, J., Fortin, C. & Campbell, P. G. C. Cell homogenization and subcellular fractionation in two phytoplanktonic algae: implications for the assessment of metal subcellular distributions. *Limnol. Oceanogr. Methods* **7**, 277–286 (2009).

313. Voigt, J. The lithium-chloride-soluble cell-wall layers of Chlamydomonas reinhardii contain several immunologically related glycoproteins. *Planta* **173**, 373–384 (1988).

314. Lee, D.-Y., Fortin, C. & Campbell, P. G. C. Contrasting effects of chloride on the toxicity of silver to two green algae, Pseudokirchneriella subcapitata and Chlamydomonas reinhardtii. *Aquat. Toxicol.* **75**, 127–135 (2005).

315. Chen, L. *et al.* Toxicological effects of nanometer titanium dioxide (nano-TiO2) on Chlamydomonas reinhardtii. *Ecotoxicol. Environ. Saf.* **84**, 155–162 (2012).

316. Perreault, F. *et al.* Toxicity of pamam-coated gold nanoparticles in different unicellular models. *Environ. Toxicol.* **29**, 328–336 (2014).

317. Wang, J., Zhang, X., Chen, Y., Sommerfeld, M. & Hu, Q. Toxicity assessment of manufactured nanomaterials using the unicellular green alga Chlamydomonas reinhardtii. *Chemosphere* **73**, 1121–1128 (2008).

318. Crist, R. H., Oberholser, K., Wong, B. & Crist, D. R. Amine-algae interactions: Cation-exchange and possible hydrogen bonding. *Environ. Sci. Technol.* **26**, 1523–1526 (1992).

319. D'Addio, S. M. *et al.* Novel method for concentrating and drying polymeric nanoparticles: hydrogen bonding coacervate precipitation. *Mol. Pharm.* **7**, 557–564 (2010).

320. Balasubramanian, S. V, Alderfer, J. L. & Straubinger, R. M. Solvent-and concentration-dependent molecular interactions of taxol (paclitaxel). *J. Pharm. Sci.* **83**, 1470–1476 (1994).

321. Chen, P., Powell, B. A., Mortimer, M. & Ke, P. C. Adaptive interactions between zinc oxide nanoparticles and Chlorella sp. *Environ. Sci. Technol.* **46**, 12178–12185 (2012).

322. Perreault, F., Bogdan, N., Morin, M., Claverie, J. & Popovic, R. Interaction of gold nanoglycodendrimers with algal cells (Chlamydomonas reinhardtii) and their effect on physiological processes. *Nanotoxicology* **6**, 109–120 (2012).

323. Pakrashi, S. *et al.* Cytotoxicity of aluminium oxide nanoparticles towards fresh water algal isolate at low exposure concentrations. *Aquat. Toxicol.* **132**–**133**, 34–45 (2013).

324. Ma, S., Zhou, K., Yang, K. & Lin, D. Heteroagglomeration of Oxide Nanoparticles with Algal Cells: Effects of Particle Type, Ionic Strength and pH. *Environ. Sci. Technol.* **49**, 932–939 (2015).

325. Gong, N. *et al.* Biotoxicity of nickel oxide nanoparticles and bio-remediation by microalgae Chlorella vulgaris. *Chemosphere* **83**, 510–516 (2011).

326. Lee, S.-W., Obregón, S. & Rodríguez-González, V. The role of silver nanoparticles functionalized on TiO 2 for photocatalytic disinfection of harmful algae. *RSC Adv.* **5**, 44470–44475 (2015).

APPENDIX A MECHANISMS OF ACTION OF THE POULTRY SANITIZER CETYLPYRIDINIUM CHLORIDE AGAINST *SALMONELLA* TYPHIMURIUM*

A.1. Overview

Cetylpyridinium chloride (CPC), a quaternary ammonium compound, is often used for the surface sanitation of fresh poultry animal carcasses to reduce human microbial pathogens, including *Salmonella enterica.* The interactions between *S. enterica* serovars Typhimurium and CPC were investigated to gain new insight into its mechanisms of action against the pathogen. *S.* Typhimurium LT2 cells were treated with increasing concentrations of the sanitizer, ranging from 0.002 to 0.8 % (w/v). Zeta (ζ) potential of bare *Salmonella* was measured to be -12.73±1.31 mV. Application of the sanitizer CPC (0.8 %) resulted in a sanitizer concentration-dependent increase to ζ-potential immediately from negative to positive, up to +16.63±1.38 mV, likely due to adsorption of cationic amine groups onto the negatively charged surface lipids. Upon CPC treatment, cell structure of microorganisms was disrupted: the outer membrane of cells was observed to either rupture or be covered by proteins to hinder the nutrient uptake. Plating experiments revealed correlation between the extent of CPC adsorption on microorganisms and bacterial growth: while cells with negative surface charge (i.e. no or very small amount of CPC adsorption) displayed bacterial growth, bacteria with positive surface charges strongly inhibited bacterial growth, producing fewer or no detectable colonies on plating medium surfaces. Overall, this study contributes to understanding the mechanisms of the sanitizer CPC to inhibit growth or inactivate the human pathogen *S.* Typhimurium.

A.2. Introduction

Salmonella is one of the most common foodborne pathogens, causing foodborne illnesses worldwide. Poultry, meat, eggs, fish, dairy, fruits and vegetables are common vehicles of

* Part of this chapter is reprinted with permission from "Cetylpyridinium chloride produces increased zeta-potential on *Salmonella* Typhimurium cells, a mechanism of the pathogen's inactivation" by Yegin, Y., J. K. Oh, M. Akbulut, and T. M. Taylor, 2019, NPJ Science of Food, 3, 1, 1-7, Copyright 2019, with permission from Nature Publishing Group.

Salmonella transfer. Nearly 1.2 million illnesses are estimated to occur from *Salmonella* consumption in human foods, resulting in an estimated 19,000 hospitalizations and 370 deaths each year in the U.S.[2] *Salmonella* causes approximately economic loss of 3.7 billion dollars annually.[166] Salmonellosis, disease caused by *salmonella*, has been associated with a wide variety of food products, especially with poultry.[167] Therefore, it is essential to reduce S*almonella* contamination in foods to reduce the risk of foodborne illnesses.[168] Poultry is a frequently identified vehicle for non-typhoidal *Salmonella* transmission to humans via consumption of contaminated foods, particularly fresh poultry products.[169] *Salmonella* Typhimurium was one of the top 10 *Salmonella* serotypes identified during testing of young chicken carcasses, ground beef, and turkey carcasses (USDA-FSIS, 2016).[170] The U.S. Department of Agriculture - Food Safety and Inspection Service (USDA-FSIS) regulates the manufacturing and safety of poultry products in the U.S., and in addition to the implementation of *Salmonella* performance standards for fresh poultry carcasses and products, there are several chemical sanitizers approved for use for the decontamination of poultry carcasses and cut pieces from this and other microbial foodborne pathogens.[171]

Quaternary ammonium compounds (QACs) are widely used as disinfectants and sanitizers in many different industries to prevent bacteria growth.[172] They display a broad spectrum of antimicrobial activity against various bacterial and fungal microbes.[173] Antimicrobial activity of QACs originates from disruption of outer and cytoplasmic membrane lipid bilayers through association of the positively charged quaternary nitrogen with anionic and/or zwitterionic polar head groups of phospholipids.[174] Hydrophobic tails of the surfactant sanitizer inserted into the hydrophobic region of the microbial membrane. As a result, QACs emulsify the membrane of the bacteria, producing membrane integrity loss, cytosol leakage, and transmembrane potential

destabilization.[175] Leakage of cytoplasmic content causes death of the microorganism.[176] These compounds display very long shelf stability without losing their antimicrobial activities.[177] The sanitizer cetylpyridinium chloride (CPC) has been approved to be used for the surface decontamination of fresh poultry carcasses in the U.S. up to a maximum content of 0.8% with requirement for rinse-off prior to final packaging.[178]

CPC demonstrates antimicrobial and bactericidal activities because of its absorption onto cell membrane and cell wall.[179,180] When a bacterial cell and antimicrobial sanitizer encounter the first time, the sanitizer binds to the cell surface of the bacteria, which changes the outer layers of the bacterial cell. Hence, the sanitizer penetrates through those layers and reaches the cytoplasmic membrane. Concentration and exposure time of the CPC affect the degree of bacterial membrane damage.[181] Some morphological changes were observed on *S.* Typhimurium cells when the bacterial cells were suspended into 0.1 % (wt/vol) of CPC for 5 min at SEM. However, bacterial membrane damage was not easy to distinguish for the bacteria cells suspended for 1 min and 3 min from non-treated cells (bare bacteria).

The impacts of CPC concentration and exposure period on resulting inhibition and reduction of *S.* Typhimurium were investigated on chicken skin surfaces.[182] After chicken surfaces were inoculated, the antimicrobial efficiency of sanitizer CPC for the concentrations of 1 mg/ml upto 8 mg/ml for 1, 3, and 10 min exposure times. Application of 4.0 mg/ml CPC for 3 min produced a 4.87 $\log_{10}$-cycle reduction of inoculated *S.* Typhimurium counts. 4.5 $\log_{10}$-cycle reductions in the number of bacteria were obtained: 8 mg/ml for 1 min CPC exposure; 4 mg/ml for 3 min CPC exposure; and 2 mg/ml for 10 min CPC exposure. Therefore, their study demonstrated that the reduction of *S.* Typhimurium was both CPC concentration and sanitizer exposure dependent. As the sanitizer exposure time was increased the necessary sanitizer

concentration was decreased for the same number of bacteria reductions. Effect of different concentrations of CPC and other chemical sanitizers such as trisodium phosphate (TSP), lactic acid (LA), and grape fruit seed extract were tested for the reduction of the number of inoculated *Salmonella* on chicken skin.[183] *S.* Typhimurium were inoculated on chicken skins and chemical solutions were then sprayed on skin surfaces for 30 sec at 20 °C and 206 kPa. Researchers reported that while varying the concentrations of TSP, LA, and grapefruit seed extract application did not produce significant differences in *Salmonella* reduction, 0.5% CPC yielded a higher reduction in numbers of *S.* Typhimurium than that by 0.1% CPC application. A 1.9 $\log_{10}$ and 1.5 $\log_{10}$ bacteria reduction obtained when chicken skins were sprayed with 0.5% and 0.1% CPC, respectively. Li et. al. also investigated the efficiency of different sanitizers on reductions of *S.* Typhimurium.[184] They designed a spray testing chamber to evaluate the effectiveness of 0.85% sodium chloride (NaCl), 5% or 10% TSP, 5% or 10% sodium bisulfate (SBS), 1% LA, and 0.1% CPC at varying concentrations, pressures (207, 345, or 827 kPa), and exposure times (30 or 90 sec). 0.85% NaCl treatment of chicken carcasses did not show a significant reduction of *Salmonella* as compared to the treatment with tap water. The longer spraying time (90 seconds) resulted in more *Salmonella* reduction than the shorter spraying time (30 sec). The treatment of higher concentration (10%) of TSP and SBS showed higher reduction in the number of bacteria than the treatment of their lower concentration (5%). 30 sec spraying with 0.1% CPC resulted in 0.8 $\log_{10}$ reduction while 90 sec spraying with 0.1% CPC resulted in 1.6 $\log_{10}$ reduction in the number of bacteria at 827 kPa pressure. The 90 sec spraying of chicken carcasses with 10% TSP, 10% SBS, or 0.1% CPC at 827 kPa showed 3.8, 2.6, and 1.6 $\log_{10}$ reduction of the bacteria, respectively. They did not observe any significant bacteria reduction between 207 and 345 kPa of chemical application pressures. However, spraying applications at 827 kPa pressure showed significant reduction in the number

of *Salmonella*. Same bacteria reduction (1.6 log) was observed for 0.1% CPC at 827 kPa or 1% LAC at 345 kPa spraying for a spraying time 90 sec. Antibacterial activity of CPC to reduce Salmonella and Campylobacter on different chicken parts in a post chill tank were examined.[185] Treatment of 0.35% CPC was able to reduce 2.5 log CFU/mL *Salmonella* and 4 log CFU/mL *Campylobacter* while 0.6% CPC was able to reduce 3.5 log CFU/mL *Salmonella* and 5 log CFU/mL *Campylobacter*.

There is a significant number of research reports in literature discussing the antibacterial efficiency of CPC on *Salmonella*. However, there is a lack of information about the physico-chemical antimicrobial mechanisms of *Salmonella* inhibition and inactivation as related to outer membrane surface charge neutralization resulting from the interaction between CPC and the bacterium. The objective of this study was to investigate the interaction between outer membrane surface charge and membrane potentials of *Salmonella* Typhimurium and the sanitizer CPC, as well as to investigate cellular integrity loss by sanitizer application under concentration conditions used in poultry slaughter. While changes in surface charges of *Salmonella* cells were measured by ζ-potential analysis, size distributions of treated bacterial cells were measured by dynamic light scattering (DLS). The effect of sanitizer application on the bacterial structure and geometry was visualized via scanning electron microscopy (SEM). CPC-treated *Salmonella* were non-selectively enumerated test bacterial inhibition and culturability loss by sanitizer use.

A.3 Materials and methods

A.3.1 Preparation of sanitizer solutions

The sanitizer containing CPC (Cecure®, CPC: 40% active agent per manufacturer guidance) was provided by Safe Foods Corp. (N. Little Rock, AR). Working solutions of the sanitizer were prepared to deliver increasing concentrations of sanitizer; sanitizer was diluted in

sterilized, tempered deionized water to produce the concentrations of CPC (0.002, 0.005, 0.006, 0.013, 0.025, 0.05, 0.1, 0.2, 0.4, 0.6, and 0.8%) upon addition to reaction tubes containing bacterial cells.

A.3.2 Microorganism preparation

Salmonella Typhimurium LT2 (American Type Culture Collection [ATCC] No. 700720) (Manassas, VA) was revived from cryo-storage (-80°C) from the culture collection of the Food Microbiology Laboratory (Department of Animal Science, Texas A&M University, College Station, TX) by duplicate sequential passages in volumes of sterile tryptic soy broth (TSB; Becton, Dickinson and Co., Fairfield, NJ) followed by 24 hr incubation at 35°C. Following revival from cryo-storage, slants of the organism were prepared for refrigerated storage and use. Tryptic soy agar (TSA; Becton, Dickinson and Co.) slants, previously sterilized by autoclaving at 121°C for 20 min, were inoculated and then incubated for 24 hr at 35°C. Following incubation, slants were overlaid with 1.0-2.0 mL sterilized mineral oil and refrigerated until needed. At the initiation of experiments, a loop (10 μL) of culture was scraped from TSA slants and transferred into 9.0 mL sterile TSB and incubated at 35°C for 24 hr. A second passage in fresh sterile TSB was then completed to produce a culture for inoculum preparation and use.

A.3.3 Size measurements of Salmonella Typhimurium cells following CPC treatment

Salmonella Typhimurium LT2 cells following revival were centrifuged (4,000 rpm, benchtop mini-centrifuge) for 15 min at ambient conditions (25°C) to produce a bacterial pellet. Following centrifugation, the supernatant was poured off and cell pellets were suspended in one volume of sterilized phosphate-buffered saline (PBS; Sigma Aldrich, St. Louis, MO) with agitation. Three identically completed centrifugation and washing procedures were completed in PBS. After the preparation of approximately 8.99 ± 0.03 $\log_{10}$ CFU/mL bacteria, *Salmonella* were

treated with CPC to one of the concentrations indicated in Section 3.1. Immediately thereafter, size distribution of treated cells was measured by DLS using a Zetasizer ZS90 particle size and zeta-potential analyzer (Malvern Instruments, Ltd., Westborough, MA). The measurements were carried out at a scattering angle of 90º at 25 ºC.

A.3.4 ζ-potential measurements of Salmonella Typhimurium following CPC treatment

Impacts of the differing concentrations of sanitizer application on outer surface charge of *Salmonella* cells were measured at multiple increments over a 60 min period at ambient temperature using a Zeta-Sizer ZS90 Instrument (Malvern Instruments, Ltd., Westborough, MA) after bacteria cells were treated with CPC. Zeta potential measurements of *Salmonella* were performed in 0.5mM PBS (pH of 7.31±0.02) to minimize the effect of pH fluctuations.

A.3.5 Microbiological analysis of survival of Salmonella Typhimurium cells treated with CPC

Salmonella Typhimurium cells were serially diluted in PBS after three centrifugation and washing process (Section 2.3) prior to addition to sanitizer. For non-treated (control) and treated cell suspensions alike, 3M™ Petrifilm™ Aerobic Count Plate films were used to non-selectively enumerate sanitizer-surviving *Salmonella* cells, following serial dilution and incubation of Petrifilms at 37 °C for 48 hr.

A.3.6 Microscopic evaluation of Salmonella Typhimurium cell shape and morphology following CPC sanitizer treatment

Microscopic images were obtained by scanning electron microscopy (SEM) using a JSM-7500F electron microscope (JEOL, Tokyo, Japan). SEM images were taken of *Salmonella* cells after ~0 min (only few sec exposed), 1, 3, and 9 min treatment with 0.8% CPC. After the treatment cells were rinsed in sterile milli-Q water to remove CPC residue.

A.3.7 Statistical analysis of data

All DLS, ζ-potential, and plating (cell enumeration) experiments were replicated three times over three differing dates (N=3). Additionally, SEM imaging was completed for three identically prepared sets of samples over three differing dates. Data analysis was completed using ORIGIN® v.8 software (OriginLab Corp., Northampton, MA). All microbiological data were $\log_{10}$-transformed prior to statistical analysis. One-way analysis of variance (ANOVA) with Tukey's Honestly Significant Differences (HSD) post hoc test was used to determine whether there were significant differences in data between the treatments, at a significance level of P<0.05.

A.4 Results and Discussion

A.4.1 Size and surface charge changes in Salmonella Typhimurium cells following sanitizer exposure as a function of sanitizer concentration

Shape, size, and surface characterization of non-treated *Salmonella* cells (bare bacteria) are shown in Figure 42. Scanning electron microscopy revealed *Salmonella* cells were rod-shaped with a width of 1.95± 0.3 μm and a diameter of 0.9±0.17 μm (Fig. 42A). Mean hydrodynamic radius of *Salmonella* was measured to be 1.3±0.07 μm via DLS (Fig. 42B). Likewise, mean ζ-potential of *Salmonella* cells not CPC-treated was electro-negative (–12.73±1.31 mV) in PBS (Fig. 42C). Phosphates and carboxylic acid groups in lipopolysaccharides is responsible for the observed negative zeta potential.[186]

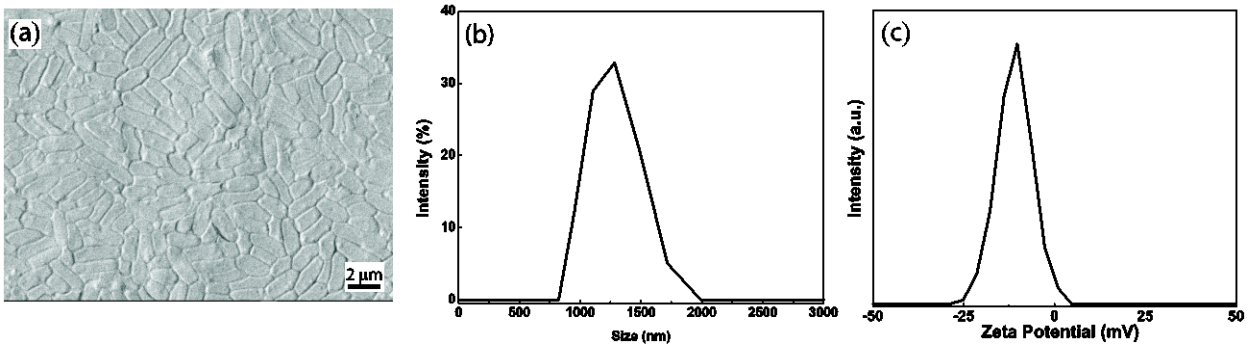

Figure 42: Shape, size, and surface characterization of *Salmonella Typhimurium* cells not treated by CPC: (a) scanning electron micrograph (SEM) of the bacteria cells, (b) size distribution for *salmonella* cells obtained by dynamic light scattering (DLS) analysis, and (c) surface charge of the cells obtained by ζ-potential measurements.

A.4.2 Electrostatic interactions between CPC and Salmonella

Bacterial surface components and functional groups are primarily responsible for the observed zeta potential values.[70] Bacterial surfaces charges originate from phosphoric, carboxylic, and amino groups. In addition, other components located in the cell membranes and cell wall of bacteria cells such as teichoic acid, proteins, lipopolysaccharides, phospholipids, and teichuronic acid can affect the surface charges.[187,188] These groups can display different electrostatic interactions against different agent.[77] Figure 43A shows the effect of CPC on the ζ-potential of *S.* Typhimurium cells as a function of sanitizer application. In these experiments, *Salmonella* cells were treated with different concentrations of CPC (0, 0.002, 0.005, 0.006, 0.013, 0.025, 0.05, 0.1, 0.2, 0.4, 0.6, and 0.8%); surface charge was measured as soon as cells were treated with CPC. After the bacterial cells were treated with different concentrations of CPC, ζ-potential immediately increased in exponential fashion, likely due to the cationic amino groups of CPC and its covering of negatively-charged surface components of cell membrane. There was a sharp increase observed in samples' ζ-potential upon treatment with up to 0.2% CPC: a change from –12.73±1.31 mV (0%

CPC) to +14.43±1.78 mV (0.2% CPC) (Fig. 38A). Above 0.2% CPC, the ζ-potential plateaued, asymptotically approaching to +16.63 ± 1.38 mV at 0.8% CPC. This finding indicates the full coverage or saturation of negatively charged functional groups on the cell wall.

The distribution of mean bacterial cell sizes shifted to larger values upon CPC treatment of increasing concentration (Figure 43B). The mean size distribution changed from 1.3±0.07 µm to 4±1.12 to µm by exposure to CPC at concentrations ranging from 0% to 0.8%. The addition of CPC also broadened the size distribution of the cells, producing a unimodal distribution with a larger full width at half maximum. These findings would indicate sanitizer treatment at increasing concentrations of CPC resulted in development of cell aggregates. This could be due to the reduction of cell surface charge repulsion via covering over of anionic functional groups on the cell's outer membrane, the colloidal stabilization of bacteria or the complexation and bridging of neighboring bacteria walls with oppositely charged CPC.

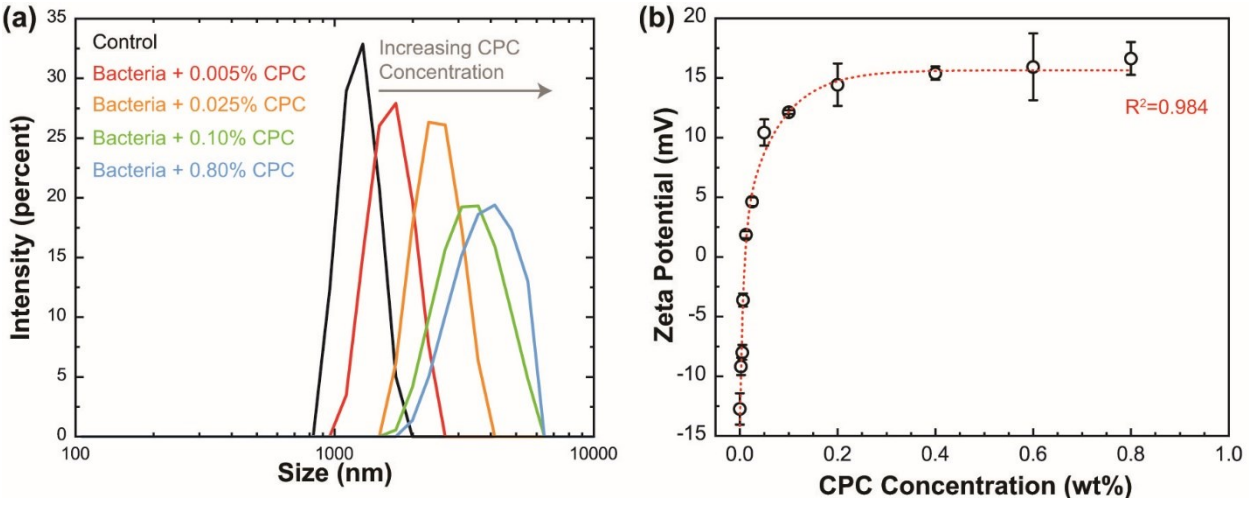

Figure 43: Hydrodynamic size (intensity averaged) of *Salmonella* Typhimurium as a function of concentration of CPC **(a)** obtained by dynamic light scattering and the change in the average ζ-potential (mV) of *Salmonella* Typhimurium cells with addition of CPC **(b)**. Symbols depict mean values from three independent replications while

error bars depict one sample s.d. (N=3). The fitted trend line (dashed) is the two-phase (double) exponential decay model with the coefficient of determination of 0.984.

A.4.3 Influence of different CPC concentration on Salmonella growth

The dependence of *S.* Typhimurium cells growth on the CPC concentration is depicted in Figure 44. The numbers of culturable bacterial cells declined with increased concentrations of CPC. The number of bare bacteria (non-treated control) was 8.99 ± 0.03 $\log_{10}$ CFU/mL, whereas no bacterial growth was detected for 0.2, 0.4, 0.6, and 0.8% CPC treatments. Interestingly, these concentrations also corresponded to positive zeta potential values for the bacteria/CPC systems. Between 0.0 and 0.2% CPC, bacterial survival decreased with increasing CPC concentration in a dose-dependent exponential manner (Fig. 39). At 0.005% CPC treatment, the numbers of *S.* Typhimurium cells decreased from 8.99 to 3.24 $\log_{10}$ CFU/mL, a 5.76 $\log_{10}$ CFU/mL reduction. It is important to highlight that even at very low concentrations (0.005%), CPC is able to disinfect 5.76 log CFU/ mL, indicating very strong potency of CPC as a sanitizer when there is direct contact between the sanitizer CPC and bacteria cells However, the antimicrobial efficacy of sanitizers also depends on organic load, such as fat and protein during immersion chilling. Organic loads in immersion chilling tanks can decrease the efficiency of sanitizers. The zeta potential was –7.99 ± 0.62 mV for 0.005% CPC treatment (Fig. 43A). Thus, even a small content of sanitizer in a liquid buffer led to a statistically significant decrease in the number of *Salmonella* CFU, indicating a strong correlation between the number of bacteria and CPC treatment. Whereas an increase in ζ-potential after the sanitizer CPC applied would likely reduce the repulsion between cells based on charge distribution across outer membranes, a decline of 5.74 $\log_{10}$-cycles with a change in surface charge of only 4.74 mV (-12.73 - -7.99 mV) was not expected to produce such a significant decline

in cell counts of the bacterium. Hamaud and Baker investigated the antimicrobial mechanism of action of 8N8, a water-in-oil emulsion, and W60C, a liposome, against Gram-negative bacteria.[189] Depending on their study, positively charged W60C showed much stronger antimicrobial activity than negatively charged 8N8 against negatively charged Gram-negative bacteria. While identical charged bacteria and 8N8 repelled each other, different surface charged bacteria and W60C attracted each other. Their electron microscopy showed fusion and internalization of W60C on bacteria cells. Ionic attraction forces between the antimicrobial agent (W60C) and bacteria increased their interactions. Ionic repulsion between negatively charged bacteria and 8N8 increased its resistance against 8N8. Interactions between bacteria and cationic and anionic surfactants were also investigated by Zhang et al.[190] Cationic surfactant, tetraphenylethene-dodecyltrimethylammonium bromide (TPE-DTAB), showed high interaction with negatively charged *Escherichia coli* while anionic surfactant, tetraphenylethene-sodium dodecyl sulfonate (TPE-SDS), did not show any interaction. Positive surface zeta potential of TPE-DTAB attracted bacteria through electrostatic attraction, after that long alkyl chain of the surfactant inserted into bacterial membrane and caused the death of bacteria due to damaging the membrane permeability. However, negatively charged TPE-SDS did not attract bacteria and could not come closer to the negatively charged bacteria due to electrostatic repulsion between them. In essence, there is a high correlation between the surface charge and bacterial growth results. No *Salmonella* growth was observed when surface charge of the bacteria was turned into positive due to the addition of sanitizer CPC. However, *Salmonella* growth was observed when surface charge of the bacteria was negative after the treatment with no or very small amount of CPC.

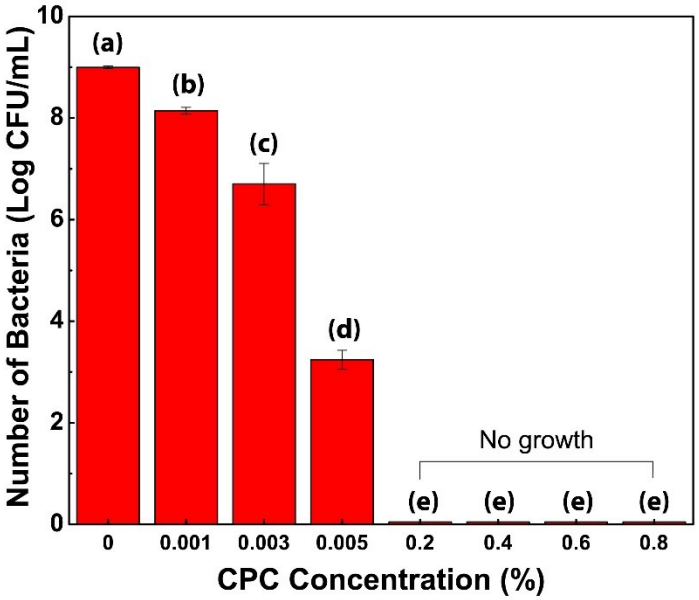

Figure 44: Least square means of *Salmonella* Typhimurium in presence of increasing CPC concentrations. Bars depict means from triplicate identically completed replicates; error bars indicate one standard deviation from means. Bars labeled e same letter are not significantly different from each other ($p<0.05$) by one-way ANOVA followed by Tukey's post hoc test.

A.4.4 Morphological disruptions of Salmonella induced by CPC

Figure 45 shows the morphology of *Salmonella* cells with CPC treatment. Microscopic images were collected from 0.8% CPC treated samples after ~0 (few seconds), 1, 3, and 9 min. Non-treated cell shape and morphology is depicted in Figure 45A. Bare bacteria (control: sanitizer untreated cells) were intact and smooth in terms of its cellular structure. Conversely, the morphology of bacterial cells started to change upon application of the sanitizer. Even short-term exposure (~ 0 min) to the sanitizer produce changes in bacterial cell shape and arrangements. The sanitizer CPC, which is a positively charged cationic surfactant can interact with negatively charged groups located on the cell membrane and destroy the cell membrane and cause the death of the bacteria cell.[191] *S.* Typhimurium is a gram-negative bacterium and its outer surface is

covered by lipopolysaccharides, polysaccharides, phospholipids, and various extracellular proteins such as pili, fimbriae, and flagella. . Negatively charged peptidoglycan and positively charged CPC can be combined by electrostatic interaction. Cells started to aggregate and clump together upon CPC addition to concentrations enough to cause *S.* Typhimurium counts to decline and caused deformation on the cell wall. As a result, cells appeared to lose their smooth rod-shaped structure as shown in Figure 45B, C, and D. As sanitizer exposure time was increased, some bacteria cells were fused together, likely through membrane lipids fusing or blending between adjacent cells following CPC-modulated loss of membrane surface anionic charges. Furthermore, some *Salmonella* cells had craters on their cell walls, indicating loss of cell membrane integrity as a result of CPC treatment (Figure 45C and 45D). Nikitina et al. obtained similar microscopy images for *Staphylococcus aureus* after treatment with quaternary bis-phosphonium and ammonium salts.[192] *Staphylococcus aureus* cells lost their intact and smooth cell morphology similar to these finding.

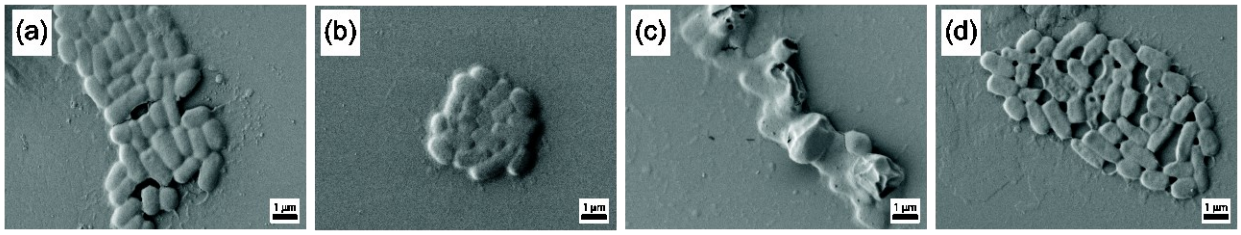

Figure 45: Scanning electron microscopy (SEM) images for 0.8% CPC-treated *Salmonella* Typhimurium cells treated by 0.8% CPC-treated cells at exposure times of 0 min (a), 1 min (b), 10 min (c), and 60 min (d). Images are representative of three independently completed experimental replications completed on differing days.

A.5. Conclusions

In this study, the interactions between *Salmonella* Typhimurium cells and the poultry sanitizer CPC were investigated to gain new insights into the sanitizer mechanism of action.

Bacterial cells were treated with different concentrations of CPC; the addition of CPC resulted in a shift in cell surface charge from electro-negative to electro-positive in a concentration-dependent manner. Increased concentrations of CPC resulted in a significant increase in the size of cell aggregates measured by DLS, indicating cells clump together and may even go membrane lipid exchange or membrane fusions, as a result of surfactant application. SEM analysis also supported the hypothesis that damage to cell shape and membrane integrity could be caused by sanitizer exposure. This study suggests a correlation between the variation of surface charge and plating results, as a result of cell inactivation following sanitizer application. Bacterial cells were reduced to non-detectable counts (from a starting load of 8.99 ± 0.03 $\log_{10}$ CFU/ml with a contact time of 1 min) at concentrations of CPC of 0.2% (2,000 ppm), but demonstrated sanitizer concentration-dependent survival at very low concentration to the sanitizer (0.005% CPC). Addition of CPC resulted in increased ST ζ-potential, likely a result of outer membrane component negative charges being covered by the cationic quaternary amino group in the CPC. These data indicate that CPC produces inhibition of the pathogen through initial charge attraction to electro-negative components on the *Salmonella* surface, and at sufficient concentration, charge neutralization leads to loss of membrane component ordering and organization. The capacity of alkyl chain components on CPC to insert into bacterial membranes was not directly investigated in this study, but possibly added to the observed antimicrobial activity of the sanitizer. In the current study we propose a mechanism of CPC interaction with *Salmonella*, that being the change in surface charge of treated cells via CPC covered anionic components of the cellular cytoplasmic membrane, resulting in disorganization and membrane integrity loss.

APPENDIX B NEUTRALIZATION BY LECITHIN AND EFFECT OF MIXING ORDERS ON *SALMONELLA* TYPHIMURIUM CELLS*

B.1. Overview

CPC is a quaternary ammonium sanitizer approved for fresh poultry animal carcass sanitization from microbial human pathogens, such as *Salmonella enterica*. Nonetheless, the interactions of CPC with *Salmonella* cells, and the mechanism of the sanitizer's neutralization by lecithin remains largely unknown. This study aimed to investigate the interaction of CPC with lecithin and *Salmonella* Typhimurium to determine the interactions of the sanitizer and neutralizer impacting the bacterium's survival. Application of 0.8% CPC is proposed to produce loss of microbial membrane integrity with loss of electrostatic repulsion between individual cells, resulting in the eventual emulsification of membrane lipids with cytoplasmic contents leakage. Our findings point to a two-phase interaction between CPC and lecithin impacting *S.* Typhimurium survival. The first consists of electrostatic attraction and charge neutralization between oppositely charged components of pathogen cell and CPC. The second involves formation of aggregates between sanitizer and pathogen, or between sanitizer, pathogen membrane lipids, and lecithin. Mixing order of CPC and neutralizer also showed a significant effect on the survival of bacteria.

B.2. Introduction

In the United States, the manufacture of fresh poultry products is regulated by the U.S. Department of Agriculture Food Safety and Inspection Service (USDA-FSIS). For poultry carcasses and fresh cut pieces, multiple chemical sanitizers are approved to decontaminate eviscerated carcasses and pieces from microbial foodborne pathogens, including *Salmonella enterica.*[193] The quaternary ammonium sanitizer cetylpyridinium chloride (CPC) has been repeatedly studied and reported effective for the sanitization of poultry carcass and meat surfaces

* Part of this chapter is reprinted with permission from "Cetylpyridinium chloride produces increased zeta-potential on *Salmonella* Typhimurium cells, a mechanism of the pathogen's inactivation" by Yegin, Y., J. K. Oh, M. Akbulut, and T. M. Taylor, 2019, NPJ Science of Food, 3, 1, 1-7, Copyright 2019, with permission from Nature Publishing Group.

from microbial pathogens at up to 0.8%.[181,194,195] Recent research has indicated that carryover of some sanitizers into poultry carcass sampling rinse fluids may prevent the successful detection of pathogenic microbes during routine verification testing.[196,197] Consequently, recent changes to routine testing methods for poultry carcass testing to detect microbial pathogens have raised questions about the utility and necessity of chemical sanitizer neutralizing agents (i.e., neutralizers) and their impact on poultry processors' ability to adhere to federal food safety performance standards for fresh poultry products.[198,199] Dey and Engley[200] previously incorporated lecithin into an antimicrobial neutralization formula for the purposes of counteracting QAC-type sanitizers. Mohammad et al.[201] reported that the incorporation of soy lecithin at 7.0 g/L effectively neutralized CPC (0.8% w/v), facilitating *Salmonella* detection in a model microbiological medium.

The antimicrobial mechanisms of the sanitizer have been previously suggested to result from the insertion of alkyl chains into microbial membranes, resulting in membrane permeation and cytoplasmic leakage.[202,203] Nonetheless, studies investigating the mechanisms of CPC antimicrobial activity against *Salmonella enterica* or other microbial pathogens on poultry carcass or meat surfaces are lacking in the scientific literature. Breen et al.[204] reported CPC addition reduced or reversed *Salmonella* cell attachment to chicken skin samples, suggested to result at least partially from electrostatic interactions of the cationic surfactant with anionic headgroups and side groups on the bacterium's outer membrane. Ma et al.[205] using a CPC-fixing clay for testing antimicrobial activity of CPC against enterotoxigenic *E. coli* and *Salmonella* Typhimurium, demonstrated cell morphology disruption by CPC application, as well as respiration inhibition in cells of both pathogens.

In addition to a general lack of data that describe mechanistic interactions of CPC with *Salmonella* or other human pathogenic bacteria, data are not known to be available detailing the

interactions of the pathogenic microbe with the sanitizer CPC when a neutralizing agent such as lecithin is introduced. Understanding the interactions between these three agents would improve food safety specialists' ability to accurately determine the reliability of poultry testing methods for pathogen detection. The objectives of this research were to identify the key components of the mechanisms of CPC neutralization by lecithin to yield increased understanding of the interaction of sanitizer and neutralizer, as impacting *Salmonella* Typhimurium (ST) survival, investigate the mixing order effect of ST, sanitizer CPC, and neutralizer agents on ST survival. It was hypothesized by researchers that CPC would exert a surfactant-type antimicrobial activity, likely resulting in membrane permeabilization and/or lipopolysaccharide (LPS) release, and that lecithin would neutralize this by counter-acting or inhibiting CPC mixing within bacterial cell membranes.

B.3. Methods

B.3.1 Bacterial isolate preparation

Salmonella enterica serovar Typhimurium (ST) Leeligen Type (LT) 2 was revived from cryo-storage (-80°C) from the culture collection in the Food Microbiology Laboratory, Department of Animal Science, Texas A&M AgriLife Research (College Station, TX, USA) by aseptically inoculating a loop of preserved culture into 10.0 mL steam-sterilized (121°C, 15 min) tryptic soy broth (TSB; Becton, Dickinson and Co., Sparks, MD, USA), and incubating statically for 24 hr at 35°C. This isolate was chosen to accommodate Texas A&M University Institutional Biosafety Committee requirements for Biosafety Level (BSL) 1 containment within microscopy and physico-chemical analytical laboratories within the Artie McFerrin Department of Chemical Engineering, Texas Engineering Experiment Station (College Station, TX, USA). Following 24 hr of incubation, a loopful (10.0 μL) of overnight culture was aseptically sub-cultured in 10.0 mL of sterile TSB and incubated in similar fashion for 24 hr at 35°C.

B.3.2 Preparation of neutralizer reagents

Refined soy lecithin (reagent grade) was purchased from Alfa Aesar (Ward Hill, MA, USA), and was prepared in sterile distilled, deionized water in order to deliver up to 1.0% lecithin upon mixing with CPC-containing samples, with or without ST cell addition. Lecithin maximal content was chosen based on USDA-FSIS incorporation of 7.0 g/L (0.7% w/v) lecithin in the formula of Neutralizing Buffered Peptone Water (nBPW) for the rinsing of poultry carcasses and fresh cut pieces.[206]

B.3.3 Salmonella Typhimurium surface ζ-potential change by lecithin exposure

The impact of lecithin inclusion was measured at 2.0, 1.5, 1.0, and 0.7% lecithin to determine concentration dependency on observed ζ-potential. Lecithin was applied to 0.8% CPC-treated bacterial cells (1.0 min treatment period prior to neutralizer addition) and ζ-potential changes measured immediately thereafter. ζ-potential measurements were collected continuously until stable.

B.3.4 Enumeration of Salmonella Typhimurium cells treated by lecithin

Salmonella Typhimurium cells were prepared as described above. Differing concentrations of lecithin (2.0, 0.7, and 0.0%) were applied to ST cells pre-exposed for 1.0 min at ambient temperature condition (25°) to 0.005, 0.2 or 0.8% CPC (CPC content at which ST cells ζ-potential became constant, intermediate CPC concentration, and maximum allowable CPC concentration allowed for poultry sanitizing, respectively). Following lecithin addition, a 40.0 min holding period was completed prior to enumeration of surviving bacterial cells. Surviving ST cells were enumerated on tryptic soy agar (TSA; Becton, Dickinson and Co.) following preparation of serial dilutions in phosphate-buffered saline (PBS; Thermo-Fisher Scientific, Waltham, MA, USA) and

incubating aerobically for at least 24 hr at 37°C. Resulting plate counts were $\log_{10}$-transformed for purposes of statistical analysis.

B.3.5 Mixing order effect on Salmonella Typhimurium survival

Survival of Salmonella Typhimurium cells will be investigated depending on the mixing order of CPC and lecithin. At first mixing condition, differing concentrations of CPC (0.005 or 0.2%) will be mixed with 2.0% lecithin for 1.0 min at ambient temperature condition (25°) then the mixture of CPC and lecithin applied to ST cells. At second mixing condition, ST cells will be mixed with 0.7% lecithin for 1.0 min at ambient temperature condition (25°) then the ST and lecithin mixture will be exposed to differing concentrations of CPC (0.005 or 0.2%). At the final mixing condition, ST cells, 0.7% lecithin, and differing concentrations of CPC (0.005 or 0.2%) will be mixed at the same time for 1.0 min at ambient temperature condition (25°). Surviving bacteria cells will be enumerated on TSA following preparation of serial dilutions in PBS and incubating aerobically for at least 24 hr at 37°C. Resulting plate counts will be log10-transformed for purposes of statistical analysis.

B.3.6 Visualization of CPC and lecithin-treated Salmonella Typhimurium cell morphology

Microscopic images were obtained by scanning electron microscopy (SEM) using a JSM-7500F electron microscope (JEOL, Tokyo, Japan), in order to visualize any changes in ST cell shape and morphology as a function of sanitizer and lecithin application. The samples were coated with 15 nm platinum/palladium (Pt/Pd) to eliminate any positive charging effects. The SEM was operated at an accelerating voltage of 1.0 kV and emission current of 20 μA. SEM images were taken of *Salmonella* cells after 1, 10, and 60 min treatment with 0.8% CPC. After the treatment cells were thoroughly rinsed in sterile milli-Q water to remove CPC residue. Identically prepared

ST cells were then subjected to 0.8% CPC treatment (1.0 min) and then treated with 0.7% lecithin, after which micrographs were collected after 1, 10, and 60 min of lecithin exposure.

B.3.7 Data analysis

All DLS, ζ-potential, and plating (cell enumeration) experiments were replicated three times in identical fashion over differing days (N=3). Additionally, SEM imaging was completed for three identically prepared independent sets of samples over three differing dates. Statistical analysis of data was completed using ORIGIN® v.8 software (OriginLab Corp., Northampton, MA, USA). All microbiological data were $\log_{10}$-transformed prior to statistical analysis. One-way analysis of variance (ANOVA) with Tukey's Honestly Significant Differences (HSD) post hoc test was used to determine significant differences in data between the treatments at a significance level of P<0.05.

B.4. Results and Discussion

B.4.1 Lecithin addition impacts on CPC-treated Salmonella

The influence of lecithin on the zeta-potential of 0.8% CPC-treated ST cells is shown in Figure 46. Lecithin effect was measured at 0.7, 1.0, 1.5, and 2.0% lecithin to determine concentration dependency on observed effects. Lecithin was applied to 0.8% CPC-treated bacterial cells (1.0 min treatment period prior to neutralizer addition) and ζ-potential changes measured immediately thereafter. Addition of 1.5-2% lecithin reduced cationic charge distribution of samples, indicating the capacity of lecithin to neutralize CPC activity.

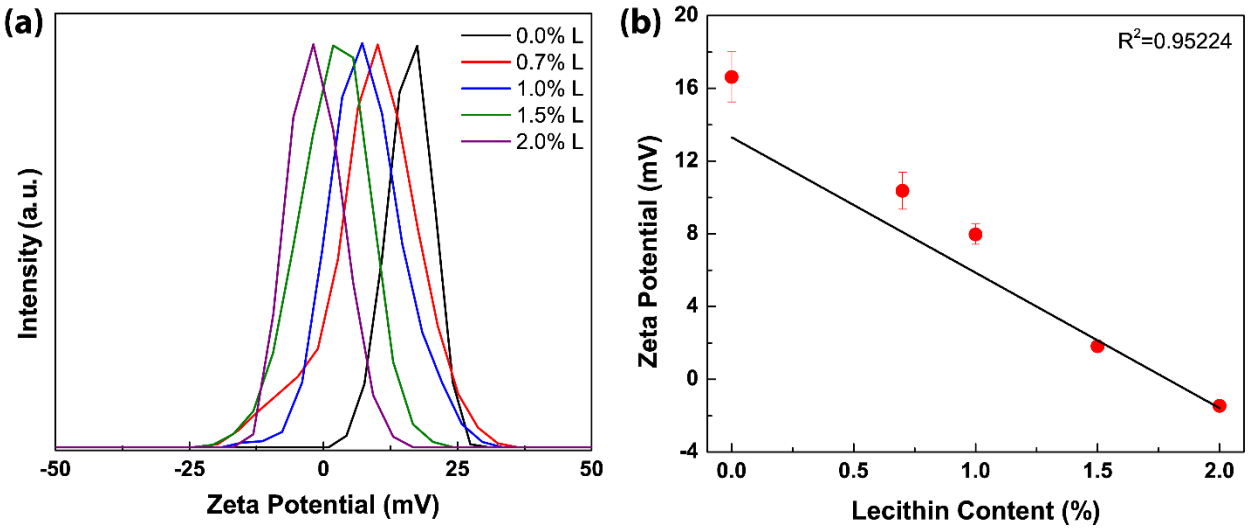

Figure 46: ζ-potential shifts depending on lecithin concentrations (a) and mean ζ-potential of *Salmonella* Typhimurium cells in the presence of lecithin after 0.8% CPC treatment. Values in panel (b) represent means of triplicate identical replications; error bars indicate one s.d. Fitted trend line depicts inverse relation of ζ-potential against increased lecithin addition, indicating increasing anionic characteristic of lecithin suspension.

B.4.2 CPC effect on Salmonella ζ-potential with 1.0% lecithin

Non-CPC-exposed ST ζ-potential readings were predictably electro-negative consistently throughout measurements (Figure 47). Similarly, the neutralizer lecithin was also electro-negative, with a ζ-potential of approximately -45 mV. Samples of ST cells treated with increasing concentrations of CPC displayed increased ζ-potential, up to 11.8-13.6 mV, at sufficient concentrations overwhelming the surface charges of ST cells. Surface electrophoretic mobility (ζ-potential) of 0.2 or 0.8% CPC was significantly impacted by contact with up to 1.0% lecithin. The surface potential of a mixture of 0.2% CPC with 1.0% lecithin hovered around 0.0 mV, whereas 0.8% CPC with 1% lecithin ζ-potential ranged between 8.0 and 8.7 mV. ζ-potential values for sanitizer and lecithin mixtures increased as sanitizer concentration was increased from 0.2 to 0.8%

(from 11.8±1.2 mV at 0.2% CPC to 13.6±0.1 mV at 0.8% CPC at 0 min incubation in sanitizer treated cells). Mixing of CPC with lecithin effectively negated the anionic charges of lecithin. In comparison, when treated with CPC, the ζ-potential of cells treated with 1.0% lecithin and sanitizer increased in a similar fashion (from -0.6±1.5 mV at 0.2% CPC in 1.0% lecithin-treated cells to 8.7±0.2 mV at 0.8% CPC in 1.0% lecithin-treated cells) (Figure 42). The increases in ζ-potential in both scenarios may indicate a mechanism of sanitizer activity, that of membrane surface charge disruption, in addition to permeabilization of the microbial membrane to water, ion, and leakage. Addition of lecithin following CPC application onto suspended cells, in reducing the ζ-potential, likely competed with the *Salmonella* cell membranes for interaction with CPC. CPC possessed strong ability to increase the surface charge of molecules and bacterial cells (Figure 47), reducing ST ability to maintain proper respiration and metabolism.

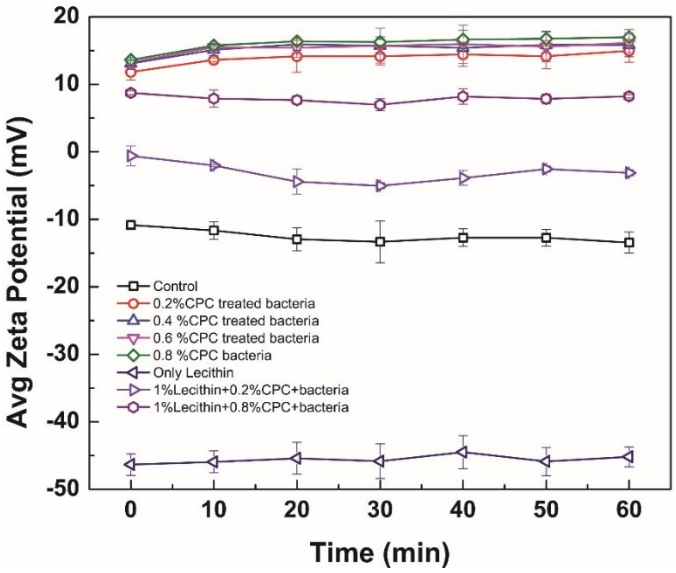

Figure 47: Change in ζ-potential of *Salmonella* Typhimurium cells immediately following mixing with CPC and 1.0% lecithin, over 60 min holding period at 25°C. Symbols and connecting lines depict means of triplicate identical replications, while error bars depict one s.d. from sample means.

B.4.3 Survival of Salmonella treated within lecithin

The dependence of ST survival on CPC concentration, and the concentration of added lecithin, is presented in Figure 48. The mean count of non-treated control bacteria was 8.99±0.03 $\log_{10}$ CFU/mL, whereas no detection of ST survivors was achieved for 0.2 or 0.8% CPC treatments (limit of detection: 1 CFU/mL). Interestingly, these sanitizer concentrations produced electro-positive ζ-potential values for the bacteria/CPC systems. At 0.005% CPC treatment, the numbers of *S.* Typhimurium cells decreased from 8.99 to 3.24 $\log_{10}$ CFU/mL, a 5.76 $\log_{10}$ CFU/mL reduction. Also, at 0.005% CPC, bacterial survival increased with addition of 0.7 or 2.0% lecithin, but not in a dose-dependent manner (Fig. 48). Thus, a small content of sanitizer in a liquid buffer led to a statistically significant decrease in the number of *Salmonella*, indicating a strong correlation between the number of bacteria and CPC treatment ($p<0.05$). The lack of an apparent dose effect for 0.7 and 2.0% lecithin at the low concentration of sanitizer, however, indicates the neutralizer was sufficient to provide protection to ST cells, possibly by competing with ST cells for electrostatic interactions between anionic members of lecithin with the cationic surfactant, or by formation of structures wherein lecithin sequestered CPC from ST cells. At higher concentrations of sanitizer (0.2 and 0.8%), however, even 2.0% lecithin was generally unable to overcome the inactivation of the microorganism by the sanitizer. Even though lecithin was added at 1 minute after addition of CPC to ST cells, inactivation of the pathogen occurred quickly. The general lack of pathogen survival at higher CPC doses, even when lecithin was added at higher concentrations, suggests that if a dose effect is to be observed, it will be at a lecithin concentration substantially higher than that approved by the USDA-FSIS in its nBPW formulation (0.7% w/v). Additionally, it may require lecithin to contact *Salmonella* cells prior to CPC, unlikely to occur

given the sequence of sanitizer and neutralizer use in commercial poultry harvest and routine testing.

Hamouda and Baker, Jr.[189] investigated the antimicrobial mechanism of action of 8N8, a negatively charged water-in-oil emulsion, and W60C, a cationic liposome, against the Gram-negative bacteria *Escherichia coli* and *Vibrio cholerae*. Their study demonstrated the positively charged W60C showed much stronger antimicrobial activity than the anionic 8N8 against negatively charged Gram-negative bacteria when divalent cations were chelated. In the current study, we utilized distilled deionized water, reducing the potential for cations to inhibit the attraction of CPC to *S.* Typhimurium cell surfaces. Interactions between bacteria and cationic and anionic surfactants were also investigated by Zhang et al.[190] The cationic surfactant, tetraphenylethene-dodecyltrimethylammonium bromide (TPE-DTAB), showed high interaction with *Escherichia coli* by fluorescence microscopy, while the anionic surfactant tetraphenylethene-sodium dodecyl sulfonate (TPE-SDS) did not show any interaction. An electro-positive surface ζ-potential of TPE-DTAB (when in excess versus TPE-SDS) likely resulted in electrostatic attraction to *E. coli* cells membrane surfaces, followed by long alkyl chain of the surfactant inserting into bacterial membrane and producing leakage of cytoplasmic contents.[190] However, negatively charged TPE-SDS did not attract bacteria and could not come closer to the negatively charged bacteria due to electrostatic repulsion between cell surface and surfactant.

It is important to highlight that at very low concentration (0.005%; 0.00015 M)), CPC (exposure period of 1.0 min) was able to produce a 5.76 $\log_{10}$ CFU/mL reduction in ST cells in the absence of lecithin, indicating strong potency of CPC as a sanitizer, despite being slightly above the critical micelle concentration (CMC) in water (0.00012 M).[207] Antimicrobial efficacy of sanitizers is impacted by organic load encountered during poultry processing, such as fat and

protein content in poultry immersion-type chilling waters. Organic loads in immersion chilling tanks can decrease the efficiency of sanitizers, potentially requiring elevated sanitizer concentrations to overcome inactivation by organic matter. In the current study, aggregation of membrane components of *Salmonella* was observed when surface charge of suspended bacteria was turned to electro-positive due to the addition of excess CPC, a cationic surfactant.

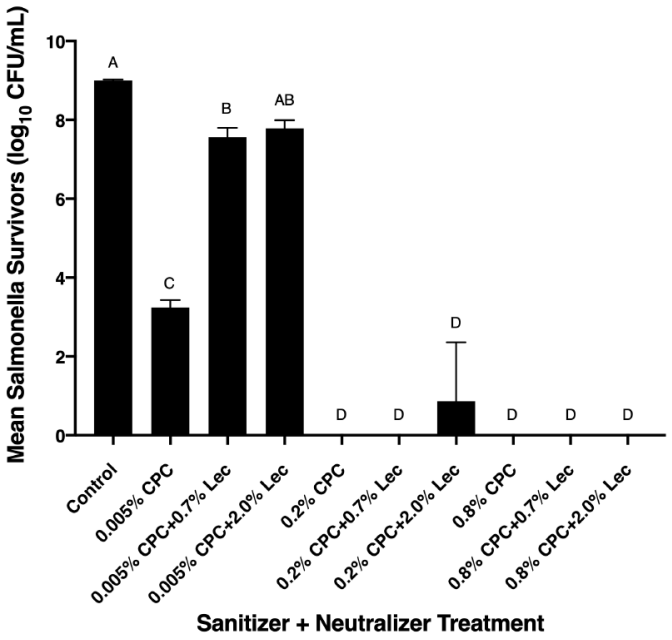

Figure 48: Least square means of *Salmonella* Typhimurium counts in presence of increasing CPC concentrations over a 1.0 min exposure period, with or without 0.7 or 2.0% Lecithin (Lec) exposure (40 min post lecithin incorporation exposure period). Bars depict means from triplicate identically completed replicates; error bars indicate one s.d. from means. Bars labeled with the same letter are not statistically different from each other (p<0.05) by one-way analysis of variance and Tukey's post-hoc means separation test.

B.4.4 Impact of lecithin on cell appearance and morphology

In experiments determining the impact of sanitizer with subsequent neutralizer addition to ST cells on cellular shape and morphology changes, micrograph images were collected at 1, 10,

and 60 min following treatment with sanitizer (Figure 49A-C). For ST cells treated only by 0.8% CPC, as the exposure time was increased, sanitizer-treated cells appeared to initially aggregate (Fig. 40B) and membrane lipids emulsify (Fig. 40C), potentially due to surface charges being covered by the cationic surfactant. *Salmonella* cells lost cell structure during prolonged exposure to the sanitizer (Fig. 45C, D; Fig. 49A-C). Conversely, Figure 49 panes D-F show embedded bacterial cells and cell matter within a layer of lecithin (added after 1.0 min CPC application at 0.8%). SEM images were quite different after lecithin addition as compared to only CPC-treated bacteria. Application of lecithin into the sample vessel resulted in a layer of surfactant forming on the glass slide, covering the remaining cells, and likely furthering emulsification of the membrane lipid components of ST cells. On solid surfaces, addition of lecithin could provide protection to ST cells by covering susceptible membrane components prior to sanitizer insertion, should the neutralizer contact the microbial cell prior to sanitizer contact. This would potentially give rise to increased pathogen survival, as reported in other research detailing neutralization of CPC by lecithin.[197] In free-swimming cells, such as those which might be found in poultry carcass rinse fluids, addition of lecithin might be expected to form complexes with CPC rather than forming a protective coating on surface-adhered bacteria, given sufficient content of lecithin.[196]

CPC has been reported effective for reducing the numbers of *Salmonella enterica* or other bacterial pathogens on surfaces of poultry carcass or cut pieces.[194,208] Gerba,[209] citing McDonnell,[210] described early steps in quaternary sanitizer antimicrobial mechanisms against bacteria, indicating requirements for attachment and penetration of the outer membrane in Gram-negative bacteria and/or the cytoplasmic membrane in Gram-negative and -positive bacteria, following membrane lipid emulsification and disorganization. However, impacts of the cationic charge component on bacterial surface charge was not discussed. Similarly, other researchers have

more recently indicated biscationic QACs demonstrated greater antimicrobial activity against the human enteric pathogen *Campylobacter* versus monocationic QACs (including CPC). The increased charge of the bis-cationic QACs led to greater pathogen reduction within the experimental period compared to CPC and other monocationic QACs.[211] On the other hand, research into the influence of CPC treatment on bacterial adherence to oil/water interfaces with the bacterium *Pseudomonas fluorescens* reported little change in cell membrane hydrophobicity following CPC treatment (200 mg/L), though cell surface ζ-potential was significantly changed, similar to findings in the current study.[212] These researchers suggested that influences of the cationic sanitizer on cell surface ζ-potential, specifically charge neutralization through interactions of oppositely charged components, likely led to increased adhesion and interaction with the oil/water interface. A similar impact was observed here, as changes in cell surface charge of CPC-treated *Salmonella* were observed, and loss of surface charge led to increased observed membrane lipid components reorganizing and/or aggregating together.

Quisno et al.[213] reported the inclusion of lecithin as effective for the neutralization of bacteriostatic activity of cationic surfactants and other cationic disinfectants, though no mechanism of activity was suggested. Recent research indicates the inclusion of sanitizer neutralizers, such as lecithin, for the neutralization of quaternary ammonium sanitizers like CPC, increases the likelihood of *Salmonella* recovery during poultry carcass or parts testing.[196,214] The formation of lecithin/CPC mixed micelles was not detected in the current study by DLS or ζ-potential analysis when mixed with *Salmonella* Typhimurium cells, though mixing of the surfactants potentially occurred, given changes in ζ-potential for lecithin:CPC mixtures where 1% lecithin was mixed with CPC at differing concentrations. Microscopy indicated mixing of sanitizer

along with bacterial membrane components, likely leading to cell death through cytoplasmic contents leakage via membrane integrity loss.

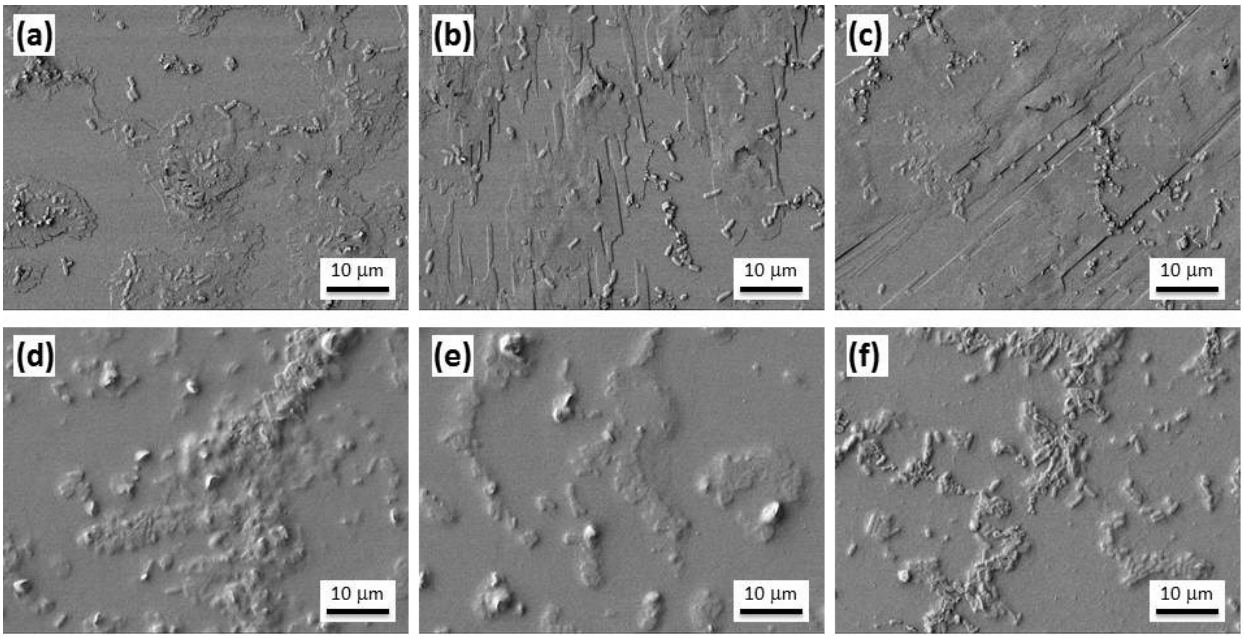

Figure 49: Scanning electron microscopy (SEM) images (a-c) for 0.8% CPC-treated *Salmonella* Typhimurium cells and (d-f) lecithin effect for 0.8% CPC-treated cells for different exposure times for 1 min (a, d), 10 min (b, e), and 60 min (c, f). Images are representative of three independently completed experimental replications completed on differing days. Scale bar is 10 µm.

B.4.5 Impact of mixing order on Salmonella Typhimurium survival

The dependence of ST survival related to the mixing order of CPC, ST, and lecithin are shown at Figure 50-53. ST cells were treated with sanitizer CPC, then the cells were mixed with lecithin, is presented in Figure 50. Sanitizer treated cells (0.005% or 0.8%) were mixed with differing concentrations of neutralizer. Addition of lecithin increased the number of bacteria at low concentrations of CPC (0.005%) which was not sufficient concentration to kill all the bacteria

cells. However, if the concentration of CPC was high (0.8%) enough to inactivate the microorganisms, lecithin did not increase the number of cells or recover them.

The other mixing condition is presented in Figure 51. Two different CPC concentrations (0.005 or 0.2%) were mixed with 2.0% lecithin and then the mixture of CPC and lecithin mixed with ST. Lecithin concentration was high enough to neutralize CPC for both concentrations. Mixing sanitizer with neutralizer before mixing with bacteria cells significantly decreased efficacy of the sanitizer. Even though 0.2% CPC concentration is high enough to kill ST when it is first applied to ST, it could not overcome neutralizing effect of lecithin and could not inactivate the cells.

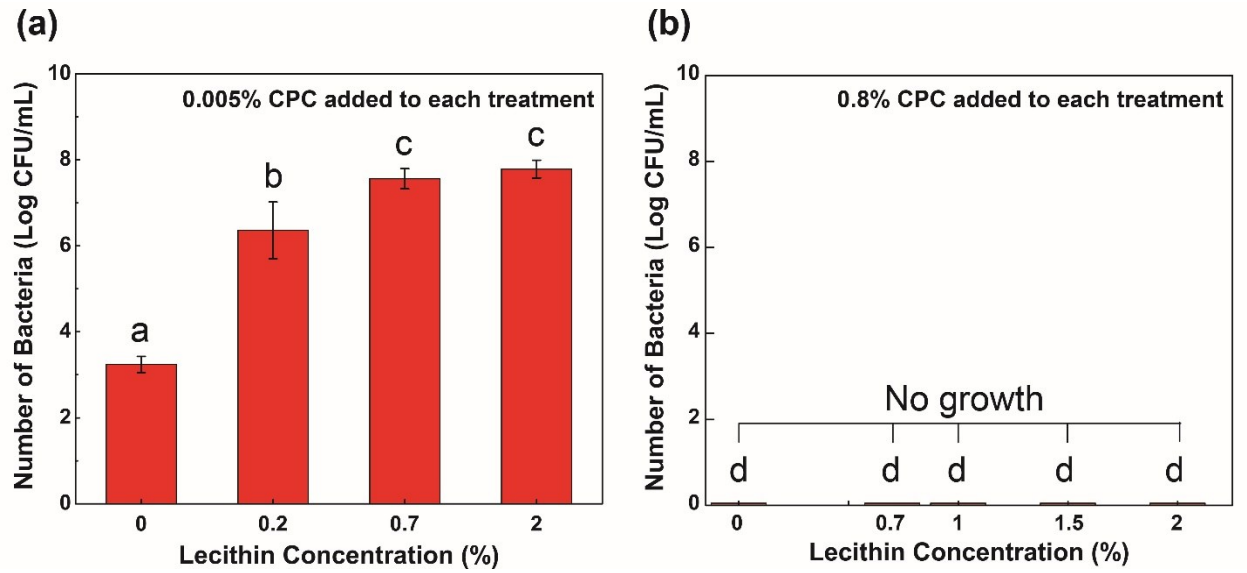

Figure 50: Least square means of *Salmonella* Typhimurium counts, after the cells were treated with CPC (0.005% or 0.8%CPC) over a 1.0 min exposure period then mixed with various concentrations of lecithin. Bars depict means from triplicate identically completed replicates; error bars indicate one s.d. from means. Bars labeled with the same letter are not statistically different from each other (p<0.05) by one-way analysis of variance and Tukey's post-hoc means separation test.

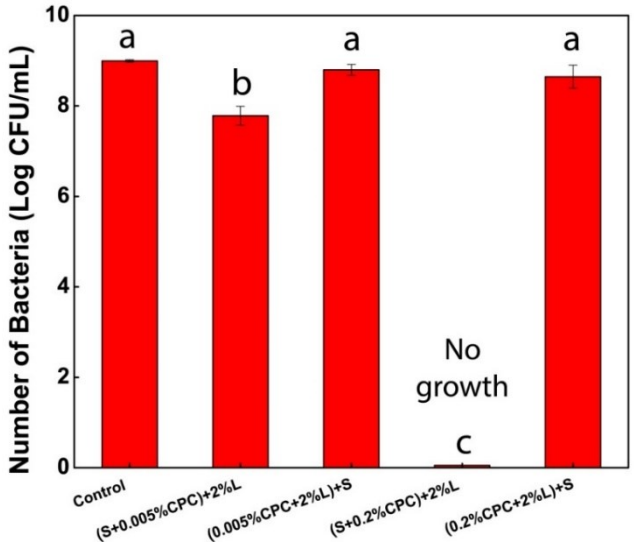

Figure 51: Least square means of *Salmonella* Typhimurium counts, after CPC (0.005% or 0.2%CPC) was mixed with 2.0% lecithin over a 1.0 min exposure period then mixed with the cells. Bars depict means from triplicate identically completed replicates; error bars indicate one s.d. from means. Bars labeled with the same letter are not statistically different from each other (p<0.05) by one-way analysis of variance and Tukey's post-hoc means separation test.

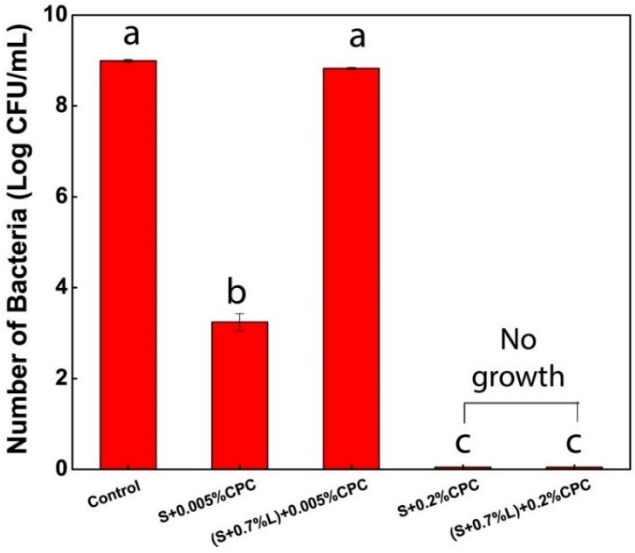

Figure 52: Least square means of *Salmonella* Typhimurium counts, after the cells were mixed with 0.7% lecithin over a 1.0 min exposure period then mixed with CPC (0.005 or 0.2%). Bars depict means from triplicate identically

completed replicates; error bars indicate one s.d. from means. Bars labeled with the same letter are not statistically different from each other (p<0.05) by one-way analysis of variance and Tukey's post-hoc means separation test.

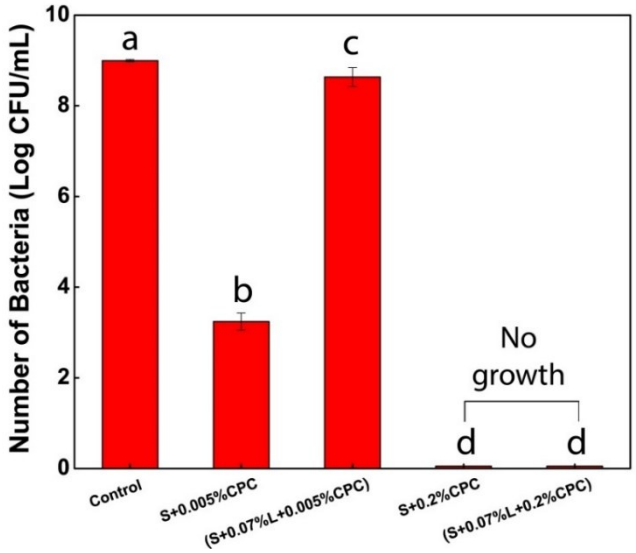

Figure 53: Least square means of *Salmonella* Typhimurium counts, after the cells, 0.7% lecithin, and CPC (0.005 or 0.2%) were mixed all together at the same Bars depict means from triplicate identically completed replicates; error bars indicate one s.d. from means. Bars labeled with the same letter are not statistically different from each other (p<0.05) by one-way analysis of variance and Tukey's post-hoc means separation test.

The third mixing condition is ST cells were mixed with 0.7% neutralizer, after that the ST and lecithin mixture was exposed to differing concentrations of CPC (0.005 or 0.2%) in Figure 52. Mixing with lecithin decreased the efficiency of sanitizer by covering the surface of the cells and minimizing the interaction of sanitizer with ST. 0.005%CPC did not show any significant decrease in ST cells when applied after the cells mixed with lecithin as compared to control bacteria while the same concentration of CPC was able to produce a 5.76 $\log_{10}$ CFU/mL reduction in ST cells in the absence of neutralizer. 0.2% CPC treatment after cells were mixed with lecithin was high enough to kill ST cells.

Final mixing condition is mixing of ST, 0.7% lecithin, and CPC (0.005 or 0.2%) all together at the same time (Figure 53). High concentration of CPC (0.2%) inactivated ST cells while lower concentration of CPC (0.005%) could not inactivate the cells. As a result, if the sanitizer concentration is not enough to inactivate all the cells, mixing order of neutralizer, sanitizer, and bacteria can make significant difference in terms of bacterial inactivation.

B.6. Conclusions

In the current study, we present hydrodynamic radius, ζ-potential (electrophoretic mobility), microbiological and microscopic data describing the interactions of the cationic poultry sanitizer CPC with the bacterium *Salmonella* Typhimurium, with the inclusion of the sanitizer neutralizer lecithin. Addition of lecithin at up to 2% potentially provided some degree of neutralization to CPC by competing for charge attraction with *Salmonella* cells, though plate count data indicate even this concentration of neutralizer was insufficient to afford pathogen survival post-CPC exposure. The use of sanitizer neutralizers during poultry carcass and cut pieces routine sampling has been reported necessary to improve the accuracy of testing for *Salmonella* and *Campylobacter* by the USDA-FSIS. Lecithin as a neutralizer, at lower CPC concentrations, competed for electrostatic attraction with CPC and *Salmonella* membrane components, though at higher concentrations of CPC, lecithin at concentrations used in USDA-FSIS routine testing media was insufficient to neutralize all sanitizer activity via charge neutralization or mixed micelle complex formation, determined by *Salmonella* inactivation by CPC.

APPENDIX C ANTIFUNGAL ACTIVITY OF NEEM OIL-LOADED POLYMERIC NANOPARTICLES AGAINST ASPERGILLUS FLAVUS

C.1. Overview

Molds causes a health concern because of their mycotoxins production. These compounds are toxic to humans and animals. The aim of this study was to develop and characterize neem oil-loaded nanoparticles that can be used to effectively control the growth of *Aspergillus flavus*. This study demonstrates neem oil can be loaded into polymeric nanoparticles with sustainable release profile. Neem oil-loaded NPs were characterized for size, zeta-potential, release, encapsulation efficiency, and inhibition of *A. flavus*. The NPs showed a size 300.6 nm, zeta potential -16 mV, with an encapsulation efficiency 84.78%. Both encapsulated neem oil and non-encapsulated neem oil treatments inhibited the growth of the fungi. However, neem oil-loaded NPs inhibited *A. flavus* growth at much lower concentrations as compared to unencapsulated neem oil. Neem oil-loaded NPs displayed sustained release with a time constant of 120 h, maintaining their anti-pathogenic properties over a prolonged time period. Encapsulated neem oil prevented the growth of *A. flavus* at day 7 while non-encapsulated neem oil treated *A. flavus* showed an increased growth. Antimicrobial NPs may be useful decontamination of various crops.

C.2. Introduction

Fungi can cause negative health effects as some strains release toxins to the environment causing allergies and other health issues like cancer.[215] Cereal grains can be contaminated with filamentous fungi that produce mycotoxins under inappropriate conditions.[216] The most known mycotoxins are produced by *Aspergillus*, *Fusarium*, and *Penicillium*.[217,218,219] Peanuts, rice, figs, sorghum, cocoa beans, spices, oil seeds, fruits and vegetables are high risk group food commodities to aflatoxin contamination.[220]

Aflatoxigenic strains of *Aspergillus* can produce aflatoxins which are known as carcinogenic, hepatotoxic, and teratogenic.[221] Aflatoxins can cause various heath issues such as acute liver damage, hormonal imbalance, skin disorders, tumor and liver cirrhosis.[222]

Nanotechnology is a technology provided advantage to synthesize antifungal compounds.[223] For example, silver nanoparticles are commonly used antimicrobial agents and inhibit fungal pathogens effectively.[224] Polymeric nanoparticles have received great interest for agricultural applications among various carrier systems because of solid matrices that can protect active compound and enable release of active compound over time.[225] Polymeric nanoparticles provide numerous advantages such as biodegradability, incorporation of active compounds with no need of chemical reactions, and prolonged release of active compounds with the selection of materials used during the nanoparticle preparations.[164,226] The objective of this study was to develop antifungal nanoparticles loaded with neem oil using the triblock copolymer Pluronic F-127 and characterize resulting physico-chemical and antifungal properties. Resulting neem oil-loaded NPs were characterized for size, zeta potential, drug release profile, and antifungal capacity of neem oil NPs against Aspergillus flavus.

C.3. Materials and Methods

C.3.1. Preparation of neem oil-loaded nanoparticles

Organic cold-pressed filtered un-refined 100% neem oil (Deepthi Organics LLC, Greeensboro, NC, USA) and Pluronic F-127 (CAS #9003-1-6; Sigma-Aldrich Corp., St. Louis, MO, USA) were dissolved in tetrahydrofuran (CAS #109-99-9; Sigma-Aldrich Corp.; THF), to a ratio of 1:2 (neem oil:pluronic F-127). Then THF solution was added in milli-Q water, to a ratio of 1:10 (THF mixture:milli-Q water) and sonicated for 3 min. Neem oil-loaded nanoparticles are placed into a standard regenerated cellulose membrane (molecular weight cut-off 12,000-14,000

Da; approximately 2.0 nm diameter cut-off) (Spectrum Laboratories, Inc., Rancho Dominguez, CA); membranes were then placed into beakers containing 2.0 L milli-Q water to remove THF.

C.3.3. Characterization of Neem Oil-loaded Nanoparticles

Particle size distribution of neem oil-loaded NPs was measured by dynamic light scattering (DLS) following four-fold dilution in milli-Q water using a Zeta-sizer ZS90 particle size and zeta potential analyzer (Malvern Instruments, Ltd., Westborough, MA). The measurements were carried out at a scattering angle of 90° at 25°C to determine sizes and size distribution. Zeta potential (ζ-potential) of the NPs were also measured using a Zeta-Sizer ZS90 Instrument (Malvern Instruments, Ltd.)

C.3.4. Release Kinetics of Neem Oil from Polymeric NPs

Neem oil-loaded NPs (10.0 mL) were added into standard regenerated cellulose membrane (molecular weight cut-off 12,000-14,000 Da; approximately 2.0 nm diameter cut-off) (Spectrum Laboratories, Inc., Rancho Dominguez, CA). After that, the membranes were placed into beakers containing 200.0 mL milli-Q water. Unencapsulated neem oil was expected to passively diffuse through dialysis membranes, while NPs were expected to be unable to diffuse through membranes, preventing entrapped neem oil from diffusion. Changes in concentration of free neem oil were tracked by spectroscopy using a UV-1800 UV/Visible scanning spectrophotometer (Shimadzu Corp., Columbia, MD), scanning all wavelengths from 200 to 800 nm. UV measurements were performed at ambient temperature at 1, 2, 4, 8, 24, 48, 72, 96, 120, 144, 168, 192, 216, 240, 264, 288, and 312 h. Three independent replications were completed for each measurement.

C.3.5. Preparation of Aspergillus Flavus

Plate counts were used to observe the microbial growth. *Aspergillus flavus* was counted by identifying the fungus in color and growth stages. A concentration of 16.4x10^4 CFU/ml of *A.*

flavus (Carolina Biological Supply Company, Burlington, NC) was plated onto 100 mm × 15 mm sterile petri dishes containing Potato Dextrose Agar (Sigma Aldrich, Merck KGaA, Darmstadt, Germany). Three replicates from each diluted sample group were observed for microbial growth. After 7 days of incubation at 25°C, colony-forming units (CFUs) per ml were counted to compare the microbial growth of different treatments.

C.3.6. Antifungal Assays

After *Aspergillus flavus* cultures were prepared, various concentrations of treatments were applied to determine their antifungal activities. *A. flavus* were treated with neem oil-loaded NPs, non-encapsulated neem oil, and polymer. Various concentrations of unencapsulated neem oil and encapsulated neem oil were applied on *A. flavus* to determine antifungal activity. The assay was replicated three times; antifungal activity of free or entrapped neem oil were determined. Neem oil-containing (free, encapsulated) A PF127 control was included to determine fungal growth. Antifungal activity of free or encapsulated neem oil was assayed following plate counting. Numbers of surviving pathogens from tubes containing free or encapsulated neem oil were determined by spreading 0.1 mL of culture fluid directly from a sample well onto the surface of a Potato Dextrose Agar-containing Petri dish. Inoculated Petri dishes were incubated at 35°C. The growth of the cells was observed every 24 hr.

C.3.7. Statistical Analysis of Data

Data analysis was completed using ORIGIN® v.8 software (OriginLab Corp., Northampton, MA). One-way analysis of variance (ANOVA) was used to test the differences between treatments and Tukey's Honestly Significant Differences (HSD) test was performed to separate means differing at $p<0.05$.

C.4. Results and Discussion

C.4.1. Characterization of Nanoparticles and Encapsulation Efficiency

Size distribution of NPs were obtained by DLS (Figure 54). Hydrodynamic NP size distribution ranged between 100 to 1000 nm. Average diameter of NPS were 300.6±6.2 nm. Polydispersity index (PDI) values approximated 0.21. Average zeta-potential of NPs were -16±0.4 mV (Fig. 55).

The neem oil-loaded were synthesized using pluronic F127 as stabilizer, which coated the surfaces of the particles and provided steric stabilization. Therefore, surface electron repulsion was not the main factor affecting colloidal stability.

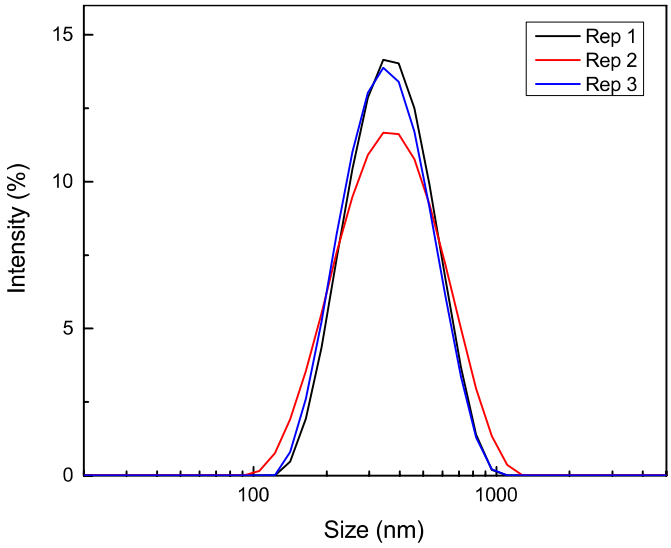

Figure 54: Particle size distribution of neem oil-loaded nanoparticles.

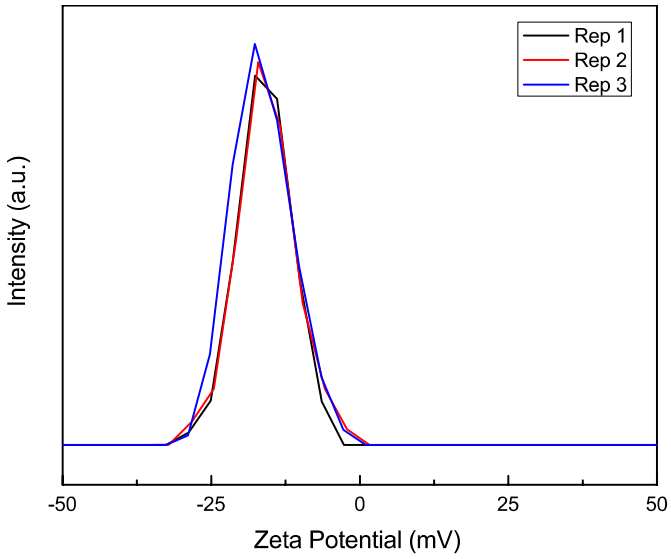

Figure 55: Zeta-potential of neem oil-loaded nanoparticles.

Encapsulation efficiency determination can provide an information about the percent of drug entrapped within a polymeric matrix from the amount of drug added in NP synthesis. Encapsulation efficiency for neem oil in Pluronic F127 was 84.8±3.3%. Non-encapsulated neem oil was removed during dialysis while removing THF.

C.4.2. Release of Neem Oil from PF127 Nanoparticles

The release of neem oil from NPs into water was measured by the spectroscopic determination of neem oil concentration as shown in Figure 56. The measurements were collected up to 312 h at 25°C. The concentration of neem oil diffusion through the dialysis membrane increased from 0 to 120 h. After that, the concentration of neem oil diffusing across the dialysis membrane reached to a plateau from 144 h to 312 h of storage.

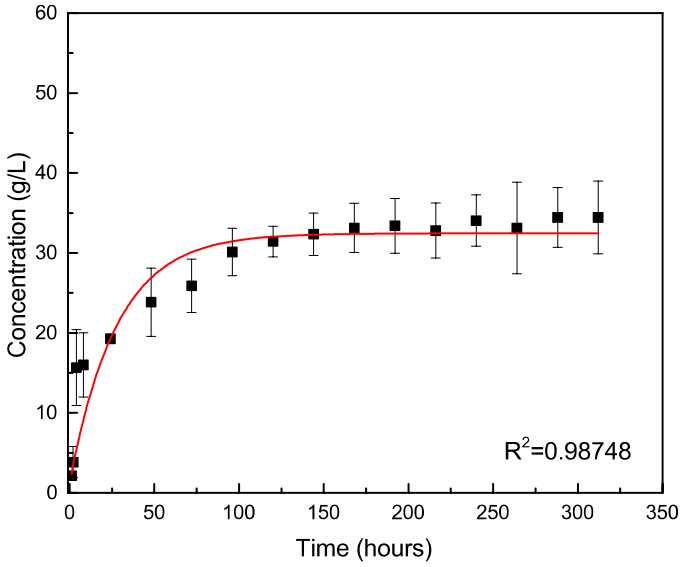

Figure 56: Neem oil release from nanoparticles stored at 25°C as a function of time. Symbols depict means from three independent replications while error bars depict one sample standard deviation (n=3).

C.4.3. Antifungal Activity of Neem Oil NPs against Aspergillus flavus

Antifungal activity of nano-encapsulated and unencapsulated neem oil applied to *A. flavus* are provided in Table 10. The reductions of the fungi for nano-encapsulated neem oil were greater than those obtained for unencapsulated neem oil. Antifungal neem oil-loaded NPs inhibited pathogen growth at lower neem concentrations as compared to unencapsulated neem oil (Table 10). The growth of *A. flavus* observed at day 5 in Petri dishes. Only polymer treated fungi showed the highest growth with 20±2 CFU at day 5. Mold covered the entire Petri dishes at day 7 and not possible to count the colonies. Therefore, Pluronic F127 used for the encapsulation of neem oil did not have any antifungal effect against *A. flavus*. The number of fungi growth without any treatment was 15.33±2.08 and 17.67±2.08 CFU at day 5 and day 7, respectively. Fungi growth was decreased with the increased concentrations of encapsulated and unencapsulated neem oil. Highest concentrations of neem oil (10%) for encapsulated and unencapsulated resulted in a fungicidal

effect. Unencapsulated neem oil treated A. flavus showed an increased growth from day 5 to day 7 for neem oil concentrations between 0.5% to 4%. However, *A. flavus* treated with NPs did not show any growth increase at day 7. Neem oil-loaded NPs showed sustained release behaviors. Therefore, neem oil continued to be released over time and inhibited the growth of fungi. These results suggest that encapsulation of neem oil can enhance their bioavailability and transport of neem oil, which may explain observed reductions in *A. flavus* for encapsulated versus unencapsulated neem oil (Table 10).

Table 10: Antifungal effect of free and polymeric NP-encapsulated neem oil against *Aspergillus flavus*.

Neem Oil Concentration (%)	Condition	Day7	
		Average	St-dev
0.5	NP1	7.33	0.58
1	NP2	1.67	1.53
1.5	NP3	1.33	1.53
2	NP4	1.00	0.00
2.5	NP5	0.67	1.15
3	NP6	0.67	0.58
4	NP7	0.33	0.58
10	NP8	0	0
0.5	FD1	11.33	1.53
1	FD2	7.00	3.00
1.5	FD3	6.67	1.53
2	FD4	4.33	0.58
2.5	FD5	4.33	2.08
3	FD6	2.67	1.53
4	FD7	1.67	1.15
10	FD8	0	0
0	Control (only mold)	17.67	2.08
0	Control Polymer	Covered entire plate (hard to count)	

C.5. Conclusions

Encapsulation of neem oil in the polymer Pluronic® F-127 demonstrated a significantly greater decrease on the number of *A. flavus* as compared to unencapsulated neem oil. Nano-encapsulation of neem oil enhanced antifungal activity against *A. flavus* by lowering the required amount of neem oil necessary for inhibition through improved transport of neem oil to the mold membranes. Release profile indicates that neem oil continued to release over time and kept showing antifungal activity. Neem oil-loaded NPs are very promising application for the inhibition of *A. flavus* growth on the crops. Further, release profile analysis indicates that encapsulation of neem oil will help the slow release of neem oil and maintain the efficacy of neem oil. Physico-chemical and antifungal properties of Pluronic® F-127 NPs containing neem oil were characterized for the potential of the application neem oil-loaded NPs for the determination of their antifungal capacity on food surfaces.

APPENDIX D ECOTOXIC EFFECTS OF PACLITAXEL-LOADED NANOTHERAPEUTICS ON FRESHWATER ALGAE, *PSEUDOKIRCHNERIELLA SUBCAPITATA* AND *CHAMYDOMONAS REINHARDTII**

D.1. Abstract

The contamination of water bodies and water pollution with pharmaceutics are global issues receiving increasing attention, stemming from the population growth and resultant rises in pharmaceutical consumption, disposal, and excretion. However, little is known about how emerging classes of pharmaceutics, in particular nanopharmaceutics, influence water bodies and organisms living in them. In this work, we investigate the interactions of paclitaxel-load nanomedicine with freshwater algae *Pseudokirchneriella subcapitata* and *Chamydomonas reinhardtii*. For a given paclitaxel concentration, the nanomedicine form of paclitaxel was found to lead to a higher localization/internalization of paclitaxel on/in algal cell surfaces and to inhibit algal growth more than molecular (free) paclitaxel. In addition, while the molecular paclitaxel at the solubility limit in water could not significantly hinder algal growth to reach a IC50 level, the nanomedicine form had a 72-h IC50 value of 0.8 ± 0.1 µg paclitaxel/mL for *C. reinhardtii* and 1.6 ± 0.1 µg paclitaxel/mL for *P. subcapitata*. In the case of paclitaxel-load nanomedicine, concentrations above 16.2 µg paclitaxel/mL for *P. subcapitata* and above 5.4 µg paclitaxel/mL for *C. reinhardtii* resulted in an algaecidal effect, i.e. algal necrosis and complete stoppage of algal growth. These findings indicate that nanopharmaceutics can cause ecotoxic effects on freshwater algae that are otherwise not possible by traditional lipophilic pharmaceutics, owing to their ability to solubilize water-insoluble drug molecules in them.

* Reprinted with permission from "Ecotoxic effects of paclitaxel-loaded nanotherapeutics on freshwater algae, *Raphidocelis subcapitata* and *Chlamydomonas reinhardtii*" by Yegin, Y., C. Yegin, J. K. Oh, A. Orr, M. Zhang, N. Nagabandi, T. Severin, T. A. Villareal, M. M. Sari, A. Castillo, E. A. Scholar, and M. Akbulut, 2017, Environmental Science: Nano, 4, 5, 1077-1085, Copyright 2017, with permission from Royal Society of Chemistry.

D.2. Introduction

Nanotherapeutics are defined as nanoscale or nanostructured materials used for medical diagnosis and treatment.[227] The main motivation behind to use nanotherapeutics is their size-specific unique medical and physiological properties. For instance, the bioavailability of therapeutics, increases with decreasing size and increasing surface area to volume ratio of drug particles, which is especially beneficial for water-insoluble therapeutics.[228] In addition, nanopharmaceutics in the range of 10 nm to 200 nm tend to passively target disease sites through the enhanced permeability and retention effect.[229,230] By relying on such intriguing properties, a number of nanotherapeutics have successfully been developed from the laboratory to the clinic to the market: According to a recent study, there were 33 marketed nanotherapeutics worldwide in 2012.[231] Another study identified 158 startups and small and medium enterprises focusing on the development of nanotherapeuticss.[227] The global market value of nanotherapeutics was estimated to reach about $7 billion in 2004,[227] between $17 and $73 billion in 2011,[232,233] and between $178 and $528 billion in 2019.[233,234] The increased production and consumption of nanotherapeutics have brought along concerns regarding the potential consequences of their occurrence and distribution on environmental and ecological health.

The abovementioned concerns have intensified in light of recent studies indicating that some of the administered nanotherapeutics can be excreted from the human body via excretory or hepatobiliary systems.[235–237] Hepatobiliary system generally provides a partial or a full metabolization of the nanomedicines that is followed by fecal or biliary excretion.[238,239] On the other hand, kidney and other parts of the excretory system rapidly remove them, in particular small ones (i.e. <50 nm), from the vascular compartment in a relatively unaltered form.[238] Upon excretion, nanotherapeutics are destined to reach the sewer system and then go through a waste

treatment facility. However, the elimination of nanoparticles from wastewater is a challenge and standard wastewater treatment plants do not completely capture some nanomaterials.[240,241] While it is currently unknown how nanotherapeutics interact with waste treatment plants, the occurrence and detection of conventional therapeutic agents in waterbodies[242–244] suggest nanotherapeutics may also find its way to rivers, lakes, and oceans through the discharge of liquid effluent from wastewater treatment plants. In addition, sewage systems may leak or become defective, and these leaks can eventually infiltrate to subsoil and reach underground streams.[245–247] Overall, owing to these reasons, the ecotoxicity of nanotherapeutics is an emerging concern from environmental science perspectives.

Algal communities have many characteristics as biological indicators of spatial and temporal environmental variations owing to their position at the base of aquatic foodwebs.[248] Furthermore, algae play a role on the purification of polluted water.[249,250] Algae respond promptly various types of pollutants and provide warning signals related to the deterioration of ecological conditions, making them useful as model organisms for assessing the toxicity of pollutants.[251–256] There is extensive literature on the interactions of pharmaceuticals and nanomaterials with algae and subsequent outcomes of these interactions on survival and growth of algae.[257–264] Mechanisms by which nanomaterials cause ecotoxicity on algae include modifications of membranes and other cell structures, local nutrient depletion and shading induced by physical restraints (clogging effects), solubilization of toxic compounds, and/or production of reactive oxygen species.[265–284] Regarding pharmaceuticals, the main modes of pharmaceutical toxicity for algae are specific and nonspecific inhibition of photosynthesis, estrogenic effects, and reactive toxicity.[285–291] The severity of these ecotoxic effects depend on the chemical nature of pharmaceuticals. For instance, cytostatics, used for cancer therapy, tend to inhibit algal growth at doses much below than that

analgesics and antibiotics can.[263,264] Despite the existence of numerous ecotoxicity studies of nanoparticles and pharmaceuticals with algae, little has been reported on the ecotoxicity of nanotherapeutics on algae. In addition, the very nature of nanotherapeutics resulting in increased bioavailability, ability to solubilize hydrophobic molecules, higher payload capacity, excellent stability in aqueous environments and in blood, and prolonged blood circulation times further motivates ecotoxicity studies with nanotherapeutics. This is because the abovementioned properties can cause nanotherapeutics to persevere for extended periods of time in the environment, and thus have a larger impact on uncontrolled releases and accidental spills.

In this study, we investigate the interactions of paclitaxel-loaded nanotherapeutics with *Pseudokirchneriella subcapitata* and *Chlamydomonas reinhardtii*. Here, paclitaxel is focused on because it is a commonly used antineoplastic agent for treatment of pancreatic, breast, ovarian, lung, and other types of cancer and the active ingredient of three different nanotherapeutics on the market.[292] *Pseudokirchneriella subcapitata* and *Chlamydomonas reinhardtii* are well-established green algae models for ecotoxicity studies.[268,270,293,294] To systematically study how paclitaxel-based nanomedicine adsorb and absorb on/in algae and such processes influence algal proliferation, a comprehensive and complementary set of experimental techniques were used, including transmission electron microscopy, dynamic light scattering, spectrofluorometry, optical microscopy, and laser confocal microscopy.

D.3. Experimental

D.3.1 Materials

Paclitaxel (99%) was purchased from Selleck Chemicals (Houston, TX); poly (ethylene oxide)-*block*-poly (ε-caprolactone) (PEO-*b*-PCL, 5k-b-6k, Mw/Mn = 1.3) was purchased from Polymer Source Inc. (Dorval, Quebec, Canada); and tetrahydrofuran (THF, 99+ %) and poly-L-

lysine were procured from Sigma-Aldrich Co. (St. Louis, MO). Oregon Green® 488 Conjugate (Oregon Green® 488 Taxol, Flutax-2) was purchased from ThermoFisher Scientific (Waltham, MA). All chemicals were used as received.

D.3.2 Preparation of Paclitaxel-Loaded Nanotherapeutics

Paclitaxel-loaded nanomedicine was prepared as described elsewhere.[142,295,296] Briefly, paclitaxel (0.002 g) and PEO-*b*-PCL (0.03 g) were dissolved in 1 mL THF, which was then intensely mixed with 9 mL Milli-Q water using a probe sonicator at 1200 W for 5 min (SJIA-2000W, Ningbo Haishu Sklon Electronics Instruments Co., Zhejiang, China). Then, the dispersion of paclitaxel-loaded particles was dialyzed in OECD media using a standard regenerated cellulose membrane (molecular weight cut-off 12,000-14,000 Da, Spectrum Laboratories, Inc., Rancho Dominguez, CA) to remove THF from the dispersion. To facilitate the removal of THF, the OECD media was replaced with fresh OECD media every 30 min until no THF was detected by olfactory analysis.

D.3.3 Characterization of Paclitaxel-Loaded Nanotherapeutics

Particle size distribution of paclitaxel nanoparticles after the dialysis was measured using dynamic light scattering (DLS) with a Zetasizer ZS90 particle size and zeta potential analyzer (Malvern Instruments, Ltd., Westborough, MA). The measurements were carried out at a scattering angle of 90° at 25 °C. The morphology of nanotherapeutics was characterized by a JEOL JEM-2010 transmission electron microscope (JEOL USA, Inc., Peabody, MA). In these measurements, nanotherapeutics dispersion was added drop-wise onto a copper grid (400 mesh) with carbon film (CF400-Cu, Electron Microscopy Sciences, Hatfield, PA). Then, the sample was fully dried at ambient conditions prior to TEM analysis. Observations were done at 200 kV accelerating voltage, $<2.5 \times 10^{-5}$ Pa pressure, and at 25°C.

D.3.4 Algal Growth and Exposure Experiments

Pseudokirchneriella subcapitata and *Chlamydomonas reinhardtii* algae cells were obtained from Carolina Biological Supply Company (Burlington, NC). These microorganisms were grown in algal growth medium described in the guidelines by Organisation for Economic Cooperation and Development (OECD).[297] The resultant algal cultures were counted using a hemocytometer and then diluted into 200 mL of fresh OECD media to yield a concentration of 10^6 cells/L. Then, the algae cultures were exposed to free paclitaxel at the solubility limit in water (0.2 μg/mL)[298] or paclitaxel-loaded nanotherapeutics at varying concentrations where the net paclitaxel concentration was 0.2, 0.6, 1.8, 5.4, or 16.2 μg/mL in the suspension of paclitaxel-loaded nanotherapeutics. Algal culture with no treatment was control group. Each of these conditions were performed in triplicate. The point of exposure was taken as time zero. The number of algae after the treatments was determined by taking 3 mL aliquots from the treated solutions and by measuring fluorescence levels using a spectrofluorometer (PTI QuantaMaster, the Fluorescence Solutions Company, Edison, NJ) at day 0, 1, 2, 3, 5, and 7. The inhibitory concentration of paclitaxel-based nanomedicine leading to a 50% reduction in algal growth rate compared to the controls (i.e. IC50) were calculated using a linear interpolation.[299]

D.3.5 Characterization of Algae and Nanoparticulate Uptake by Algae

The shape and dimensions of algae were characterized using optical microscopy (Zeiss LSM 780 NLO, Carl Zeiss Microscopy GmbH, Pleasanton, CA). To enable fluorescent tracking of therapeutic agent needed in uptake studies, paclitaxel/Oregon Green® 488 conjugate rather than just paclitaxel was used for the preparation of paclitaxel-loaded nanotherapeutics. The exposure studies were conducted using paclitaxel/Oregon Green® 488 conjugate and nanotherapeutics containing paclitaxel/Oregon Green® 488 conjugate. Here, Oregon Green® 488 was particularly

selected to ensure that the fluorescence emission of the tracked particles peaks at a wavelength sufficiently away from that of algal chlorophylls. After the preparation of fluorescently-tagged materials, 1.0 mL aliquot from each algae stock solution at a concentration of 10^6 cells/L was mixed with 1.0 mL fluorescently-tagged free paclitaxel (0.2 µg/mL) or paclitaxel-based nanotherapeutics with a net paclitaxel concentration of 0.2 µg/mL and incubated for 2 hr. Before confocal microscopic imaging, the exposed algal cultures were washed once with OECD media and immobilized on glass cover slides that were coated with poly-L-lysine solution. The images were obtained using a confocal laser scanning microscope (Leica TCS SP5, Leica Microsystems Inc., Buffalo Grove, IL) at an excitation wavelength of 488 nm.

D.3.6 Statistical Analysis

Data and statistical analyses were carried out using ORIGIN® v8 software (OriginLab Corp., Northampton, MA). One-way analysis of variance (ANOVA) was used to test the differences between treatments and Tukey's Honestly Significant Differences (HSD) test was performed to separate means differing at $p<0.05$.

D.4. Results and Discussion

D.4.1 Characterization of Paclitaxel-based Nanomedicine and Microorganisms

Nanoparticle size is known to affect the efficacy and pathway of cellular uptake and blood circulation of nanoparticles. Commercial nanotherapeutics for intravenously administration are often prepared in a way to result in a particle size in the range of 50-300 nm to ensure a prolonged blood circulation and passive tarageting.[300–302] The mean intensity-weighted hydrodynamic size of paclitaxel-based nanomedicine prepared, which was obtained by the DLS analysis, was found to be 84 ± 4 nm with a relatively narrow size distribution having polydispersity index (PDI) of 0.19 (Fig. 57A). Since the size of the prepared nanomedicine lies within the range of optimum size for

intravenous drug delivery applications, the prepared nanomedicine represents a suitable model from a size perspective. The shape of nanoparticles is another important parameter influencing their cellular uptake.[303] For instance, Chithrani et al.[304,305] reported that spherical particles of similar size were taken up 500% more than rod-shaped particles, which was attributed to the greater membrane-wrapping time required for the elongated particles. Hence, to better interpret the algal uptake data, we characterized the morphology of the prepared nanomedicine using TEM (Fig. 57B), which revealed that particles are spherical in shape as most commercial nanotherapeutics.

Figs. 57C and D show the size and shape of *P. subcapitata* and *C. reinhardtii* cells, respectively, before any treatments. It was observed that while *P. subcapitata* cells have a curved and twisted appearance, with an arc length of 9.3 ± 1.8 μm and width of 1.9 ± 0.4 μm, *C. reinhardtii* cells were mostly spherical with a diameter of 9.8 ± 1.2 μm. In summary, these microorganisms are approximately two order of magnitude larger in size than nanomedicine (i.e., about six order of magnitude larger in volume).

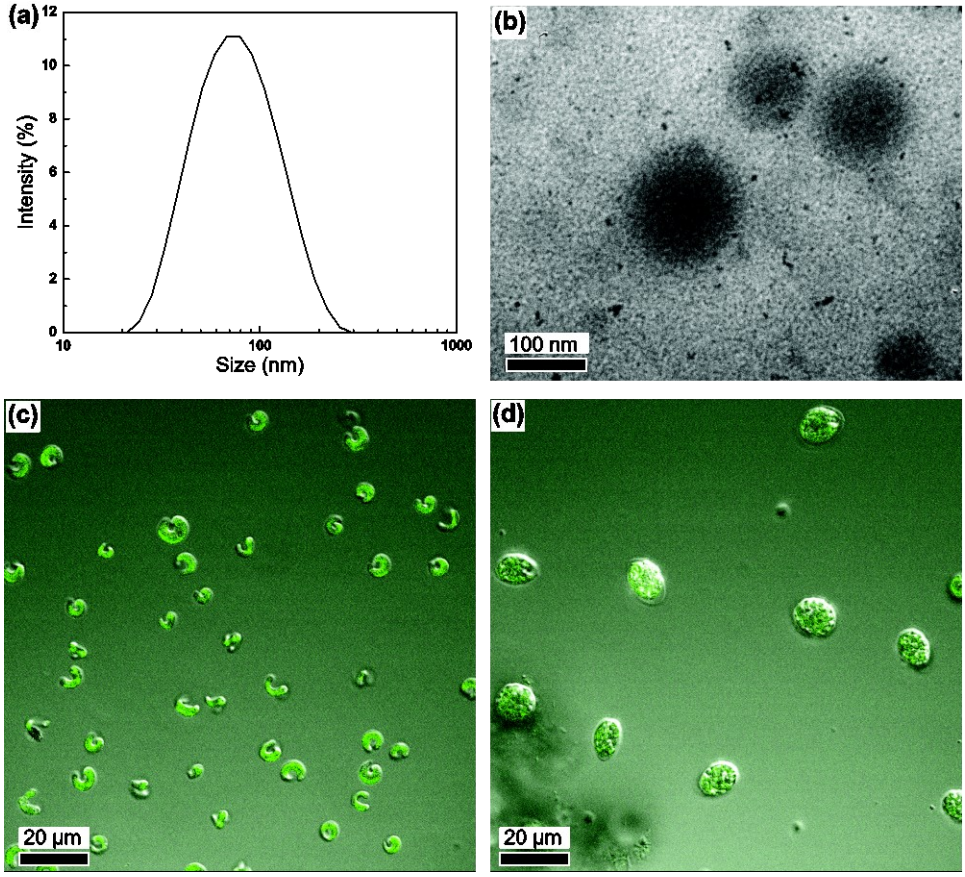

Figure 57. (a) Size distribution for paclitaxel NPs obtained via DLS analysis, (b) transmission electron micrograph of paclitaxel NPs, and microscopic images of (c) *P. subcapitata* and (d) *C. reinhardtii* algae cells.

D.4.2 Effect of Free-Paclitaxel and Paclitaxel-based Nanomedicine on Algal Growth

To compare the effect of paclitaxel in solution and nanoparticulate formulation on algae growth, *P. subcapitata* and *C. reinhardtii* cells were exposed to free paclitaxel at the solubility limit in water or varying concentrations of paclitaxel-based nanomedicine for up to 7 days and the resultant algal growth was spectrofluorometrically determined as a function of time (Fig. 58). In the case of *P. subcapitata, t*hese studies revealed the following (Fig. 58A): First, both free- and nanoparticulate- form of paclitaxel reduced the algal population in short term (up to day 1). Second, for a given paclitaxel concentration (0.2 µg/mL), the nanoparticulate-form of paclitaxel

hindered the algal growth more than the free-form, indicating an enhanced algal toxicity of nanoparticulate-form. Third, the algal growth slowed down with increasing nanomedicine concentration in the range of a net paclitaxel concentration of 0.2 to 5.4 μg/mL and completely ceased at a nanomedicine concentration corresponding to 16.2 μg paclitaxel/mL. Fourth, in the case of paclitaxel nanomedicine, IC50 value was 1.6 ± 0.1 μg paclitaxel/mL for 72-h. On the other hand, free-paclitaxel could not lead to a growth inhibition to IC50 level due to the poor water solubility of paclitaxel in water, 0.2 μg/mL. To put the IC50 value into a perspective, we compare this value with IC50 values of other nanomaterials and chemicals in the literature. For instance, toxicity studies involving 10–20 nm CeO_2 nanoparticles and P. *subcapitata* indicated a 72-h IC50 value of 10.3 ± 1.7 μg/mL.[306] Franklin et al.[307] reported that *P. subcapitata* was sensitive to ZnO nanoparticle (30 nm) stress, with a 72-h IC50 value of 68 μg Zn/L, mostly due to dissolved zinc. Aruoja et al.[308] found that *P. subcapitata* EC50 values (72-h) of most nonpolar narcotic chemicals, including pentachloroethane, 2,4-dichlorotoluene, m-xylene, trichloroethene, and hexanol were in the range of 2-200 μg/mL. Common antibacterial agents such as triclosan, triclocarban, roxithromycin, and clarithromycin were shown to inhibit *P. subcapitata* growth with 72-h IC50 of 0.5 to 46 μg/L.[309] Overall, while most nonpolar narcotic compounds and CeO_2 nanoparticles yield lower toxicity to *P. subcapitata* compared to paclitaxel-based nanomedicine, ZnO nanoparticles and antibacterial agents such as triclosan, triclocarban, roxithromycin, and clarithromycin were significantly more toxic to *P. subcapitata* than paclitaxel and paclitaxel-based nanomedicine.

Similar trends were also observed for the case of *C. reinhardtii* with a few differences (Fig. 58B). First, free-paclitaxel did not give rise to a decrease in algal population at any time point. Second, paclitaxel-based nanomedicine inhibited *C. reinhardtii* growth to a greater extent in comparison to *P. subcapitata* growth. Third, algaecide effect of paclitaxel-based nanomedicine

was observed at a lower concentration (5.4 µg paclitaxel/mL) instead of 16.2 µg paclitaxel/mL. Fourth, 72-h IC50 value of paclitaxel-based nanomedicine was 0.8 ± 0.1 µg paclitaxel/mL (for *C. reinhardtii*) rather than 1.6 ± 0.1 µg paclitaxel/mL (for *P. subcapitata*). Considering that paclitaxel is highly lipophilic, a higher fatty acid content of *C. reinhardtii*, i.e. ~9% of dry cell weight (DCW)[310] compared to ~7% fatty acid of DCW in *P. subcapitata*[311] can account for this difference. Furthermore, the ratio of unsaturated fatty acids to all fatty acids is larger for P. *subcapitata* (~75%)[311] than for *C. reinhardtii* (~65%).[310] *C. reinhardtii* cells are much fragile than *P. subcapitata* cells because *P. subcapitata cell* wall is comprised of cellulose and other polysaccharides while cell wall of *C. reinhardtii* contains several layers of hydroxyproline-rich glycoproteins but not cellulose and other polysaccharides.[312,313] This difference implies a more rigid and ordered membrane structure and, hence, a lower permeability of cell membrane for P. *subcapitata*. The lower tolerance of *C. reinhardtii* to toxic compounds have also previously observed. For example, Lee et al.[314] evaluated the toxicity of dissolved Ag for *P. subcapitata* and *C. reinhardtii* cells and reported that EC50 value for the growth rate of *P. subcapitata* and *C. reinhardtii* cells were 2.8 µg Ag/mL and 1.3 µg Ag/mL, respectively. They attributed this difference to the higher uptake rates of *C. reinhardtii*, which may also be the case for paclitaxel.

Regarding the prior studies focusing on the effect of nanomaterials on *C. reinhardtii* growth, Chen et al.[315] reported that the *C. reinhardtii* algae cells were significantly damaged by the increased concentration of TiO_2 nanoparticles. The algae cells were exposed to the nanoparticulate dispersions with 0.1, 1, 10, 20 and 100 µg/mL TiO_2 nanoparticles, and the growth of algae cells were shown to stop at an exposure concentration of 100 µg/mL. Perreault et al.[316] measured a 30-min and 24-h EC50 of 0.114 mg/mL and 0.083 mg/mL for the polyamidoamine-coated gold nanoparticle-*C. reinhardtii* system, respectively. CuO NP was shown to cause growth

inhibition on *C. reinhardtii* with 72-h EC50 of 150.45 ± 1.17 µg/mL.[278] Hu and co-workers[317] found that 4 nm CdTe quantum dots (QDs) inhibited *C. reinhardtii* growth above a concentration of 1 µg/mL and these microorganisms were more sensitive to QDs than to TiO_2 nanoparticles.

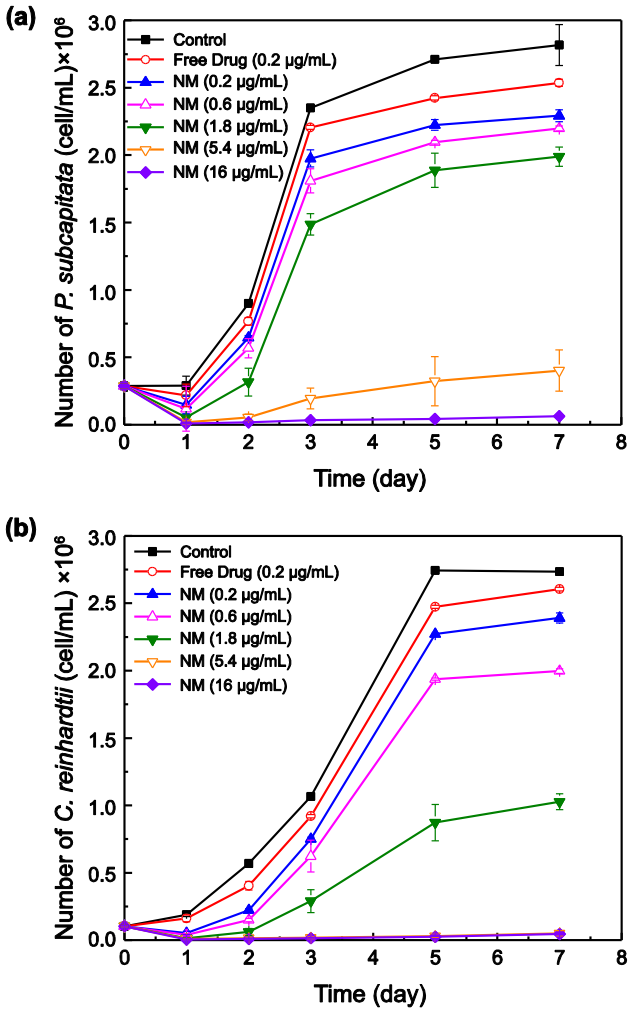

Figure 58. Effect of free-paclitaxel and paclitaxel-based nanomedicine on the growth of (a) *P. subcapitata and* (b) *C. reinhardtii algae* cells. The concentrations of nanomedicine (NM) concentration is given in terms of the net paclitaxel concentration.

D.4.3 Interactions of Free Paclitaxel and Paclitaxel-based Nanomedicine with Algae Cells

To gain mechanistic insights into the interactions of paclitaxel-based nanomedicine and algal *P. subcapitata* and *C. reinhardtii* cells, we carried out confocal microscopy studies with the aid of paclitaxel conjugated with a fluorophore, in free (molecular) form as well as nanoparticulate form. As can be seen from Figs. 59A and B, for a given paclitaxel/fluorophore concentration, the ratio of *P. subcapitata* cells with fluorophores to all cells were higher in the case of exposure to paclitaxel-loaded nanomedicine: >79±11% in comparison to 38±5%. While the exposure to paclitaxel-loaded nanomedicine led to a similar degree of localization for both types of microorganisms (one-way ANOVA, $P > 0.05$), the exposure to free-paclitaxel gave rise to a higher localization for *C. reinhardtii* cells (66±2%) compared to *P. subcapitata* cells (38±5%) (Figs. 59 and 60). The reason behind the enhanced localization of paclitaxel in/on algae for the nanoparticulate form can be attributed to two phenomena. First, the adsorption of free-paclitaxel and paclitaxel-based nanomedicine on algae surface is mainly governed by van der Waals interactions, which are well-known to be body-forces. This indicates a stronger attraction between larger objects i.e., nanomedicine and algae cell compared to drug molecule and algae cell. Furthermore, owing to the existence of hydrogen bonding groups on algae cell[318] and because the shell of nanomedicine, poly(ethylene oxide)-*block*-poly(ε-caprolactone), contains a large number of hydroxyl and ether groups,[319] favorable hydrogen bonding interaction arises between nanomedicine and algae cells.

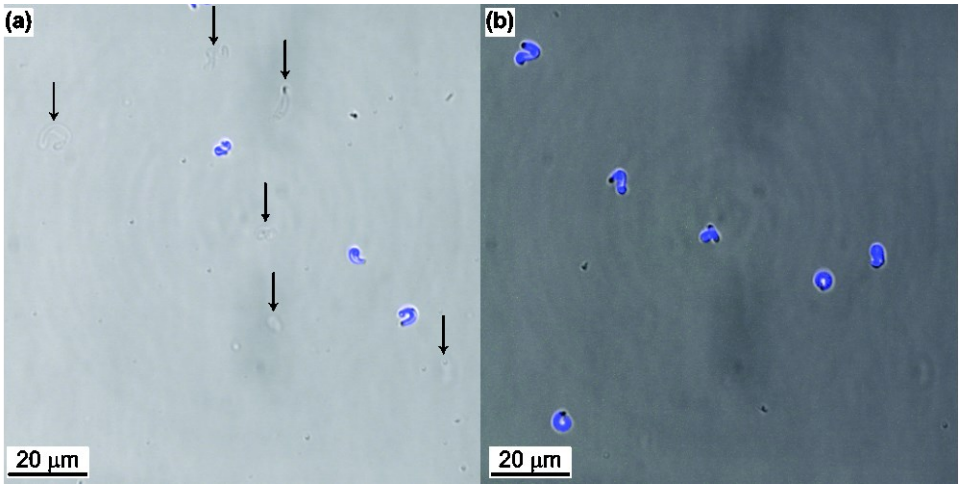

Figure 59. Confocal microscopy images of *P. subcapitata* cells in presence of (a) free drug (paclitaxel) and (b) paclitaxel-based nanomedicine. Arrows indicate the empty cells (i.e. cells without drug localization).

The presence of paclitaxel (both forms) resulted in a flocculation of *C. reinhardtii* cells but not *P. subcapitata* cells (Fig. 59 and 60), suggesting a stronger interaction between paclitaxel/paclitaxel-based nanomedicine and *C. reinhardtii*. To explain this discrepancy between C. *reinhardtii* and *P. subcapitata*, we measured their zeta potentials and found the zeta-potential to be –21.9 ± 0.9 mV for *P. subcapitata* and –8.51 ± 0.2 mV for *C. reinhardtii*. These values indicate that double-layer electrostatic repulsion between *C. reinhardtii* cells are much weaker, i.e. more likely to aggregate. Furthermore, the introduction of paclitaxel having hydroxyl, carbonyl, and amino groups[320] or poly(ethylene oxide)-*block*-poly(ε-caprolactone) having hydroxyl and ether groups[319] may link algae cells and form "algal coacervates" through hydrogen bonding. It is also possible that aggregation could be a self-protection mechanism of algal cells, which relies on the minimization of their surface area through aggregation.[321] Similar to our findings, Perreault et al.[322] also found that when *C. reinhardtii* cultures were exposed to mannose-functionalization Au nanoparticles, 90.5 ± 6.3% of algae cells were in an aggregated form, indicating nanoparticle

induced aggregation and clustering of algal cell culture. Likewise, Behra and co-workers[279] reported that exposure to CeO_2 nanoparticulate aggregates resulted in a flocculation of *C. reinhardtii* cells.

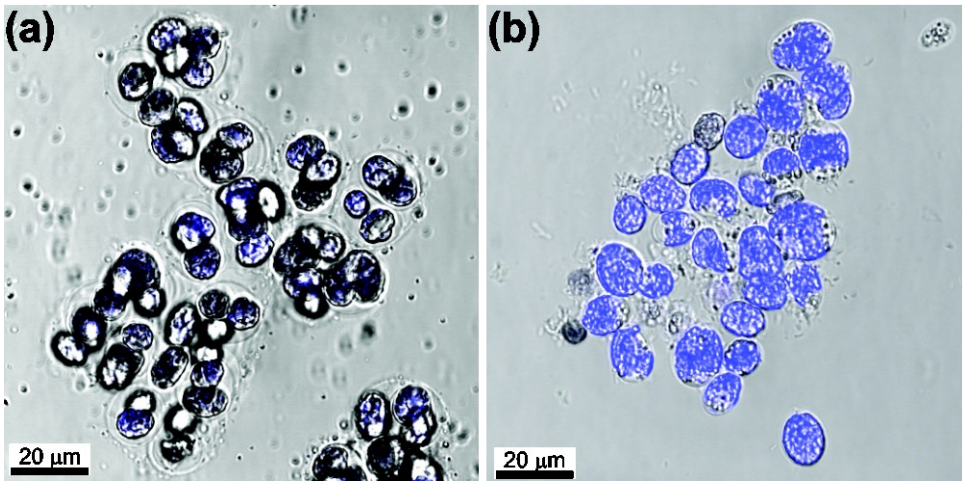

Figure 60. Confocal microscopy images of *C. reinhardtii* cells in presence of (a) free paclitaxel and (b) paclitaxel-based nanomedicine.

For both types of microorganisms, the cells exposed to paclitaxel or paclitaxel-loaded nanomedicine slightly shrank and deformed (Figs. 52, 54, and 55). The deformations were slightly more noticeable for the case of *C. reinhardtii* presumably owing to soft and flexibly hydroxyproline-rich glycoproteins layers. In addition, lipophilic paclitaxel prefers to internalize lipid-rich environment as in the case of *C. reinhardtii* compared to *P. subcapitata*.[310,311] However, the degree of morphological alterations induced by paclitaxel-loaded nanomedicine are much smaller than those observed with hard inorganic nanoparticles such alumina, silica, titania, nickel oxide.[323–326] This difference may be ascribed to the dynamic nature of nanomedicine in which there are continuous rearrangements of building blocks (i.e., diblock copolymers) due to thermal energy

and entropic factors, its ability to re-assemble and dis-assemble in the presence of certain stimuli, and its soft and deformable nature.

D.5. Conclusion

This work is concerned with the interactions of paclitaxel-load nanomedicine with *P. subcapitata* and *C. reinhardtii* algae cells as well as the potential consequences of these interactions on the dynamics of algal growth. The key findings are as follows: First, the for a given drug concentration, paclitaxel-load nanomedicine inhibits algal growth more than molecular (free) paclitaxel. While the molecular paclitaxel at the solubility limit (i.e. maximum solubility in water, ~0.2 μg/mL) was not enough to hinder the algal growth to reach a IC50 level, paclitaxel-loaded nanomedicine had a 72-h IC50 value of 0.8 ± 0.1 μg paclitaxel/mL for *C. reinhardtii* and 1.6 ± 0.1 μg paclitaxel/mL for *P. subcapitata.* This result indicates that due to its ability to solubilize water insoluble (lipophilic) drug molecules in them, nanomedicine can cause ecotoxic effects on algae that is not otherwise possible. Second, the nanomedicine form of paclitaxel also demonstrates higher localization/internalization on algal cell surfaces suggesting favorable interactions between hydrogen bonding groups on algae cell and the stabilizing shell of nanomedicine, poly(ethylene oxide)-*block*-poly(ε-caprolactone), which contains a large number of hydroxyl and ether groups. Third, an increasing exposure concentration of paclitaxel-loaded nanomedicine results in a decrease in the growth rate. In addition, concentrations above 16.2 μg paclitaxel /mL for *P. subcapitata* and *above* 5.4 μg paclitaxel /mL for *C. reinhardtii* lead to algaecidal effect (i.e. inability to grow any algae). Overall, increasing production and consumption of nanomedicine is a valid ecological and environmental concern given that nanomedicine form of paclitaxel, a commonly used drug for cancer treatments, can inhibit the growth of freshwater algae and even show algaecidal effect at fairly low concentrations.

D.6. Acknowledgements

This material is based upon work supported the National Science Foundation under Grant No. 1236532.